

ENHANCEMENT OF D-LACTATE PRODUCTION IN A
CONTINUOUS CULTURE OF A MUTANT ESCHERICHIA COLI
THROUGH PERIODIC OPERATION

By

JONATHAN BEN RODIN

A DISSERTATION PRESENTED TO THE GRADUATE SCHOOL
OF THE UNIVERSITY OF FLORIDA IN PARTIAL FULFILLMENT
OF THE REQUIREMENTS FOR THE DEGREE OF
DOCTOR OF PHILOSOPHY

UNIVERSITY OF FLORIDA

1992

ACKNOWLEDGMENTS

I would like to thank my committee chairmen, Professors Spyros Svoronos and Gerasimos Lyberatos, for providing guidance above and beyond the call of duty. They are appreciated for being there to help and encourage me during the bad times when the project was going down seemingly blind alleys.

There are other faculty members who have truly been of great assistance. I would like to thank my other committee members first, Professors Gerald Westermann-Clark, Seymour Block, Ben Koopman, and Lonnie Ingram. Dr. Ingram is especially appreciated for all of his very useful advice without which this project would not have been completed. He has also been very generous with use of his laboratory and equipment. In addition to my committee members, Professors Bitsanis and Crisalle are thanked for all of their guidance.

Several graduate students have helped me out during my research project. Three deserve special mention, Jeff Mejia, Pratap Pullammanappallil, and Christina Stalhandske for all the technical assistance they provided. If only one student was to be mentioned, Jeff Mejia would be the one. He is the one who initially suggested the reversion problem with this system. If not for his advice, I would still be in the dark as to the cause of all of the problems associated with continuous anaerobic operation. Christina's help was instrumental in the work performed on the aerobic characterization of bacterial growth. Pratap, besides being one of my closest friends during my years in Gainesville, has been an indispensable resource of information and help with my project. Additionally, Jeffrey Harmon has lent a helping hand on several occasions. Lastly, in addition to those

mentioned above, I have been very fortunate to have had numerous other friends among the graduate students in this department.

Several undergraduates from this department have assisted me at various times during the duration of this project. I have been very fortunate to have had these people work with me. The following undergraduates have worked as laboratory assistants or completed small research projects with me: Dawn Mackland, Mike Hinson, Reann Soodeen, Craig Moates, Erik Dunmire, and John Walker. Among these students, Dawn, Craig, and Mike have each shown dedication above and beyond what was expected from them. Like the graduate students that have gone through this department, I have been fortunate to call several of the undergraduates, again in addition to those mentioned above, friends.

This section would not be complete without mentioning Mr. Tracy Lambert, the department's maintenance specialist. He has been of invaluable help to me during this project.

Finally, I would like to thank my parents, sister, brother, and sister-in-law. Without their love, support, and encouragement, I probably would not have been able to endure this whole ordeal. My brother was also generous with allowing me free use of the facilities and equipment at his business, Gallery Graphics.

TABLE OF CONTENTS

	<u>page</u>
ACKNOWLEDGEMENTS	ii
ABSTRACT	vi
CHAPTERS	
1 INTRODUCTION	1
2 THEORETICAL METHODS	4
2.1 Overview	4
2.2 Determination of Optimal Steady-state Operation	5
2.3 A New Method of Determining Optimal Periodic Pulsing	7
2.3.1 Carleman Linearization	7
2.3.2 Performance Measure Calculation	10
2.4 Model Fitting with Nonlinear Least Squares Methods	15
3 EXPERIMENTAL METHODS	19
3.1 Organism Description	19
3.2 Analytical Methods	21
3.2.1 Biomass and Cell Number Determination	21
3.2.2 Glucose Analysis	25
3.2.3 d-Lactate Measurement	26
3.2.4 Other Analyses	28
3.3 Feed Medium Composition	30
3.4 Feed Preparation	32
3.5 Experimental Operation	38
3.5.1 Operational Conditions	38
3.5.2 Shake Flask Experimental Procedure	40
3.5.3 Reactor Experimental Procedure	42
3.5.3.1 System Description	42
3.5.3.2 System Startup and Operation	44
4 ANAEROBIC GROWTH OF <i>E. COLI</i> LCB898	48
4.1 Background	48
4.2 Batch Growth	51
4.3 Continuous Growth	65
4.4 Modeling	73
4.4.1 Presentation of Model	73
4.4.2 Model Parameter Fitting	74

5	AEROBIC GROWTH OF <i>E. COLI</i> LCB898	84
5.1	Background	84
5.2	Experimental and Modelling Results Introduction	85
5.3	Batch Growth	87
5.4	Continuous Growth	87
5.5	Modeling	95
5.5.1	Presentation of Model	95
5.5.2	Model Parameter Fitting	101
6	THE EFFECTS OF SHIFTS IN AERATION OF <i>E. COLI</i> LCB898 ..	113
6.1	Background	113
6.2	Development of the Combined Aerobic-Anaerobic Model ...	114
6.3	Testing of the Model	116
7	EFFECTS OF AERATION CYCLING ON LACTATE PRODUCTIVITY OF <i>E. COLI</i> LCB898	122
7.1	Background	122
7.2	Theoretical Investigation into Cycling	123
7.3	Experimetal Confirmation of Lactate Productivity Optimization Results	135
8	REVERSION OF <i>E. COLI</i> LCB898 AND A POSSIBLE NEW METHOD OF AVOIDANCE OF REVERSION	151
9	CONCLUSIONS	163
APPENDIX		
	MATHEMATICA PROGRAMS FOR COMPUTATION OF CARLEMAN LINEARIZATION MATRICES	165
	LIST OF REFERENCES	171
	BIOGRAPHICAL SKETCH	175

Abstract of Dissertation Presented to the Graduate School
of the University of Florida in Partial Fulfillment of the
Requirements for the Degree of Doctor of Philosophy

ENHANCEMENT OF D-LACTATE PRODUCTION IN A
CONTINUOUS CULTURE OF A MUTANT ESCHERICHIA COLI
THROUGH PERIODIC OPERATION

By

Jonathan Ben Rodin

December, 1992

Chairman: S. Svoronos
Cochairman: G. Lyberatos
Major Department: Chemical Engineering

In some biological systems, the environmental conditions that are optimal for microbial growth differ from the optimal conditions optimal for producing a desired metabolite. If production of this metabolite were the process objective, one could continuously operate a reactor system at the optimal production conditions. However, for a given reactor volume, changing the conditions periodically could increase overall production of the desired metabolite. This is possible since, due to higher growth rates under the optimal growth conditions, one could operate the system at significantly higher flowrates and, thus, obtain more product. A system involving *E. coli* mutant LCB898 was used as a model system. Under anaerobic conditions this bacterium will produce large amounts of d-lactic acid, whereas under aerobic conditions, this bacterium will grow faster. The possibility of increasing total lactate production by cycling dissolved oxygen was investigated.

Before any optimization work could be done, an adequate model for describing the behavior of this system under both steady-state and transient conditions had to be developed and tested. Such a model was developed using batch and continuous data and then tested by comparison with shifts between conditions.

A method for determining the optimal waveform for the proposed cycling was developed by extending previous work by Lyberatos and Svoronos. The method involved Carleman linearization of the model equations around a steady state and subsequent development of a term for the performance measure. The system studied oscillated between purely aerobic and anaerobic metabolisms with no intermediate conditions. Thus, an “imaginary” steady state of intermediate metabolism had to be used for linearization.

In numerical simulation of the determined optimal cycling, significant improvement over strictly anaerobic operation was found. Experimental verification of this was performed and improvement, though not as significant as theoretical predictions would indicate, was found. Additionally it was found that the mutant was probably reverting to a form where little d-lactic acid was produced. Cycling of dissolved oxygen apparently helps delay this reversion.

CHAPTER 1 INTRODUCTION

Chemical processes are usually operated in one of three different manners, batch, fed-batch, or continuous, each with its own advantages and disadvantages. Batch operation is advantageous when small quantities of a product are desired. This type of operation is perhaps the simplest since it only involves charging the reactor with the appropriate reactants at the start of the process and removal of the products at its completion. Unfortunately, this type of operation includes frequent downtimes where the reactor is being either charged or purged, and production is thus temporarily stopped. Fed-batch operation, where feed is added continuously but nothing is being withdrawn, is also advantageous when small quantities of a product are desired. This type of operation is optimal, for example, when it is desired to keep reactant concentration low. Fed-batch operation has the same downtime problems that batch operation does. Continuous operation is typically used when large quantities of a product are desired. It has advantages over the batch-type processes in that no downtimes for charging or purging the reactor are necessary. However, higher control and instrumentation costs are incurred. When large quantities of product are desired, continuous operation is the usual method of choice.

When continuous processes are used, they are usually operated, after start-up transients die out, in a steady-state manner. This involves keeping the process variables constant. This type of operation is relatively easy to model and control. However, optimal operation may involve taking the reacting volume through multiple steps of processing, for example, operating the system in a neutral environment for an amount of time, and then in an acidic environment. The simplest solution to this type of problem for a two-step process

would be to have two tanks in series, where one has a particular set of environmental conditions maintained in it, and the other has a different set of environmental conditions maintained. However, this increases the total volume and instrumentation (and thus cost) of the system. An alternative approach is periodic operation. This involves only one tank, but the environmental conditions are manipulated with respect to time. In general chemical systems small time constants are the rule. As a result, conditions in the reactor would have to be changed frequently to observe a significant improvement over steady-state operation. This would lead to substantial control costs. However, in biological systems the time constants are relatively large. Thus conditions may not have to be changed rapidly. Therefore, biological systems may be suitable for periodic operation.

Periodic operation of continuous culture systems has been investigated by other workers [e.g. 1-8] and it has been found to be useful in achieving desired process goals. For example, it has been used for enhancing the production of yeast in continuous cultures [7] and for solving the problem of plasmid stability in continuous recombinant cultures [8]. To establish appropriate operating conditions, kinetic models are required that adequately describe the transient behavior of the culture being investigated. Such models have been developed previously [e.g. 9-11].

Biological reactors can be operated to achieve one of the following process objectives: utilization of nutrient (e.g., wastewater treatment), biomass production, production of a particular metabolite, or conversion of one chemical substance to another (bioconversion). The productivity of a continuous culture is determined by two variables, number and state of cells. To achieve high productivity or substrate utilization, it is desirable to have a large number of cells in the optimal state for the particular objective. A system can be manipulated to change the state of the cells through control of environmental conditions. However, in microbial growth processes, the optimal cell state for maximum growth of the cells is generally not the same as the optimal state for production of a desired metabolite. A solution to this problem is cycling environmental conditions (and thus cell

state) in the reactor. A large number of cells producing the desired metabolite could result. Previous efforts in cycling of conditions will be described later in this work.

As an example, an *E. coli* mutant (LCB898), which produces d-lactic acid in large amounts, was examined in this work. Under aerobic growth conditions this organism produces high amounts of biomass but insignificant amounts of d-lactic acid. Under anaerobic conditions it produces significant amounts of d-lactic acid and less biomass. If the goal is to maximize lactate production per reactor volume per time, one could simply operate the system under strictly anaerobic conditions. Alternatively, cycling dissolved oxygen level (and sometimes residence time) may improve productivity over that achieved by strict anaerobic operation. This improvement, in the case of constant residence time, is achieved by operating the system at higher flowrates. The higher flowrates are allowed by the aerobic (faster growth) portion of the cycle. Improvement by cycling is explained further in the chapter on cycling.

An unexpected problem that occurred while investigating this process was that of reversion of the genotype of *E. coli* LCB898 under anaerobic continuous operation. This reversion led the organism into a state where little d-lactic acid was produced. The proposed cycling of aeration also appears to be a new method for avoiding reversion or mutation of organisms under continuous operation.

This dissertation reports theoretical and experimental investigations on aeration cycling for *E. coli* LCB898. First, the general theoretical problem of optimizing a system undergoing cycling of environmental conditions will be formulated. A description of the particular microbial system under anaerobic and aerobic conditions, including modeling results, will then be given. Transient behavior of the system will then be discussed, followed by cycling predictions and experimental results. The question of reversion delay will subsequently be addressed. Conclusions will then be presented.

CHAPTER 2 THEORETICAL METHODS

2.1 Overview

An important job of the engineer is to determine the best way to operate a system. This usually will be the way that maximizes profitability within safety limits. It can involve anything from deciding how best to place workers on an assembly line to finding the optimal control setting for the temperature of a chemical reactor. The engineer will usually attack this problem by devising a mathematical formulation of the system and then use one or more optimization methods to design the best operation. The formulation will involve a statement of some sort of performance criterion to be optimized, along with descriptions of various equality and/or inequality constraints on the system. Examples of the performance criterion include maximizing the number of automobiles produced or minimizing the amount of byproduct from a reactor. Examples of constraints are the number of workers available at any given time or the maximum operating temperature of a reactor. Two kinds of constraints usually encountered are equality constraints, where some quantity of the system must always be equal to some other quantity, and inequality constraints, where some quantity of the system is bounded within certain value(s). The optimization method used will be selected by the engineer based on several factors including the system under study, available computing power, and others. Much work has been devoted to finding such optimization methods [e.g. 12-14].

A class of optimization problems exists where the equality constraints are not algebraic equations but differential equations. These are called optimal control problems [13, page 364]. Frequently, for this type of system, the engineer will want to vary the

control settings with time to maximize the productivity. Many methods have been developed for handling this kind of problem and one will be discussed later. Others can be found elsewhere [e.g. 15,16].

Continuous-flow reactor systems are typically operated at optimal steady-state conditions. However, several workers [17-23] have looked into operating systems at nonconstant conditions by cycling control variables around the optimal steady-state control settings and found improvement for certain performance criteria. Sometimes, though, there may be a need to examine systems where there is no true optimal steady-state control setting to cycle around [e.g. 8], and an imaginary intermediate state, only existing mathematically, may be used to design the best cyclic operation. As an example of this type of system one could imagine a reactor whose air pumps can be either on or off, with the on setting resulting in complete aeration. A mathematical model of the system may show that intermediate aeration is optimal for production. Then the engineer must decide how to best operate the air pumps to get optimal production.

In this chapter, the problem of determining optimal steady-state operation will be addressed first. The method used to determine optimal square-wave cycling will then be discussed, and finally a short description of some of the model-fitting techniques will be given.

2.2 Determination of Optimal Steady-state Operation

The typical system examined is one described by a set of differential equations:

$$\frac{dx_i}{dt} = f_i(x_1, x_2, \dots, x_n; u_1, u_2, \dots, u_r) \quad (1)$$

$$i = 1, 2, \dots, n$$

where $x_i =$ state variable i

$f_i =$ function describing the rate of change of variable i

$n =$ number of state variables

$u_i =$ control variable

$r =$ number of control variables

$t =$ time

Steady states for such a system are found by setting the right-hand side of equation 1 equal to a zero vector and solving (by algebraic manipulation or by use of numerical methods [24]) for the values of x_i . The optimum steady-state operating conditions (i. e. the optimal control settings) for such a system can be found by treating the resulting steady-state model equations as equality constraints, expressing necessary inequality constraints and stating a performance measure. Since the equations become algebraic at steady state, many methods of optimization can be used. If the steady-state model equations can be solved to yield an explicit expression of the performance measure as a function solely of the control variables (and if inequality constraints do not come into play), then classical theories of determining the optimal control settings involving setting the partial derivatives with respect to each control variable to zero and solving for the settings can be used [12]. Frequently an explicit expression cannot be found and other methods have to be used.

One can find the optimum steady-state settings by performing, when possible, a simple numerical search for the control values giving the maximum (or minimum) value of a stated performance measure, but it will frequently be necessary to use a different method when the system increases in complexity. As stated before, many methods exist. A few of them include quasi-Newton and conjugate gradient methods. These methods are described elsewhere [12,13].

2.3 A New Method of Determining Optimal Periodic Pulsing

This new method involves Carleman linearization of a general nonlinear system, expression of an explicit formula of the performance measure for pulsed cycling of the linearized system, and then a search, using the explicit performance measure, for the optimal settings for the system.

2.3.1 Carleman Linearization

Carleman linearization is a method of describing a general nonlinear system of first order differential equations in a linearized form. It was first introduced in 1932 [25] and has been applied to various problems in nonlinear system dynamics and control [17,26-34]. A brief overview of this method is presented here. This description was composed using earlier descriptions [17,35].

A restatement of equation 1 would be as follows:

$$\dot{\underline{x}} = \underline{f}(\underline{x}, \underline{u}) ; \quad \underline{f}(\underline{0}, \underline{0}) = \underline{0} \quad (2)$$

with $\underline{x} \in \mathbb{R}^n$ a vector of deviation state variables and $\underline{u} \in \mathbb{R}^m$ a vector of deviation control variables from a nominal steady state. This system is defined to have n dimensions. It is assumed that the functions f are differentiable up to order r at $\underline{0}$. Taylor expansion is then performed on system (2) and the monomials of order up to r are introduced as new variables. These monomials are then differentiated and terms of order up to r are retained. The result is a linear system in the new variables and is called the r th order Carleman linearization. For example, the system

$$\begin{aligned} \dot{x}_1 &= -x_1 + 3x_2 + x_2^2 \\ \dot{x}_2 &= -x_1^2 + 4u \end{aligned} \quad (3)$$

where the manipulated variable u is treated as a parameter, would have the following monomials approximated as variables w_j .

$$\begin{bmatrix} x_1 \\ x_2 \\ x_1^2 \\ x_1 x_2 \\ x_2^2 \end{bmatrix} \equiv \begin{bmatrix} w_1 \\ w_2 \\ w_3 \\ w_4 \\ w_5 \end{bmatrix} \quad (4)$$

The second order Carleman linearization for the system in equation 3 is

$$\dot{\underline{w}} = \begin{bmatrix} -1 & 3 & 0 & 0 & 1 \\ 0 & 0 & -1 & 0 & 0 \\ 0 & 0 & -2 & 6 & 0 \\ 4u & 0 & 0 & -1 & 3 \\ 0 & 8u & 0 & 0 & 0 \end{bmatrix} \underline{w} + \begin{bmatrix} 0 \\ 4u \\ 0 \\ 0 \\ 0 \end{bmatrix} \quad (5)$$

The computation of the necessary partial derivatives for expressions of higher order Carleman linearization can be tedious, and, in the case of elaborate differential equations, can lead to errors. A new program written in Mathematica [36] has been developed for computing the necessary Carleman matrices and vectors and is presented in Appendix A, along with an associated program used to compute necessary Kronecker products (the Kronecker package offered by Mathematica is not usable for this type of problem). This program, using the capabilities of Mathematica, does not require the user to provide necessary derivatives; it computes the derivatives analytically. A description of the algorithm used in the program was given by Lyberatos and Svoronos [17], but will also be presented here.

Let \otimes represent Kronecker multiplication. The Taylor series expansion about $\underline{x} = \underline{0}$ can be expressed as

$$\dot{\underline{x}} = \sum_{k=1}^{\infty} A_{1k} x^{[k]} + A_{10} \quad (6)$$

where $\underline{x}^{[k]} = \underline{x} \otimes \underline{x} \otimes \dots \otimes \underline{x}$ (k terms)

and \otimes represents Kronecker multiplication

e.g. [27, page 11] if A is an $m \times n$ matrix and B is a $p \times q$ matrix then

$$A \otimes B = \begin{pmatrix} a_{11}B & a_{12}B & \dots & a_{1n}B \\ a_{21}B & a_{22}B & \dots & a_{2n}B \\ \vdots & \vdots & \ddots & \vdots \\ a_{m1}B & a_{m2}B & \dots & a_{mn}B \end{pmatrix}$$

The resulting matrix has the dimensions $mp \times nq$.

The following system then comprises the r th order Carleman approximation to the original system

$$\begin{bmatrix} \dot{\underline{x}} \\ \dot{\underline{x}}^{[2]} \\ \vdots \\ \dot{\underline{x}}^{[r]} \end{bmatrix} \equiv \underline{\dot{w}} = \begin{bmatrix} A_{1,1} & A_{1,2} & A_{1,3} & \dots & A_{1,r} \\ A_{2,0} & A_{2,1} & A_{2,2} & \dots & A_{2,r-1} \\ 0 & A_{3,0} & A_{3,1} & \dots & A_{3,r-2} \\ 0 & 0 & A_{4,0} & \dots & A_{4,r-3} \\ \vdots & \vdots & \vdots & & \vdots \\ 0 & 0 & \dots & A_{r,0} & A_{r,1} \end{bmatrix} \underline{w} + \begin{bmatrix} A_{1,0} \\ 0 \\ 0 \\ \vdots \\ 0 \end{bmatrix} \quad (7)$$

where $A_{i,j} = I_n \otimes A_{i-1,j} + A_{1,j} \otimes I_{n^{i-1}}$

$I_g = g \times g$ Identity Matrix

The above system will have a dimensionality of $n + n^2 + n^3 + \dots + n^r$. Since the vector \underline{w} will contain monomial redundancies (e.g. $x_1 x_2$ and $x_2 x_1$), the system should be simplified. This is done by eliminating rows that correspond to the same monomial and adding the corresponding columns together. The Carleman system will then have a

dimensionality of $\sum_{j=1}^r {}_{n+j-1}C_j$ or equivalently $\sum_{j=1}^{\min(n,r)} {}_rC_j {}_nC_j$ where ${}_mC_q$ is the number of combinations of m objects taken q at a time $\left({}_mC_q = \frac{m!}{q!(m-q)!} \right)$ [14,23].

2.3.2 Performance Measure Calculation

In this section we will develop a method to determine an explicit performance measure for a Carleman linearized system when we cycle our controls on a system between two fixed settings. Consider the waveform in figure 1. In this figure u_δ and u_ρ are the two control settings available, and u_i represents a fixed intermediate (though not necessary realistic) control setting. These settings can be vectors or scalars. δ and ρ represent the vector or scalar deviations of the two respective control settings from u_i . T represents the period of the cycle, and ϵ represents the fraction of the period spent at one of the control settings (u_δ).

This problem is very similar to one looked at by Lyberatos and Svoronos [17]. In that work, they looked at square-wave cycling around an optimal steady state. The deviations from that state were allowed to vary. The intermediate state mentioned above is analogous to the optimal steady state that Lyberatos and Svoronos examined. Additionally, in the present problem, the deviations from the intermediate are fixed. Thus, the previous mathematical development that they performed can be used to a large extent here with only minor changes. The main parts of their derivation will also be given here.

Again, the problem to be examined is (in deviation variables)

$$\dot{\underline{x}} = \underline{f}(\underline{x}, \underline{u}); \quad \underline{f}(\underline{0}, \underline{0}) = \underline{0} \quad (8)$$

where $\underline{f}(\underline{x}, \underline{u})$ is analytic in \underline{x} at $\underline{0}$ for all admissible \underline{u} vectors (or scalars). The \underline{u} vectors (scalars) are treated as staying constant for either part of the cycle. Taylor

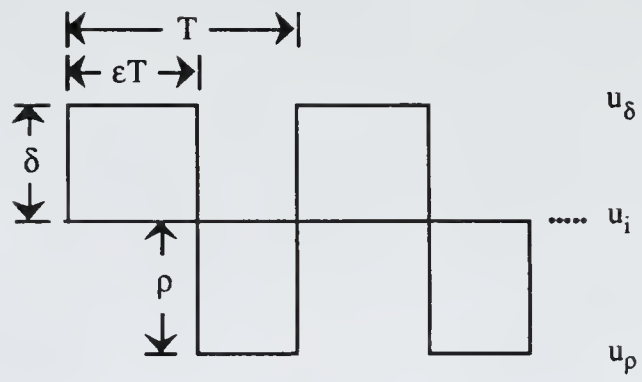


Figure 1. Section of control waveform being analyzed

expansion around $\underline{x}=0$ is performed on this system and the n th order Carleman linearization is obtained

$$\dot{\underline{w}} = \begin{cases} S(\delta)\underline{w} + \underline{z}(\delta) & t \in [nT, (n+\epsilon)T) \\ S(\rho)\underline{w} + \underline{z}(\rho) & t \in [(n+\epsilon)T, (n+1)T) \end{cases} \quad (9)$$

The performance measure under cyclic conditions can be represented as the following:

$$J = \frac{1}{T} \int_0^T P(\underline{x}, \underline{u}) dt \quad (10)$$

where J =time-averaged performance measure

T =period of the cycle

P =instantaneous performance measure

It is assumed that $P(\underline{x}, \underline{u})$ is analytic in \underline{x} at $\underline{0}$, in which case it can be linearized.. This is done by Taylor series expansion around $\underline{x}=0$ and is cast in terms of the Carleman coordinates \underline{w} . The performance measure then takes the representation

$$J = \frac{1}{T} \int_0^T [r_o(\underline{u}) + \underline{r}'(\underline{u})\underline{w}(t)] dt \quad (11)$$

where ' represents the matrix transpose.

In the derivation that follows, the following identities, which apply to any invertible $n \times n$ matrices and were proved by Lyberatos and Svoronos [17], will be needed

$$(\mathbf{I}_n - \mathbf{A}\mathbf{B})^{-1} \mathbf{A} = \mathbf{A}(\mathbf{I}_n - \mathbf{B}\mathbf{A})^{-1} \quad (12)$$

$$(\mathbf{I}_n - \mathbf{A}\mathbf{B})^{-1} - \mathbf{A}(\mathbf{I}_n - \mathbf{B}\mathbf{A})^{-1} \mathbf{B} = \mathbf{I}_n \quad (13)$$

$$(I_n - A)(I_n - BA)^{-1}(I_n - B) = (I_n - B)(I_n - AB)^{-1}(I_n - A) \quad (14)$$

Now, equation 9 can be integrated to give the following ultimate periodic solution:

$$\underline{w}(t) = \begin{cases} e^{S(\delta)(t-nT)} \underline{w}^0 - \left[I - e^{S(\delta)(t-nT)} \right] S(\delta)^{-1} \underline{z}(\delta) & \text{for } t \in [nT, (n+\epsilon)T) \\ e^{S(\rho)(t-(n+\epsilon)T)} \underline{w}^\epsilon - \left[I - e^{S(\rho)(t-(n+\epsilon)T)} \right] S(\rho)^{-1} \underline{z}(\rho) & \text{for } t \in [(n+\epsilon)T, (n+1)T) \end{cases} \quad (15)$$

Defining

$$\begin{aligned} D &= e^{S(\delta)\epsilon T} \\ R &= e^{S(\rho)(1-\epsilon)T} \end{aligned} \quad (16)$$

\underline{w}^0 and \underline{w}^ϵ can be expressed as:

$$\underline{w}^0 = -[I - RD]^{-1} \left[[R - RD]S(\delta)^{-1} \underline{z}(\delta) + [I - R]S(\rho)^{-1} \underline{z}(\rho) \right] \quad (17)$$

$$\underline{w}^\epsilon = -[I - DR]^{-1} \left[[I - D]S(\delta)^{-1} \underline{z}(\delta) + [D - DR]S(\rho)^{-1} \underline{z}(\rho) \right] \quad (18)$$

From (15) it can be seen that

$$\underline{w}^\epsilon = D\underline{w}^0 - [I - D]S(\delta)^{-1} \underline{z}(\delta) \quad (19)$$

and

$$\underline{w}^0 = R\underline{w}^\epsilon - [I - R]S(\rho)^{-1} \underline{z}(\rho) \quad (20)$$

Using equation 15, the cycle average performance measure given in equation 11 can be expressed as

$$\begin{aligned}
 J(T, \epsilon, \delta) = & \frac{1}{T} \underline{r}'(\delta) \left[e^{S(\delta)\epsilon T} - I \right] S(\delta)^{-1} \underline{w}^0 + \\
 & \frac{1}{T} \underline{r}'(\rho) \left[e^{S(\rho)(1-\epsilon)T} - I \right] S(\rho)^{-1} \underline{w}^\epsilon - \\
 & \frac{1}{T} \underline{r}'(\delta) \left[S(\delta)\epsilon T + I - e^{S(\delta)\epsilon T} \right] S(\delta)^{-2} \underline{z}(\delta) - \\
 & \frac{1}{T} \underline{r}'(\rho) \left[S(\rho)(1-\epsilon)T + I - e^{S(\rho)(1-\epsilon)T} \right] S(\rho)^{-2} \underline{z}(\rho) + \\
 & r_0(\delta)\epsilon + r_0(\rho)(1-\epsilon)
 \end{aligned} \tag{21}$$

Using that $S(\delta)^{-1}$ commutes with D and $S(\rho)^{-1}$ commutes with R along with equations 19 and 20, equation 21 can be rewritten as:

$$\begin{aligned}
 J(T, \epsilon, \delta) = & \frac{1}{T} \underline{r}'(\delta) S(\delta)^{-1} \left[\underline{w}^\epsilon - \underline{w}^0 - \epsilon T \underline{z}(\delta) \right] + \\
 & \frac{1}{T} \underline{r}'(\rho) S(\rho)^{-1} \left[\underline{w}^0 - \underline{w}^\epsilon - (1-\epsilon) T \underline{z}(\rho) \right] + \\
 & r_0(\delta)\epsilon + r_0(\rho)(1-\epsilon)
 \end{aligned} \tag{22}$$

Using equations 12-14, equation 17 and equation 18 the following is obtained:

$$\begin{aligned}
 \underline{w}^\epsilon - \underline{w}^0 = & (I - R)(I - DR)^{-1}(I - D) \\
 & \left[S(\rho)^{-1} \underline{z}(\rho) - S(\delta)^{-1} \underline{z}(\delta) \right]
 \end{aligned} \tag{23}$$

Finally, from equations 22 and 23 follows

$$\begin{aligned}
J(T, \varepsilon, \delta) = & -\left[\underline{r}'(\rho)S(\rho)^{-1} - \underline{r}'(\delta)S(\delta)^{-1} \right] \\
& \frac{(I - R)(I - DR)^{-1}(I - D)}{T} \left[S(\rho)^{-1} \underline{z}(\rho) - S(\delta)^{-1} \underline{z}(\delta) \right] \\
& + \varepsilon \left[r_0(\delta) - \underline{r}'(\delta)S(\delta)^{-1} \underline{z}(\delta) \right] \\
& + (1 - \varepsilon) \left[r_0(\rho) - \underline{r}'(\rho)S(\rho)^{-1} \underline{z}(\rho) \right]
\end{aligned} \tag{24}$$

This is the form of the cyclic average performance measure that is the most useful.

2.4 Model Fitting with Nonlinear Least Squares Methods

This topic is not directly related to the above discussion which led to an expression for the performance measure, but this fitting, used in some parts of this work, is an optimization technique and belongs in a chapter discussing the theory behind the overall project. The type of problem that is being considered here is one where data are being collected from some experiment and parameters for a model have to be determined. One can manipulate the data in some fashion, such as semilog or log-log plotting, to find necessary parameters, but, if no apparent manipulation exists for the proposed model, then some other method must be used. One can attack such a problem by varying the parameters of a model and determining how good the fit is to the data with those guessed parameters. One can use methods of optimization to find the best way to vary the parameters. The method of choice was Levenberg-Marquardt optimization due to its wide use in prepackaged computer programs such as MATLAB and Kaleidagraph. A description of the problem being examined, along with a short description of Levenberg-Marquardt optimization, is appropriate here. A further description of the method of optimization used can be found in numerical analysis texts such as Numerical Recipes [24].

Let us consider an experiment where data are taken at several times during the run. In figure 2, an example experiment where three different types (x_1 , x_2 , and x_3) of data are collected is shown .

In an experiment like that shown in figure 2, the experimenter collected all three different types of data at the same instant. This type of collection is preferable for later computational purposes, but is not necessary with the method to be described. In other words, if one of the data types is difficult to collect simultaneously with the other data types, then the following analysis still applies, but the computational effort may be increased.

Let it be assumed that a general model for a system like that shown in figure 2 is given in equation 2, but the vector of ordinary differential equations is also a function of parameters. In other words

$$\dot{\underline{x}} = \underline{\varphi}(\underline{x}, \underline{p}) ; \quad \underline{x}(0) = \underline{x}_0 \quad (25)$$

where \underline{p} =the vector of parameters for the model

For such a system, the parameter vector \underline{p} and, occasionally, the initial condition vector \underline{x}_0 (or just some parts of either of these vectors) must be determined. For any set of guessed parameters and/or the initial conditions, the model equations can be integrated, either analytically or by numerical methods such as Runge-Kutta integration, to show the predictions for that set of guesses. The model predictions for this problem would be computed for each time instant that data is available for comparison.

A performance measure for "goodness" of model fit then can be described as

$$P(\underline{x}_d, \underline{\hat{x}}, \underline{q}) = \sum_{j=1}^{nsp} \sum_{i=1}^{ndt} q_i \left(x_{d_i}(j) - \hat{x}_i(j) \right)^2 \quad (26)$$

where P =performance measure

$x_{d_i}^{(j)}$ =one type of data point at time instant j (\underline{x}_d is a vector of all data)

$\hat{x}_i^{(j)}$ =corresponding model prediction for x_{d_i} ($\underline{\hat{x}}$ is a vector of predictions)

q_i =weight of one type of measurement (\underline{q} is the vector of the weights)

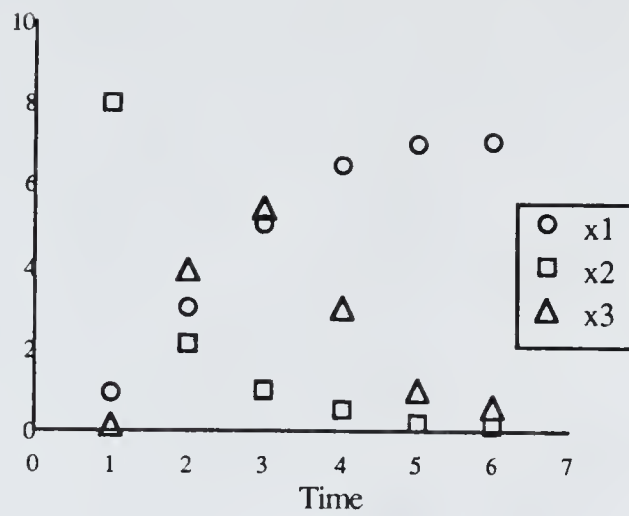


Figure 2. An example experiment where, at any time point, three different types of data (x_1 , x_2 , and x_3) are collected.

nsp=number of sampling points

ndt=number of data types

Our goal is to minimize the stated performance measure. The weighting factors q serve two purposes. First, they can be used if one type of measurement is more "trusted" than another. For example, one may give more weight to a simple measurement of temperature taken with a thermistor than to a viscosity measurement taken with a poor viscometer. This use of the weighting factor is going to be subject to the good judgment of the experimenter and should be handled with caution. The other, more important, purpose of the weighting factor is as a normalization constant. Alternative forms of the performance measure, such as summing the logarithms of the squared residuals instead of the actual squared residuals, $(x_{d_i} - \hat{x}_i)^2$, can also be useful for normalizing.

Once the performance measure is expressed in the form of equation 26, the optimization method of Levenberg and Marquardt can be used. This method is an elegant combination of steepest gradient and inverse Hessian methods of optimization. The general algorithm involves use of steepest descent methods far from the minimum, and then, as the minimum becomes more closely approximated, a smooth transition to the inverse Hessian methods [24, page 523-524]. A prepackaged program was used in this work.

CHAPTER 3 EXPERIMENTAL METHODS

3.1 Organism Description

The organism used in this project was *Escherichia coli* strain LCB898. The original culture was obtained from Dr. L.O. Ingram, Department of Microbiology and Cell Science, University of Florida. The genotype is *thr1 leu6 ton A21 str lac Y1 sup E44 pfl1* [37]. The important aspect of this organism is its mutation in the *pfl* gene causing lack of expression of that gene. This is the gene for the production of pyruvate formate-lyase (pfl), an enzyme which is primarily responsible for the conversion of pyruvate to acetyl-CoA and formate under anaerobic conditions.

The pertinent biochemical pathways for this organism are shown in figure 3 which was prepared based on the diagram in Pascal [38]. It points out the following important features: lack of pfl activity [37], anaerobic inhibition of the pyruvate dehydrogenase (PDH) pathway [38,39], and anaerobic induction of the d-lactate dehydrogenase (LDH) pathway. Further descriptions of this organism's metabolism will be given in later chapters.

The culture was maintained on plates of rich broth agar with the following composition in deionized water [40]: 10 g/l tryptone , 5 g/l sodium chloride , 1g/l yeast extract , and 15 g/l agar . The agar was prepared by mixing the ingredients together in water, heating the solution to near boiling while stirring, and then pouring approximately 12 ml aliquots of the molten agar into individual 16X125 mm tubes. These tubes were capped and autoclaved at 121°C for 30 minutes. Subculturing was performed on a monthly

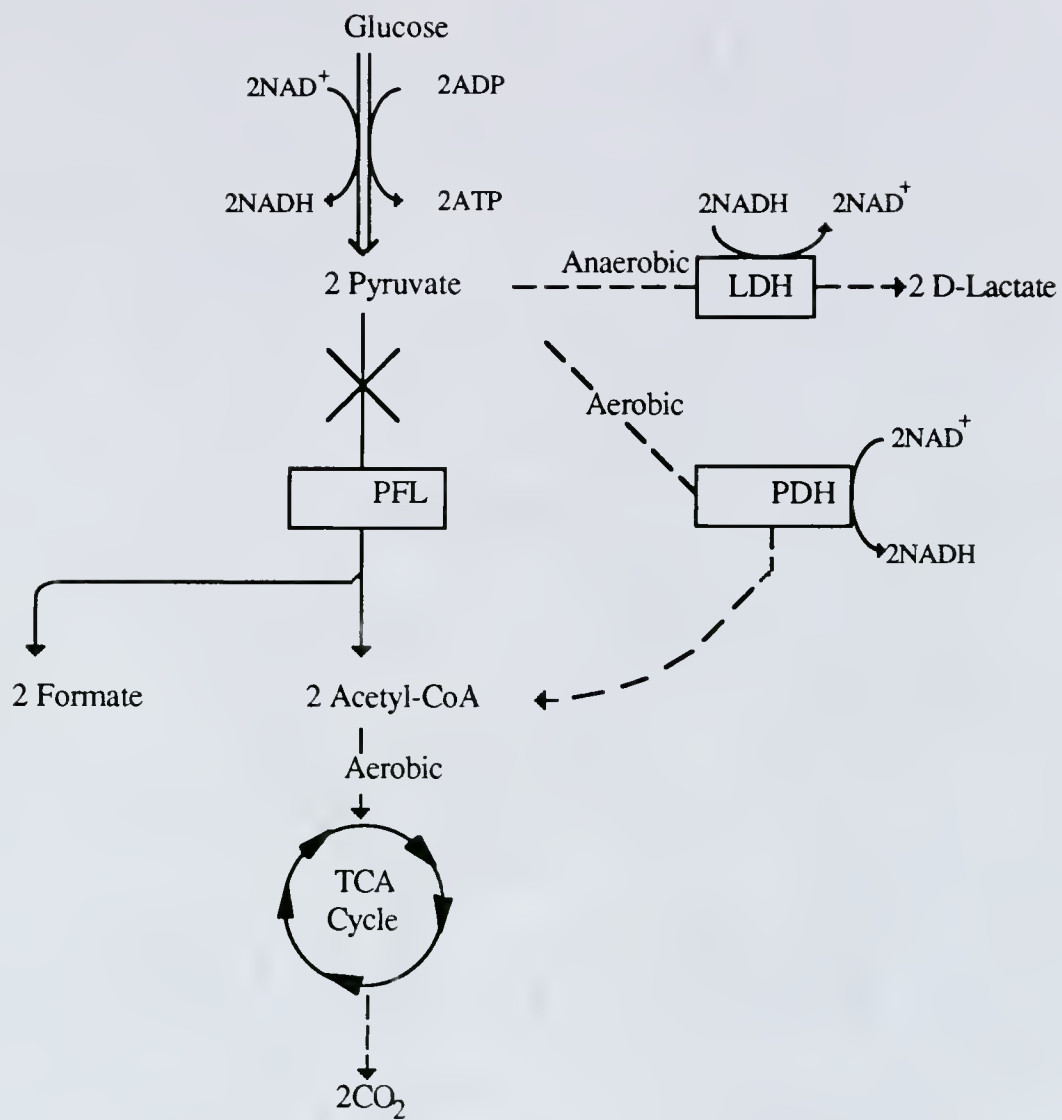


Figure 3. Pertinent Biochemical Pathways in *E. coli* LCB898.

basis with the freshly inoculated plates being incubated at 37°C in a Fisher Model 255D incubator for 24 hours then being stored in a refrigerator.

3.2 Analytical Methods

3.2.1. Biomass and Cell Number Determination

The amount of biomass in the system was determined by two different methods, cell counting and spectrophotometric turbidity (actually absorbance) measurement. The cell counting involved serial dilution of a culture aseptically withdrawn from the culture vessel. The dilutions were made in 8.5 g/l solution of sodium chloride in water[41, p. 434] and the agar used had the same composition as the rich broth agar used in culture storage. Preparations involved pouring several 9 ml aliquots of the saline solution into 16X125 mm tubes and pouring several 99 ml aliquots into bottles. Additionally, some empty capped tubes were also prepared. These were all autoclaved for approximately 30 minutes. Sterile, disposable, individually-wrapped borosilicate glass pipets (Fisher pipets) were used in this procedure. A sample procedure for serial dilution and colony counting of a culture is given in the two following paragraphs. The serial dilution procedure should be performed under a laminar flow hood.

This sample procedure is designed for experiments where cell counts are expected to be between thirty million and three hundred million cells/ml. Since it is desired to dilute to 30-300 cells/ml, it is necessary to dilute samples 100000X, one million X, and ten million X for later counting. Obviously this method can be modified for other expected cell counts. Approximately 15 minutes before a sample is to be taken, three agar tubes are placed in a boiling water bath in order to melt the tube contents. Immediately before the measurement, the tubes are withdrawn from the water bath and stored in the laminar flow hood, along with a propipettor, a pack of sterile gloves, three labeled sterile disposable Fisher petri dishes, an appropriate number of pipets, dilution bottles, and tubes. A fresh

pipet should be used after each dilution step. The sample is removed from the culture (if from a chemostat, the effluent sidearm tube (to be described later) is flamed and approximately 10 ml are allowed to flow out into a presterilized empty tube; if from a flask, the cap is removed under the laminar flow hood and a sample is aseptically pipetted out) and one ml is pipetted from the tube or culture flask into a ninety nine ml saline bottle. This bottle is then well shaken. At this point the original culture has been diluted 100 X. A one ml sample is then aseptically transferred from the first dilution bottle to another ninety nine ml saline bottle. Again, this bottle is well shaken. The culture sample has now been diluted 10000 X. A one ml sample is then aseptically transferred to a 9 ml sample tube and the tube is well shaken. 2 ml of the 100000X diluted sample is then taken. One ml is put into the next 9 ml sterile tube and the other milliliter is pipetted onto the appropriately labeled petri dish. One tubeful of agar, when it becomes lukewarm, is then poured into the petri dish and the dish is subsequently mildly swirled in order to provide a more even distribution of colony forming units. The new 1 million X dilution tube (now a 10 ml tube with the one ml of sample added) is handled in the same way as the previous 100000X tube. Lastly, the ten million X dilution tube has one ml transferred to the appropriate petri dish. The agar in the petri dishes is allowed to solidify. The dishes are then inverted and incubated at 37°C for 24 hours.

Upon sufficient incubation, the petri dishes are taken out of the incubator and are individually placed on a Quebec darkfield colony counter. A hand-held colony counter is used to ensure accounting. A marking pen is used in order to make dots under each colony appearing on the plate so that no colony gets counted twice. When counting, care must be taken to count colonies on the edge of the petri dish and to check if some of the colonies are growing directly underneath another colony. The results of each plate count are recorded, and the cell counting procedure is finished.

Biomass concentration was measured spectrophotometrically using a Milton Roy Spectronic 20D spectrophotometer. The procedure for this measurement is relatively

simple. The spectrophotometer is first set for operation at 550 nm. Deionized water is then added to a clean cuvet, the cuvet is put into the sample chamber, and zeroing is performed. The cuvet is then removed and the water is poured and then shaken out of the cuvet. Some sample is then added and the cuvet is swirled. This sample is used to eliminate the effects of residual water. At this point, the first amount of sample is poured out and at least three ml of fresh sample are added. The cuvet is then placed into the sample chamber again and an absorbance reading is then taken and recorded. If the absorbance reading is above 0.4, appropriate dilution is performed. For example, in more dense samples, three ml of deionized water would be added to one ml of sample for a 1/4 dilution. During the aerobic operation experiments, 1/16 dilutions were necessary towards the end of the batch runs and during continuous steady states.

In order to correlate the spectrophotometric absorbance reading to an actual dry mass concentration, a calibration curve has to be obtained. A large (approximately 200 ml) sample is taken from the reactor (at the end of a batch run). Eighty ml each of 75%, 25%, and 12.5% dilutions are made in three separate beakers. The spectrophotometric absorbances of each of these samples is then measured. In more turbid samples, when the absorbance readings are significantly above 0.4, the diluted samples are used for computation of the absorbance. Fifty ml of each of these dilutions are pipetted into appropriately labeled centrifuge tubes. The tubes are then placed into a Precision Universal Centrifuge set at 2000 rpm for 60 minutes. The supernatant is then decanted, the remaining contents are washed with approximately 5 ml of deionized water, and the tubes are centrifuged for 20 more minutes. The supernatant was pipetted off and the remaining contents are then emptied into preweighed and labeled petri dishes for drying. These dishes are dried at 105°C for 48 hours and the contents are weighed. In this manner, a calibration curve was prepared. The calibration curve is shown in figure 4.

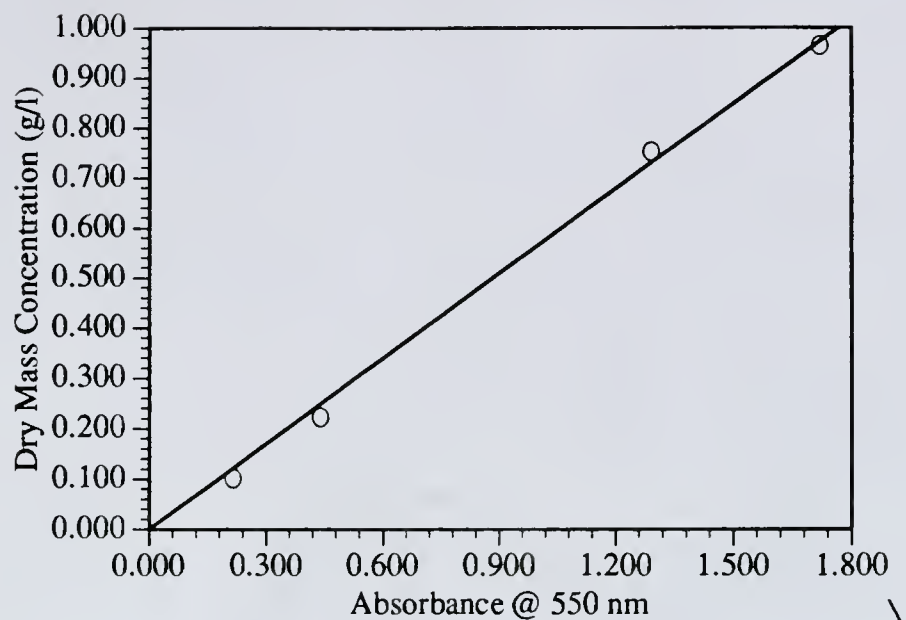


Figure 4. Dry Mass Calibration Curve. The linear fit shown is $\text{Dry Mass Concentration (g/l)} = 0.565 \times \text{Absorbance}$ with a squared regression coefficient of 0.998

3.2.2 Glucose Analysis

The device used for glucose concentration determination was an Analytical Research Model 110 Glucose Monitor. The analyzer's main component is the electrochemical sensor on which an immobilized glucose oxidase membrane is mounted. This enzyme catalyzes the reaction between glucose and oxygen to produce hydrogen peroxide. Hydrogen peroxide is detected by the sensor and an electrical signal proportional to glucose concentration is produced [42, p. 52]. The analyzer's pumps will take a small (approximately 1.5 ml) aliquot of the sample through a port and pass most of it by the membrane, leaving only a small plug of fluid for the actual analysis. This analysis is performed in approximately three minutes, at which time almost all the glucose will have reacted. Usually three aliquots are measured and the results are averaged. The following paragraph gives a brief description of the actual procedure.

In the description that follows, one cycle is defined as the time between glucose analyzer samplings. The glucose analyzer is operated as follows. Glucose calibration solutions of appropriate concentrations (operator's judgment) are prepared and allowed to dissolve for at least 2 hours. Fifty percent dilutions of calibrations should also be prepared. For example, if calibration is to be made with a 2 g/l glucose solution, a 1 g/l glucose solution should also be prepared. Additionally, the glucose analyzer is switched from idle to blank for 2 hours before calibrations are to be done. After these two hours the calibration tube is placed in 100 ml of fresh water and the switch is set to "Cal". For the next 15 minutes, water is allowed to pump through the system. After this 15 minutes, the glucose analyzer is zeroed by setting the zero dial so that the peak readout during the portion of the cycle between the ready light indicator coming on and the following sampling reads ".000" g/l. One more cycle is observed to check for appropriate zeroing. At this point, calibration of the glucose analyzer is performed. The sample tube is placed in the appropriate calibration solution. The switch is then set to "Sample". Three cycles are allowed to follow and the calibration is completed by setting the cal dial so that the peak

value of glucose read during the portion of the cycle between the ready light turning on and the following sampling reads out the calibration value of the glucose solution. This calibration is then checked with a 50% solution of the calibrator solution by putting the sample tube into the appropriate calibrator solution. Three samples are taken and calibration is checked by reading the appropriate peak value. If calibration is appropriate, samples can then be measured for glucose content. Four samplings are taken, with the last three peaks being recorded as data. Recalibration is performed once every hour that sampling is done. If the calibration stays relatively accurate, a calibration check with 50% calibration solution need not be completed. If glucose analysis results are below 1/2 of the top calibration value, recalibration is performed at one half the calibration value.

3.2.3 d-Lactate Measurement

The measurement of d-lactate was based on a modification of Sigma procedure 816-UV, which was designed for measurement of l-lactate. The major modification to this method was the use of d-lactic dehydrogenase (Sigma L-2395) instead of l-lactic dehydrogenase, provided with the original Sigma kit. The principle of this test is explained below.

In the metabolism of *E. coli* and most other chemoheterotrophic bacteria, pyruvate is converted by lactate dehydrogenase into lactate. This, however, is a reversible reaction. In other words, the same enzyme can be used to convert lactate into pyruvate. The conversion of d-lactate to pyruvate will be accompanied by a reduction of one molecule of NAD^+ into NADH. NADH shows strong spectrophotometric absorbance at 340 nm, whereas NAD^+ does not absorb at this wavelength. Thus, using the indirect method of spectrophotometrically measuring NADH in a mixture, the amount of d-lactate can be determined. The problem of backconversion of the pyruvate into d-lactate is handled by adding hydrazine to the mixture. Hydrazine reacts with the pyruvate and forms a complex that d-lactic dehydrogenase cannot convert back into d-lactate.

The experimental method involved preparation of a calibration curve of d-lactate concentration against spectrophotometric absorbance at 340 nm. The spectrophotometer used was a Milton Roy Spectronic 20D. A solution of approximately 200 mg/l d-lactic acid (Sigma L0625) or the Lithium salt (Sigma L1000) in deionized water (approximately in this case means that the experimenter knows the exact concentration within experimental accuracy, but it is not necessarily exactly 200 mg/l in concentration) was prepared when calibration was performed. When the lithium salt was used, adjustments were made for the weight of a lithium atom as opposed to a hydrogen atom in the free acid form. Dilutions of approximately 87.5%, 75%, 62.5%, 50%, 37.5% and 25% were made of this solution. Additionally, a solution of 2.50 g NAD⁺ (Sigma N7004) and 500 ml Glycine buffer (Sigma 826-3) added to 1 liter of water was prepared. The mixture will be referred to as "NAD solution" from this point. Since the NAD solution must be made immediately before the lactate measurement, the actual amount prepared would depend on the number of lactate samples to be analyzed. One would prepare 3 ml of the NAD solution (2 ml of water, 1 ml of glycine, and 5 mg of NAD⁺) per sample, plus at least one extra 3 ml solution for preparation of a blank. 2.8 ml aliquots of NAD solution were pipetted into the appropriate number of labeled test cuvetts plus one blank cuvette. Each labeled test cuvette had 0.2 ml of the corresponding full strength or diluted calibration solution added and mixed. Additionally, the blank cuvette had 0.2 ml of deionized water added and mixed. The 340 nm spectrophotometric absorbances of each test cuvette against the blank were then measured. This value, which will be referred to as the zero absorbance, was used to compensate for cuvette-to-cuvette variability.

Sixty units of d-lactic dehydrogenase were then added to each of the test cuvetts and the blank cuvette. The cuvetts were then incubated at 37°C for 30 minutes. The new absorbances against the blank were then measured, and the differences between the new absorbances and the corresponding zero absorbances were then calculated and plotted against the corresponding test lactate concentrations. The curve obtained is shown in figure

5, along with the results of a least squares fit to the data. Although the substance measured is referred to as d-lactate throughout this work, the term d-lactate is actually slightly inaccurate. D-lactic acid is the substance actually being measured. Frequently these The relatively high correlation coefficient indicates that the assumption of a linear relationship in this range of test lactate concentrations is satisfactory.

The procedure for measuring unknown lactate concentrations is essentially the same as that for measuring the net absorbances of the calibration solutions. The key differences will only be described. First, the unknowns must be diluted however many times to where their lactate concentration is in the range between 50 and 200 mg/l. The amount of dilution is usually based on previous methods, but for the first experiments this had to be determined by trial and error. Second, this dilution is also useful in diluting the effects of any residual biomass or other substances in the filtered samples on the spectrophotometric readings. Any remaining residuals would be taken into account by the zero absorbance measurement. These residuals will not affect the net absorbance measurements as the enzyme used is specific for d-lactate. Last, least, and most obvious, the calibration curve is used to determine unknown concentrations, as opposed to the preparation of the curve when calibrating.

3.2.4. Other Analyses

Other measurement methods were used in this research. These will only be mentioned briefly as they were only seldomly used. These include amino acid analysis and ethanol analysis. The amino acid measurements were made by an outside laboratory (Interdisciplinary Center for Biotechnology Research, University of Florida, Gainesville, Florida) on an amino acid analyzer. These amino acid measurements were used solely to determine whether or not leucine or threonine nutritional limitations were encountered. Ethanol concentrations, when measured, were determined using Sigma kit 332-UV.

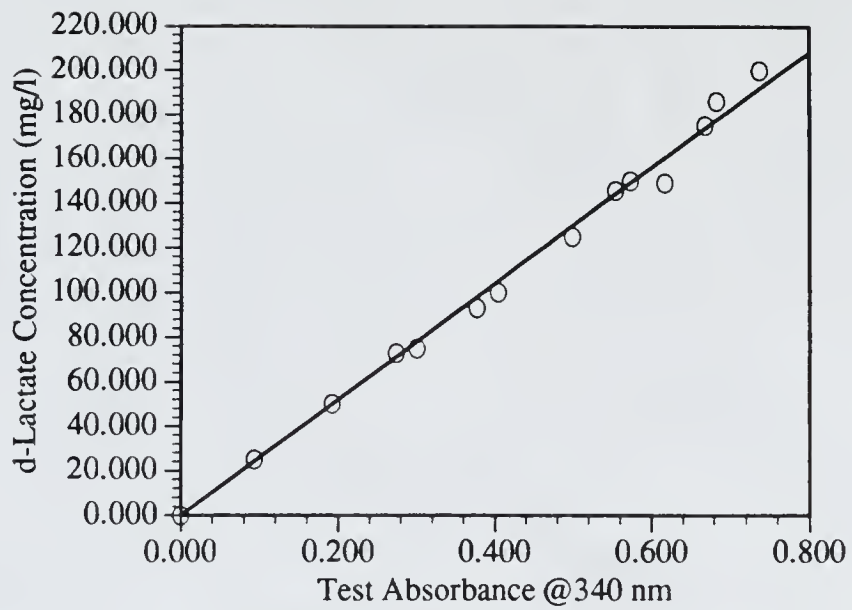


Figure 5. d-Lactate Calibration Curve. The linear fit shown is $\text{d-Lactate Concentration (mg/l)} = 260.144 \times \text{Absorbance}$ with a squared regression coefficient of 0.998

3.3 Feed Medium Composition

Many factors had to be considered in the design of the feed composition and preparation. The first consideration was whether to use a complex medium such as Luria broth or a minimal medium. A glucose minimal medium was chosen as the probability of interference of feed components with measurements is lower. Once a minimal medium was chosen, other considerations had to be taken into account. These included pH, buffering, nitrogen requirements, trace minerals and metals, genetic deficiencies, substrate amount, and interactions between these components during heat sterilization. These interactions must be considered when deciding which component solutions to autoclave in the same flask. Ideally, each component solution should be autoclaved separately. However, in order to maintain sterility during the mixing process, there should be as few separate flasks as possible. Thus, given the considerations described below, a design was chosen inbetween these two extremes. A general consideration given was the separation of inorganic from organic components in order to avoid production of toxic byproducts during autoclaving. Finally, all the ingredients were prepared in deionized water.

The medium should be buffered with target pH 7. Buffering lowers the amount of base needed to maintain pH during the experiments. M9 medium [41, p. 431 and 43, p. A.3] satisfies this requirement. Additionally the nitrogen and some of the trace mineral requirements are satisfied by the use of M9 medium. M9 medium includes sodium phosphate dibasic, potassium phosphate monobasic, sodium chloride, ammonium chloride, calcium chloride and magnesium sulfate. The exact amounts used will be given later. Miller [41, p. 431] suggests separate autoclaving of calcium chloride and of magnesium sulfate from the rest of the salts.

Other trace metals were added to the medium as suggested elsewhere[40,44,45]. These included selenium oxide, hydrated ferrous sulfate, hydrated ammonium molybdate, and hydrated manganese sulfate . The amounts used will be given later. It was suggested these should be sterilized by filtration, but sterility was a major concern in this work, so

these compounds were autoclaved together in solution. Bridson and Brecker [46] suggested autoclaving metals separately from phosphates in order to avoid precipitation.

Genetic deficiencies of *E. coli* LCB898 had to be accounted for in the medium formulation. The genotype mentioned in the organism description indicates requirements for threonine, leucine, and thiamine. Additionally, as the pyruvate-formate lyase gene is mutated, acetate may be required to satisfy some biosynthetic requirements of the cell. Several batch experiments were performed under both aerobic and anaerobic conditions in order to determine the amounts of these chemicals required to insure glucose limitation of growth. Amino acid analysis was performed on a sample of the batch at the point where growth was no longer seen to see if any residual amino acids were left in solution. The final amounts chosen were those that allowed glucose limited growth up to at least a concentration of 4 g/l glucose in the medium. This was indicated by the cessation of growth when glucose became exhausted. Miller [41, p. 431] suggests separate autoclaving of the amino acids and vitamin from the M9 salts, and Bridson and Brecker[46] suggest separate autoclaving of the amino acids from the carbohydrates to avoid Maillard reactions. Thus the amino acids and vitamin solutions were autoclaved together separately from all other components, and, to avoid any other possible feed reactions, the acetate was also separately autoclaved.

The final feed component to be discussed is the growth limiting substrate of glucose. Glucose (Sigma) was used as the limiting substrate because of its relatively straightforward measurement on the glucose analyzer previously mentioned. A main feed concentration of 4 g/l was decided on for several reasons. A feed glucose concentration too low would make batch growth measurements difficult, as the analyzer available is somewhat inaccurate at measuring glucose concentrations below 100 mg/l, and d-lactate measurements below 25 mg/l are also of questionable accuracy. Another reason to avoid low glucose concentrations is the desirability of visible turbidity in the reactor system. For example, in a batch growth experiment, the onset of visible turbidity serves as a marker for

the beginning of more frequent measurements. This onset is still well before glucose exhaustion and indicates the approximate point where glucose, d-lactate, and biomass concentrations begin to measurably deviate from the starting values. On the other hand high glucose concentrations also are not beneficial. First of all, autoclaving of high glucose concentration solutions will lead to increased caramelization of the feed glucose. Also, higher glucose concentrations represent higher biomass concentration. During aerobic growth aeration may become insufficient at higher biomass concentrations. Buffering, amino acid addition, and other feed components would have to be increased in concentration. Finally, thick growth may cause other experimental problems such as increased effluent tube wall growth, high amounts of base addition to maintain pH, and more difficult sampling and cleanup. Thus, an intermediate glucose concentration of 4 g/l was picked. However, any glucose concentration from approximately 3 g/l to 10 g/l would also have satisfied the above criteria. Glucose solutions were autoclaved separately from all other components to avoid all possible cross reactions (e.g. Maillard reactions). As glucose concentration was the one feed component measured during all experiments, this was the component that was most important to keep "pure".

The final feed composition used is given in Table 1.

3.4 Feed Preparation

The feed medium was prepared in three different configurations as follows: shake flask, reactor batch, and continuous feed. Each will be discussed separately, and the flask grouping listings in table 1 will be used. The term "2.7X concentrated" will hereafter be used to refer to concentration higher than that listed in table 1 by a factor of 2.7. For example, a 2.7X concentrated solution of flasking group 1 would be a solution of 10.8 g/l glucose in water. One stock solution was used in all three configurations, a 100X

Table 1. Feed medium recipe with flasking divisions

Feed Ingredient	Amount added per liter of deionized water	Flasking Division
Glucose	4 g	1
KH ₂ PO ₄	3 g	2
NaCl	0.5 g	2
NH ₄ Cl	1 g	2
Na ₂ HPO ₄	6 g	2
Threonine	0.5 g	3
Leucine	0.5 g	3
Thiamine	5 mg	3
CH ₃ COONa•3H ₂ O	1.66 g	4
MgSO ₄	0.24 g	5
CaCl ₂	11.96 mg	6
SeO ₂	1.1 mg	7
FeSO ₄ •7H ₂ O	27.8 mg	7
(NH ₄) ₆ Mo ₇ •4H ₂ O	1.765 mg	7
MnSO ₄ •H ₂ O	1.69 mg	7

Note: For example flask 2 would include Na₂HPO₄, KH₂PO₄, NaCl, and NH₄Cl

concentrated solution of flasking group 7. One liter of this was prepared when necessary. Ten milliliters of this solution were used for every liter of feed solution.

When shake flasks were prepared, stock solutions were used. The stock solutions prepared were 100 ml bottles of 25X concentrated solutions of flasking groups 2-6. Glucose solution was freshly prepared for each shake flask. In order to illustrate the preparation of a shake flask, the preparation of the usual 250 ml amount of flask medium will be given. 10 ml of each of the group 2-6 bottles are pipetted into separate tubes and the tubes are capped. 2.5 ml of the group 7 flask are also pipetted into a tube. Finally, 197.5 ml of deionized water is poured into a shake flask and 1 g of glucose is added. The flask is then capped with a paper towel and foil and tied with a string. All of these are then autoclaved for 25 minutes. Finally, upon cooling of the ingredients, the ingredients are poured together into the shake flask under a laminar flow hood.

The medium preparation for startup batches is described next. Although the startup medium descriptions in this section do not appear to "add up" to the concentrations given in Table 1, when the actual startup procedures are considered later, the final startup composition does "add up" to the correct medium. Two liters of 1.4 X concentrated flasking group 2 salts are prepared and poured into the chemostat and then autoclaved within the reactor. A 56 ml aliquot of the flasking group 7 stock solution is pipetted into a glass flask. Four additional glass flasks with 150 ml each of deionized water are set aside. To each of those flasks 5.6 times the mass listed in table 1 for one flasking group is added, for groups 3,4,5, and 6. These flasks are capped with paper towel and foil and then tied with string. The glucose solution is prepared by adding 22.4 g of glucose to 944 ml of water in the main feed flask, which is shown in figure 6. The main feed flask preparation is as follows. A new Supor filter is placed in the Fisher 47 mm filter holder. The connections are as follows: the flask outlet tube leads to its own filter holder, which leads to the needle for puncturing into reactor. The needle is wrapped in foil wrap. Additionally, there is a tube for a sterile nitrogen inlet into the flask for replacing the emptied fluid. The

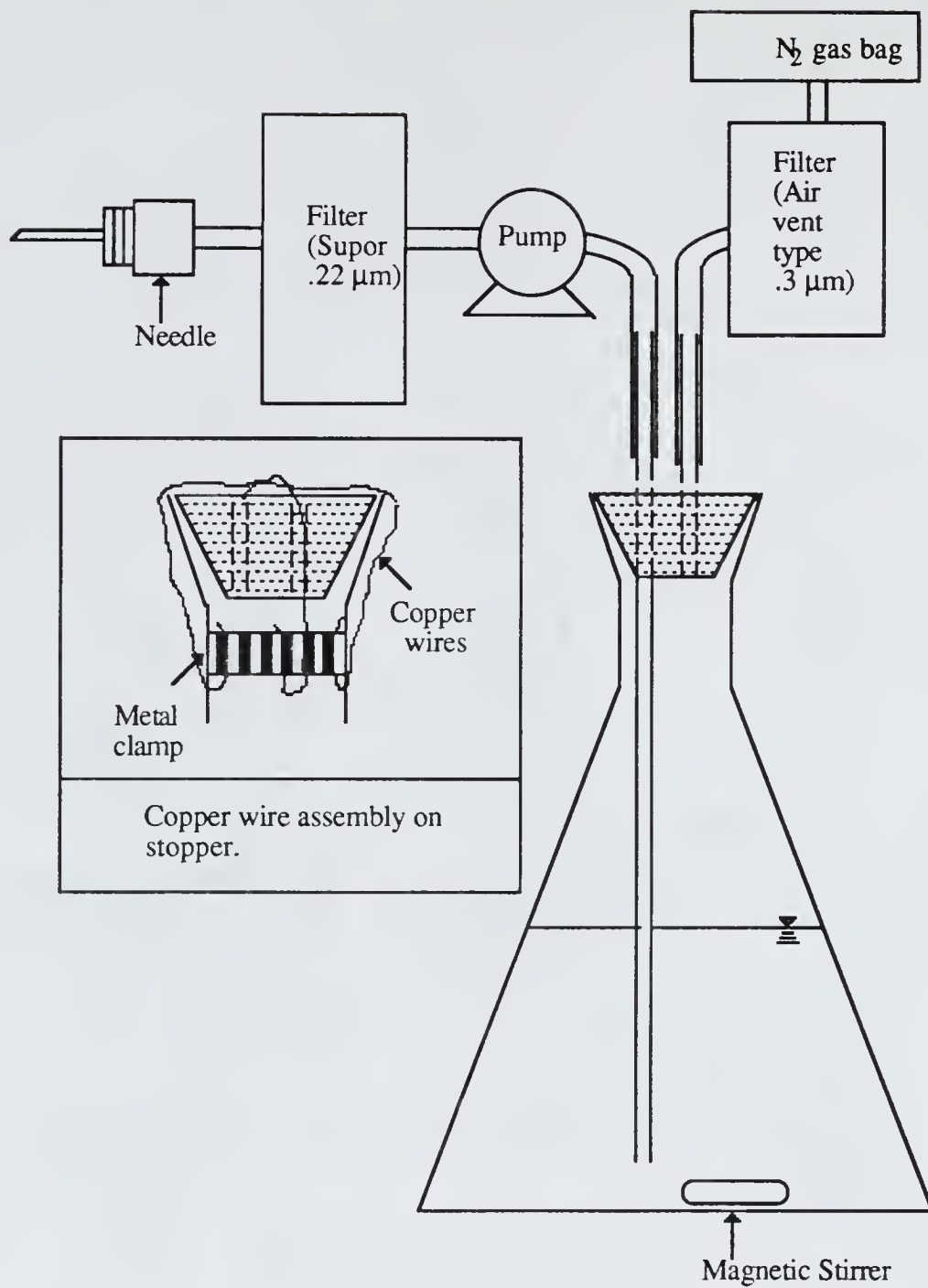


Figure 6. Main Batch Feed Flask Diagram

nitrogen introduced passes through a Bacti-Vent air filter. The rods going through the rubber stopper are made of glass. The main feed flask and the glass flasks are autoclaved for 30 minutes. After these cool down, all of the flasks are placed under a laminar flow hood. The metal clamp on the main feed flask is loosened and the contents of the glass flasks are added. The metal clamp is then retightened and the feed is ready to be added to the reactor, as will be described later in the description of reactor startup.

Finally, the continuous feed medium preparation will be described. Sixteen liters of continuous feed medium were made in any single batch, thus sixteen times the amount of each flasking group to be added per liter is added to separate amounts of water. The procedure for a single batch is described. In three large flasks, 3.5 liter aliquots of deionized water are added, along with separate additions of 16X of the Table 1 masses for flasking groups 1, 2, and 3. For example, in the glucose flask, 64 g of glucose are added to 3.5 liters of water. The group 7 flask has 160 ml of the appropriate stock solution added and then filled with deionized water to 3 liters. The acetate flask has 26.56 g of $\text{NaAcetate} \cdot 3\text{H}_2\text{O}$ added to 500 ml of water. The calcium chloride flask has 192 mg of CaCl_2 added to 250 ml of water and the last flask has 3.943 g of $\text{MgSO}_4 \cdot 7\text{H}_2\text{O}$ added to 250 ml of water. Finally, the feed carboy, diagrammed in figure 7 is prepared as follows. Two fresh .22 μ Supor filters are placed in the appropriate filter holders, along with a fresh Bacti-Vent air filter for sterile nitrogen introduction. The carboy is then autoclaved empty and uncapped. One and a half liters of deionized water are then poured into the carboy and it is capped. The tubes are then clamped, the needle and air filter are covered with foil wrap, and the whole apparatus (except the N_2 bag and the magnetic stirrer) is autoclaved for 30 minutes. All of the flasks are covered with paper towel and foil wrap and then tied with string. They are also autoclaved for 30 minutes. The cap of the carboy is removed and the contents of the other flasks are added under a laminar flow hood.

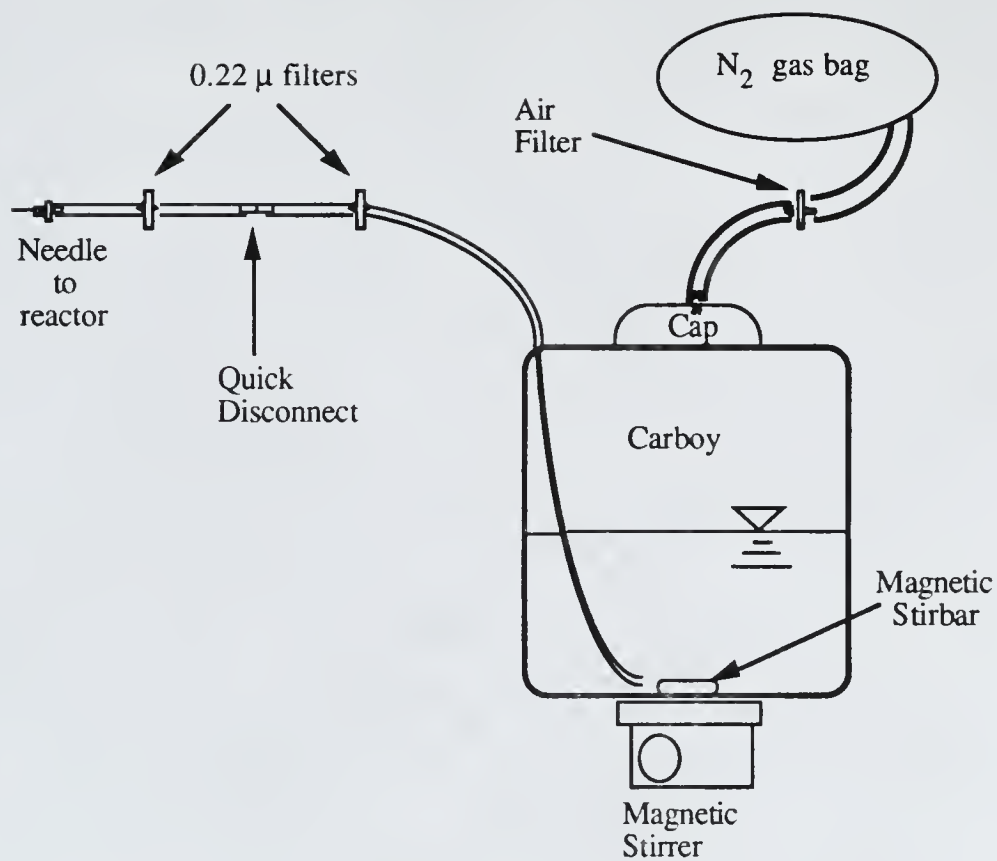


Figure 7. Continuous Feed Carboy Diagram

3.5 Experimental Operation

3.5.1 Operational Conditions

The temperature that the experiments were operated at was 37°C. This temperature was chosen as it is the normal optimal temperature for growth of *E. coli*. The other major environmental variable that was held constant was pH. It was suggested [40] that somewhat acidic pH's gave higher batch yields of d-lactic acid. As pH 7 is the optimal pH for *E.coli* growth, the possibility of cycling pH in addition to aeration was examined. Preliminary experiments were performed early in this investigation to examine the effects of pH on the anaerobic batch yield of d-lactate on glucose. The results will be described briefly. These experiments were performed before any aerobic experiments were and, thus, a slightly different medium formulation was used as shown in table 2. It should be emphasized that the pH effects experiment was the only one described in this work using the table 2 recipe. All other experiments used the main recipe given in Table 1. The use of shake flasks will be described later. A starter flask with an initial medium composition described in table 2 in 500 ml of deionized water was inoculated, placed in a 37°C AO constant temperature shaker bath and kept there until the flask contents appeared turbid. Three test flasks were prepared during the growth phase of the starter flask cultures with 150 ml of medium in each. The medium ingredients of these three flasks were the same as those in Table 2, but the concentrations of each were set so that, upon dilution with 100 ml of liquid, they were the same as those given in Table 2, except that the amounts of potassium phosphate mono- and dibasic were varied to give the desired pH values.

Table 2. First Medium Recipe

Glucose	3.0 g/l
K_2HPO_4	4.9 g/l
KH_2PO_4	3.0 g/l
NaAcetate	0.2 g/l
$(NH_4)_2SO_4$	0.1 g/l
$CaCl_2$	0.2 g/l
$MgSO_4 \cdot 7H_2O$	0.1 g/l
$FeSO_4 \cdot 7H_2O$	0.05 g/l
L-Threonine	0.05 g/l
L-Leucine	0.05 g/l
Thiamine	0.005 g/l

When the starter flask reached the appropriate turbidity, the three test flasks were each inoculated with 100 ml of the starter culture. Spectrophotometric absorbances, pH values and lactic acid concentrations were then measured at half-hour intervals. The results of this experiment are given in table 3. The large increase in lactate concentration in the pH 7 flask over a 5 hour period, along with the large increase in absorbance over a 26 hour period, would indicate that the operating pH should be kept at a value around seven. An additional benefit in choosing constant pH operation is that shifts in pH are difficult. Buffering is generally desirable in microbial systems, but buffering would require higher base or acid amounts to be added to cause a shift. High addition of these solutions have a diluting effect on the culture and thus will interfere with measurements. This problem, though, may possibly be overcome by use of gases such as CO₂ and N₂ instead of acid or base additions to manipulate pH.

3.5.2 Shake Flask Experimental Procedure

The shake flasks were prepared as described in the section on feed preparation. Further procedural details will be given here. In a starter culture, after the contents were poured together under a laminar flow hood, a small inoculum was taken off of the culture storage agar dish with a sterile loop and then transferred into the combined medium flask. In other types of shake flasks, liquid inocula may be used instead of the agar culture. When liquid inocula were used, only small amounts (~1 ml) were usually added. After inoculation, the flask was recapped with the paper towel/foil wrap cap and tied. The flask was then placed in an AO shaker bath set at 37°C. If the shake flask culture was to be used for reactor inoculation, it was usually left in the bath for approximately 12 hours. For yield experiments, the flasks would be left in for longer periods. The usual shake flask volume used was 250 ml.

Table 3. Effects of pH on Lactate Production

Initial pH	7	6.4	5.85
Initial Lactate Conc. (mg/l)	105	110	110
Initial Absorbance (550 nm)	0.186	0.186	0.186
Lactate Conc. after 5 hours (mg/l)	206	151	119
550 nm Absorbance after 5 hours	0.200	0.205	0.175
pH after 5 hours	6.98	6.4	5.87
Lactate Conc. after 26 hours (mg/l)	2900	1340	292
550 nm Absorbance after 26 hours	0.49	0.37	0.22
pH after 26 hours	5.24	5.26	5.38

3.5.3 Reactor Experimental Procedure

3.5.3.1 System Description

The reactor experimental procedures will now be described. The reactor, a Bioengineering KLF 2000, was used for all of the batch and continuous experiments. A diagram of the reactor system is shown in figure 8. In this figure the long dashed lines represent measurements for the chemostat control unit, and the dotted lines represent control outputs. Except where mentioned later, the reactor volume was always maintained at 2 liters. If the system is in continuous mode, a load cell is used to determine the system weight. A peristaltic pump maintains a constant effluent flowrate. The pumping rate is calibrated by collection of the fluid in a graduated cylinder. When a small drop in weight is detected the control unit activates the influent pump until the reactor is back up to its operating weight. Only small deviations in the level were allowed. The pH value of the system was measured with an Ingold Ag/AgCl pH electrode and controlled by a Bioengineering M7832N pH controller. This pH control maintained constant pH by controlling pumps for previously autoclaved 1 M HCl and NaOH solutions prepared separately. The constant 37°C temperature was maintained by a pt100 temperature sensor, a Bioengineering K54450 controller, and an 800 watt heater. Agitation for the reactor was set at 700 rpm, and a baffle cage within the reactor helped insure good mixing. Dissolved oxygen was monitored with a Cole-Parmer polarographic electrode and a Cole-Parmer Model 5513 dissolved oxygen meter. When anaerobic conditions were necessary, filtered (as shown in figure 8) Alphagaz oxygen-free nitrogen was bled over the top of the culture at the rate of approximately 30 ml/min. When aeration was necessary, an Air Cadet pump was used. It pumped air from underneath a UV hood, through a filter apparatus identical to the same as that used for nitrogen, and through a sparging tube with the outlet bent underneath the bottom rotor blade within the reactor. Two and a half vvm was the air flowrate obtainable with this pump into the two liter reactor. When periodic switching of

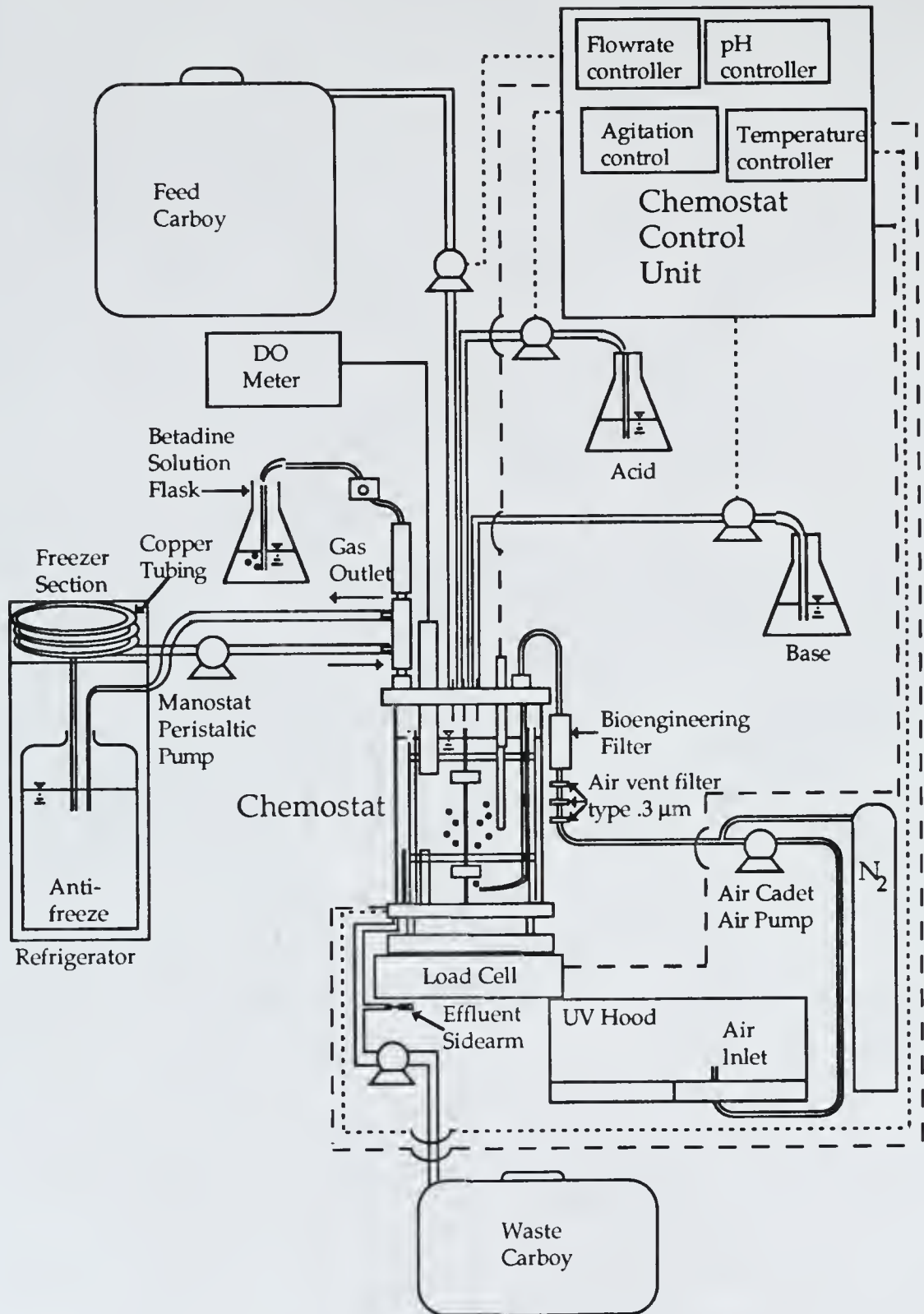


Figure 8. Experimental Reactor Setup

the aeration was performed, a slow flow of nitrogen was continuously maintained over the top of the culture so as to maintain a positive pressure (which helps prevent outside contamination). Switching of conditions during the aeration cycling was performed by simply plugging the Air Cadet pump into an X-10 wall module and setting switch times on an X-10 computer interface (X-10 (USA) Inc. 185A LeGrand Ave. Northvale, NJ). The gas was released through a Bioengineering gas outlet apparatus. This had a cooling jacket, which was maintained at about 10°C in order to minimize evaporation of culture volume. This cooling was accomplished by continuous pumping of cooled Prestone antifreeze through a Hotpoint refrigerator and freezer using a Manostat pump set on its lowest pumping speed. The end of the effluent gas hose was placed in a dilute Betadine solution in order to help prevent contamination.

3.5.3.2 System Startup and Operation

The following startup procedure was used for all batch and continuous experiments. It should be emphasized that all continuous runs were started as batch runs. The only variations were whether anaerobic or aerobic procedures were going to be used. The cycling runs were all started up under aerobic conditions. Prior to startup, the effluent tube, acid, base, and inlet gas filters were autoclaved. A batch feed was also prepared. Additionally, a starter shake flask culture was prepared and inoculated 12 hours prior to reactor inoculation. The chemostat was filled with the appropriate salts as described in the batch feed description to the 2000 ml level. The topcap and bottom attachment rings were secured in place. The pH electrode was precalibrated to pH 7 and 4 and inserted into the topcap. The reactor was now ready for autoclaving.

The autoclaving of the reactor was done *in situ*. Here, the pH electrode was pressurized to 30 psi by connecting it to an air cylinder, the stirrer was set to 800 rpm, the gas outlet was opened, and temperature set-point of the chemostat was changed to 121°C. When the temperature reached 99°C, the gas outlet was closed. The temperature was

allowed to reach 121°C, and was kept there for 30 minutes. After 121°C was held for 30 minutes, the temperature set point was changed to 104°C. When reactor temperature reached 104°C, the first thing that was done was to turn on the pump for the gas outlet apparatus reflux coolant. The reactor pressure was raised by using either air from the Air Cadet pump or nitrogen from a cylinder. The gas outlet was also opened immediately. The reactor temperature set-point was then changed to 37°C in preparation for the actual experiment.

After the reactor cooled down to 37°C, the effluent, acid, and base tubes were each placed through peristaltic pumps and then appropriate connections were made to the reactor using aseptic technique. The effluent tube was immediately clamped to avoid loss of reactor liquid. The main feed flask (described in the batch feed preparation) was then connected to the reactor. Eight hundred milliliters were then pumped into the reactor for a total volume of 2.8 liters. The reactor conditions were then set to pH 7, 37°C, and 700 rpm agitation. Finally, 20 ml of inoculum were taken by a sterile syringe from the starter flask under a laminar flow hood and then injected through one of the reactor seals. The reactor at this point was prepared and inoculated. A batch run was thus begun.

Immediately after inoculation a sample was aseptically taken through the effluent sidearm aseptically into a previously autoclaved and capped tube. Serial dilution was immediately performed and the remaining sample had its absorbance measured and then was centrifuged for ten minutes in a Fisher Centrif 228 centrifuge. After centrifugation the sample was filtered using a syringe and MSI Magna Nylon 66 .22 μ filters and then heat shocked for five minutes in boiling water. Finally, the sample was allowed to cool to room temperature and then stored in a freezer for later glucose and lactate analysis.

Frequent measurements were taken during batch runs. The acid and base levels were monitored and recorded. Upon the absorbance values reaching above 0.4, appropriate dilution with deionized water was performed in order to obtain a measurable absorbance. The batch measurements were performed until absorbance stopped increasing.

Up to this point, the batch and continuous experiments were performed in a synonymous manner (except for the obvious need for preparation of a continuous feed carboy during the batch start of a continuous run). If a run was intended to be strictly batch, measurements were continued for several hours into the stationary phase. If a run was intended to be a continuous run, the system was switched into a continuous mode before the end of exponential phase. The point of switching was usually about one hour before the expected end of exponential phase. This end point was estimated using absorbance measurements and comparing them with previous batch results.

The following procedure was used to switch the reactor from the initial batch mode to a continuous mode. The feed carboy was connected to the reactor after its tube was led through the influent peristaltic pump. Subsequently the reactor volume was lowered to 2 liters by draining through the effluent tube. The weight set point was entered into the chemostat control unit, the effluent flowrate was set, and the reactor was then in a continuous mode.

Measurements were taken in the same fashion as in the batch runs. They were taken at least three times on a daily basis, but usually the frequency was much higher. Additional considerations during continuous operation were daily monitoring of the base reservoir, checking of the tubing and overall system condition, contamination testing, effluent disposal, and feed carboy preparation and changing.

Contamination testing was usually performed by the following two methods: preparation of a shake flask deficient in the appropriate amino acids and inoculation with reactor contents, and microscopic examination of a Gram-stained sample of the reactor contents. In the former method, an additional control flask was prepared with the appropriate amino acids. The two flasks were seeded with identical volumes of reactor volume. They were then examined for growth after overnight shaker bath incubation. If the deficient flask showed significant growth, then the reactor was declared contaminated. This method is somewhat dubious, though, as the deficient flask could be selective for

leucine and threonine revertants. Thus, the primary method of contamination testing was the mentioned microscopic examination. If the slide appeared to have only red rods, the continuous operation was declared successful to that point.

When operating in continuous mode a new feed carboy had to be prepared daily. The feed was changed by switching the quick connect fitting at the end of each carboy tube while all ends were immersed in rubbing alcohol. The quick connect change in alcohol, along with the second filter placed between this connect and the reactor inlet, helped insure sterility.

CHAPTER 4 ANAEROBIC GROWTH OF *E. COLI* LCB898

4.1 Background

Under anaerobic environmental conditions, where no alternate electron acceptors such as nitrate, fumarate, or sulfate, are available, *Escherichia coli* uses fermentation as its pathway for energy production. Fermentation, as defined by Brock [47, p.802], is a group of catabolic reactions producing ATP in which organic compounds serve as both primary electron donor and ultimate electron acceptor. When compared to aerobic or anaerobic respiration, fermentation is not a very efficient method of producing ATP and, thus, overall cell biomass [48, p. 54]. In order to understand fermentation, the reactions involved are briefly described. The important reactions are diagrammed in figure 9 (this diagram was drawn with the help of Neidhardt and Brock [49, p. 153 and 47, p. 126]). First, the metabolic pathway common to both aerobic and anaerobic metabolism, pyruvate formation, will be examined. After this, fermentative pyruvate dissimilation will be considered.

The pathways of glucose degradation to pyruvate shown in figure 9 are the Embden-Meyerhof-Parnas (EMP) pathway and the pentose-phosphate pathway. Typically, in *E. coli* grown anaerobically on glucose, 92-95% of the glucose will be degraded by the EMP pathway and 5-8% will be degraded by the pentose-phosphate pathway [50,51]. The common first reaction to both pathways is the phosphorylation of glucose to glucose 6-phosphate. After this point, the split between the two pathways occurs. The pentose-phosphate pathway's major roles are formation of pentose phosphates for nucleotide

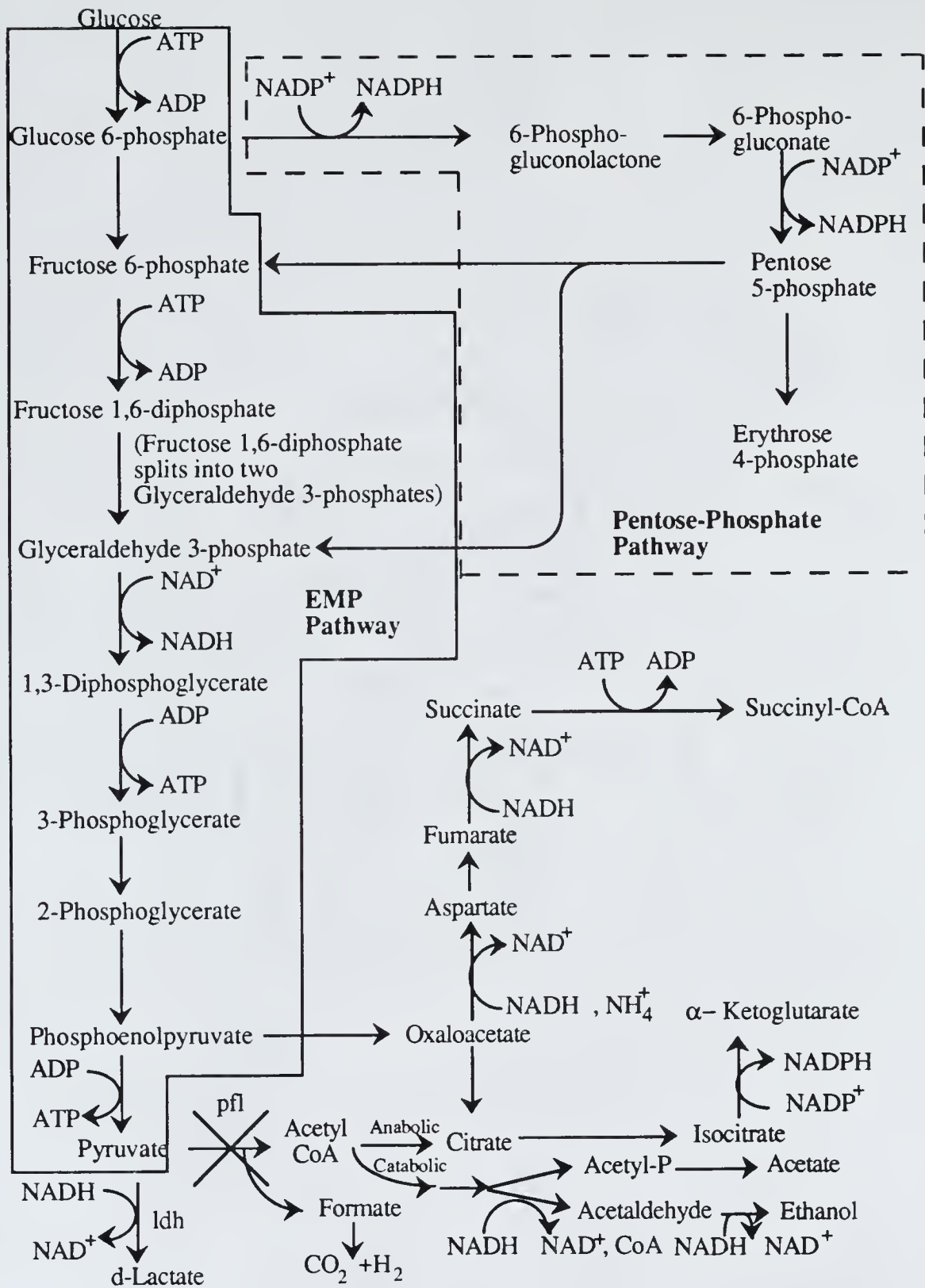


Figure 9. Main Anaerobic Biochemical Pathways in *E. coli* LCB898

biosynthesis and NADPH generation [48, p.31]. The EMP pathway will be described in the following paragraph.

During pyruvate formation, a net yield of 2 moles of ATP per mole of glucose is obtained by substrate-level phosphorylation. Additionally, 2 moles of NADH, the main source of reducing power for biosynthesis, are generated. Some of the EMP pathway intermediate metabolites also serve as biosynthetic precursors. These include fructose 6-phosphate and phosphoenolpyruvate. The point at which aerobic and anaerobic metabolisms differ is the degradation of pyruvate.

In wild-type *E. coli* cells, pyruvate is normally dissimilated under anaerobic conditions by two pathways with no additional ATP generation, one being catalysed by pyruvate formate-lyase (pfl), the other by d-lactate dehydrogenase (ldh) [52, p.151]. Pfl is inactive under aerobic conditions [53]. The products of the pfl degradation include formate, acetate, ethanol, CO₂, and H₂ [49, p. 163]. The sole product of the lactate dehydrogenase pathway is d-lactic acid. In anaerobic wild-type *E. coli* K12 batches [54], only traces of d-lactic acid are produced. This would indicate that the ldh pathway is not normally used.

In *E. coli* LCB898, a K12 mutant, a mutation exists in the gene responsible for production of pyruvate-formate lyase, thus closing off that pathway for pyruvate dissimilation [37,38,55]. High yields of d-lactic acid from glucose therefore are expected in this mutant. An additional consequence is that when growth is anaerobic in a minimal medium, the addition of acetate may be required since acetyl-CoA cannot be produced without the action of pyruvate formate-lyase.

To summarize, two points must be reiterated. The first is that when glucose is processed through the EMP pathway, a net yield of 2 ATP molecules for every glucose molecule degraded is observed. During aerobic metabolism, which is to be described later, oxidative phosphorylation can also be employed. It will be shown that the net ATP yield per glucose is much higher when the additional phosphorylation is performed. Again, ATP

yield is directly proportional to growth yield. Thus, relatively low biomass yields under anaerobic conditions are expected. The second main point is that *E. coli* LCB898 should show high yields of d-lactate on glucose.

4.2 Batch Growth

In all of the following discussed batch results, time 0 represents the point at which inoculation of the reactor was inoculated. The results for one of the anaerobic batch runs, to be designated anaerobic batch run 1, are shown in figures 10 and 11. This was one of the preliminary runs to help determine a final feed composition. It is clear that biomass concentration stopped increasing well before glucose in the system was exhausted from the results shown in figure 10. Any glucose consumed after 46 hours was strictly being used for maintenance. The results shown in figure 11 indicate that the glucose was largely being converted into lactate. In this experiment only 50 mg/l of each amino acid and no metals were used in the medium. It was hypothesized (and later confirmed with amino acid analysis) that threonine was exhausted at the point of entering stationary phase.

In the next batch experimental run, anaerobic batch run 2, the amino acid concentrations were doubled, but metals were still not added to the medium. The results for this experiment are shown in figures 12 and 13. Again, as can be seen in figure 13, the bacteria appeared to enter a stationary growth phase before glucose was exhausted. Amino acid analysis showed excess threonine and leucine. Other work with this organism [40,44,45] was then reexamined and metals were then added to the final formulation of the medium.

In figures 14-17 all of the experimental results for a batch run with sufficient amino acids and metals added to the medium are shown. This run is designated anaerobic batch run 3. At 27 hours, the point of glucose exhaustion, growth had essentially stopped, as can be seen in figures 14-16. During this growth phase, as shown in figure 17, lactate was being produced in what appears to be a growth-associated manner. Lactate concentration

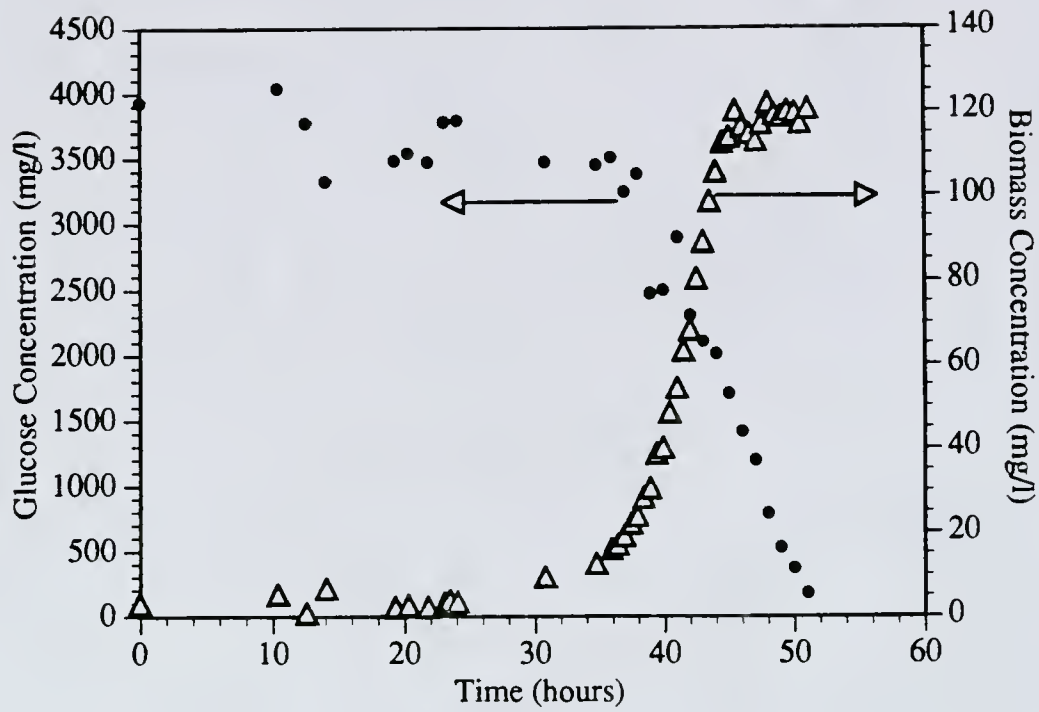


Figure 10. Anaerobic batch run 1. Glucose and biomass concentration against time.

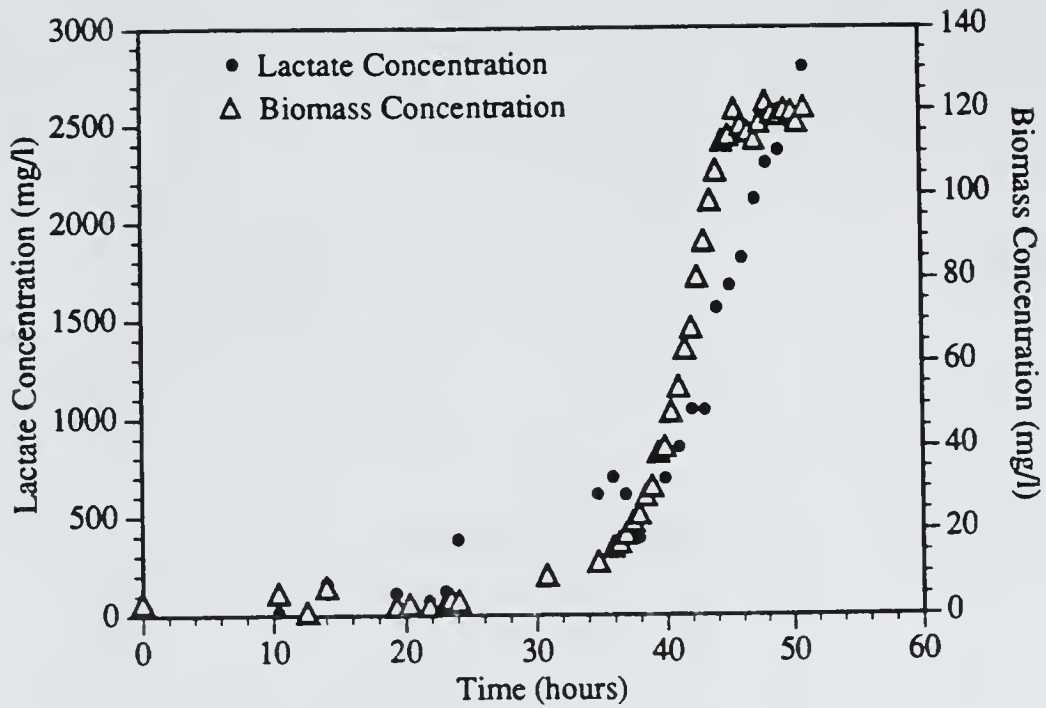


Figure 11. Anaerobic batch run 1. Lactate and biomass concentration against time.

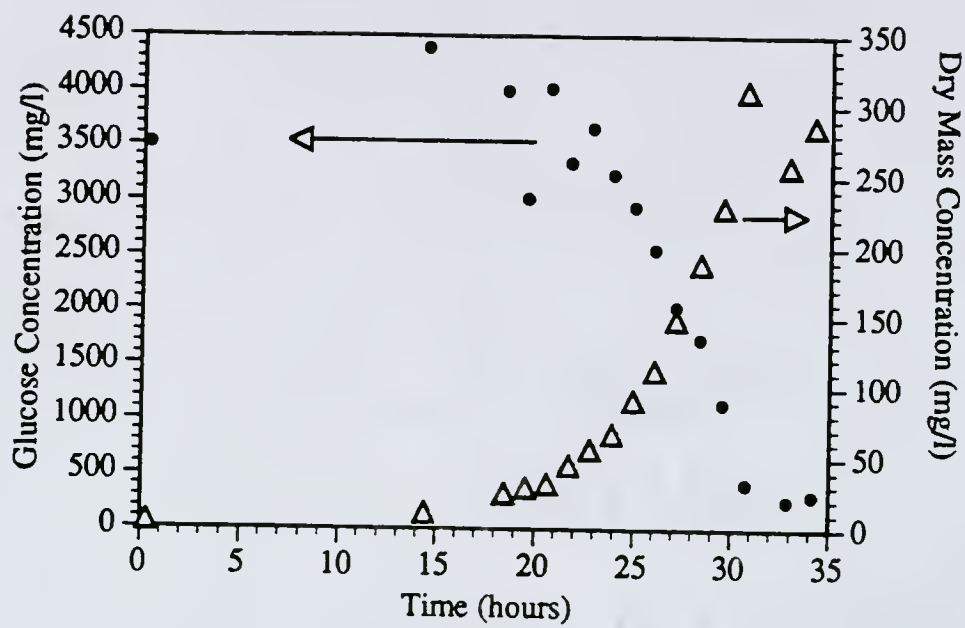


Figure 12. Anaerobic batch run 2. Glucose and biomass concentration against time.

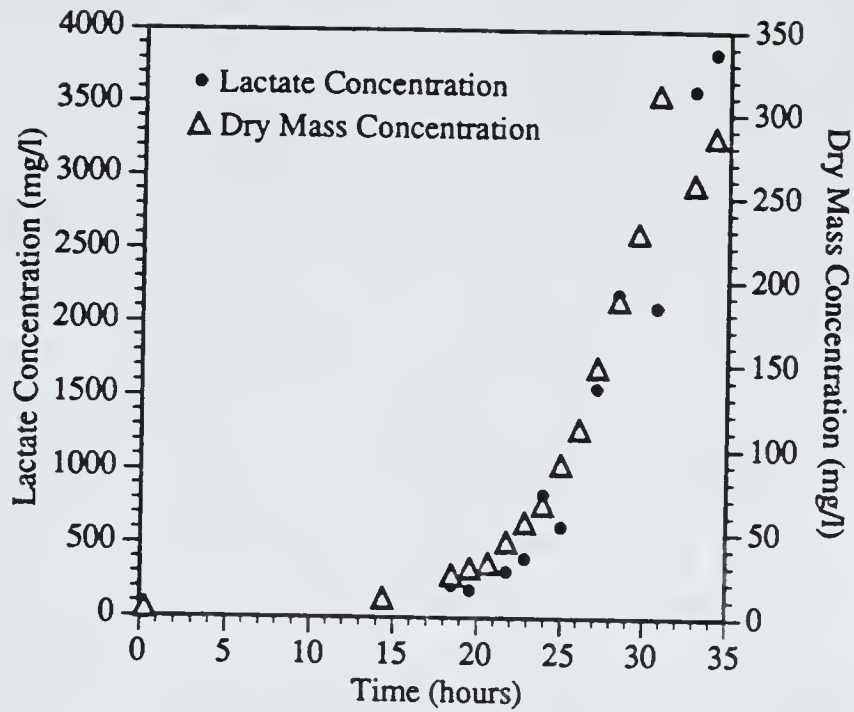


Figure 13. Anaerobic batch run 2. Lactate and biomass concentration against time.

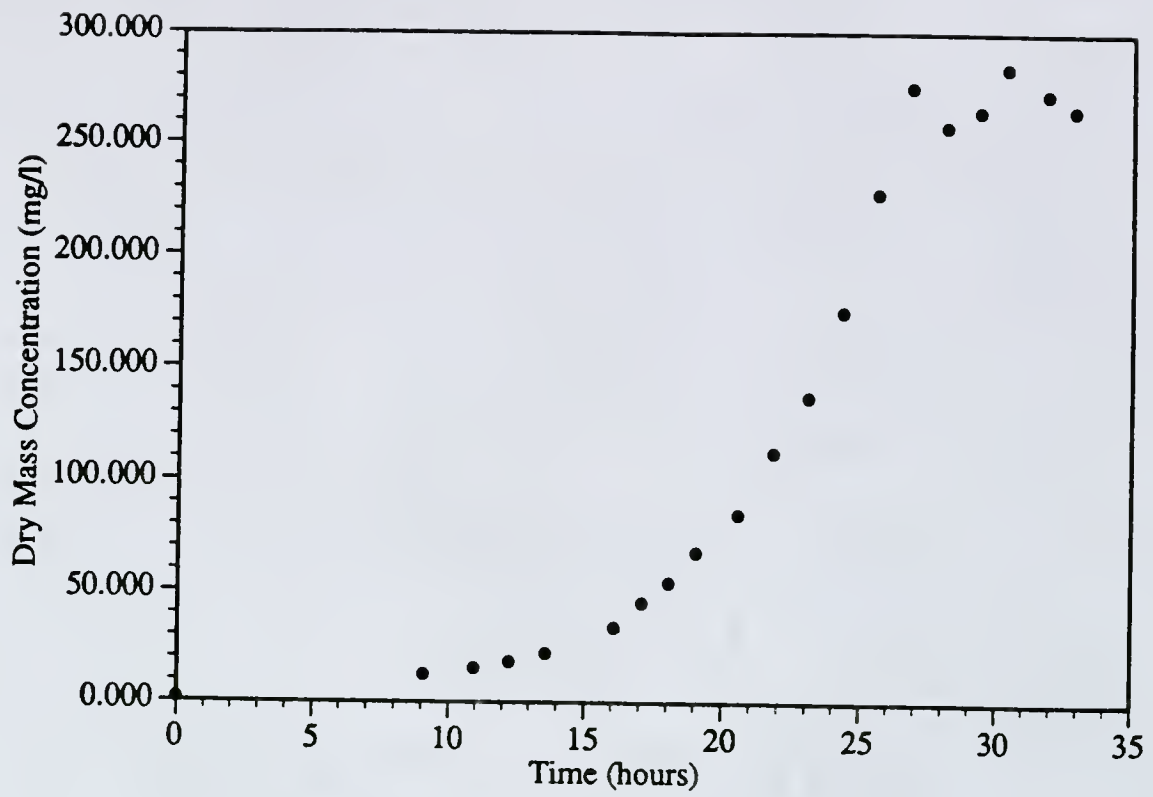


Figure 14. Anaerobic batch run 3. Biomass concentration against time.

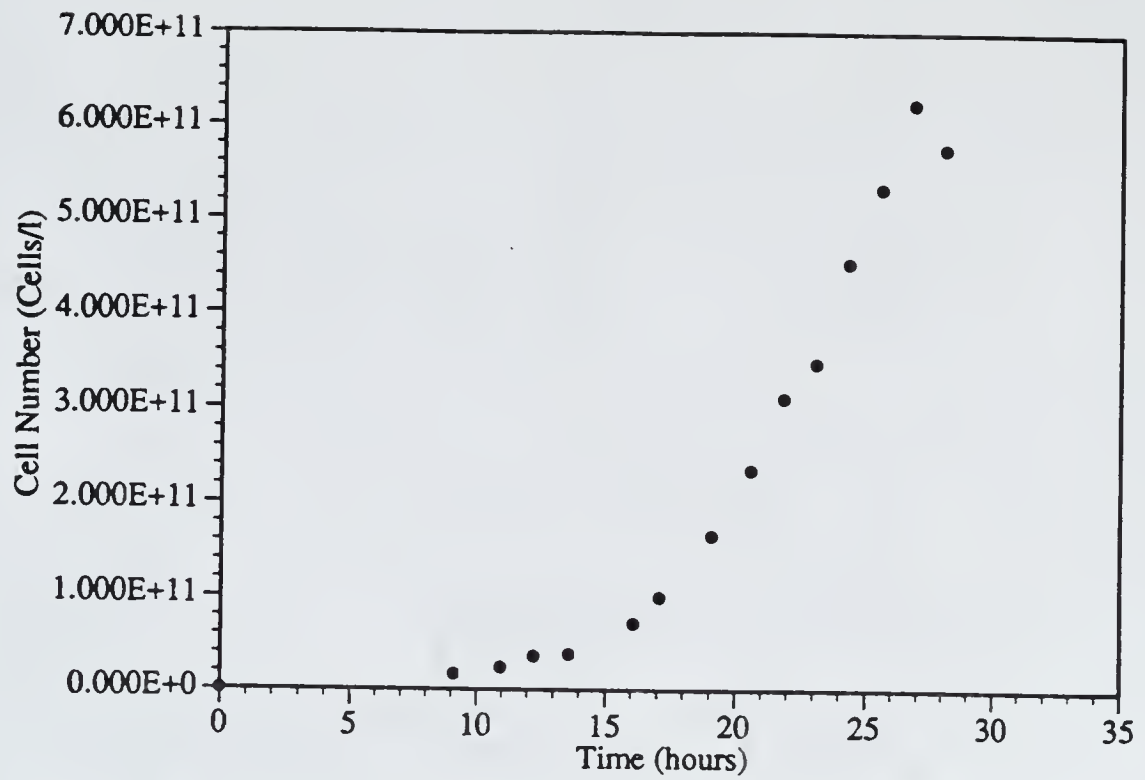


Figure 15. Anaerobic batch run 3. Cell number concentration against time.

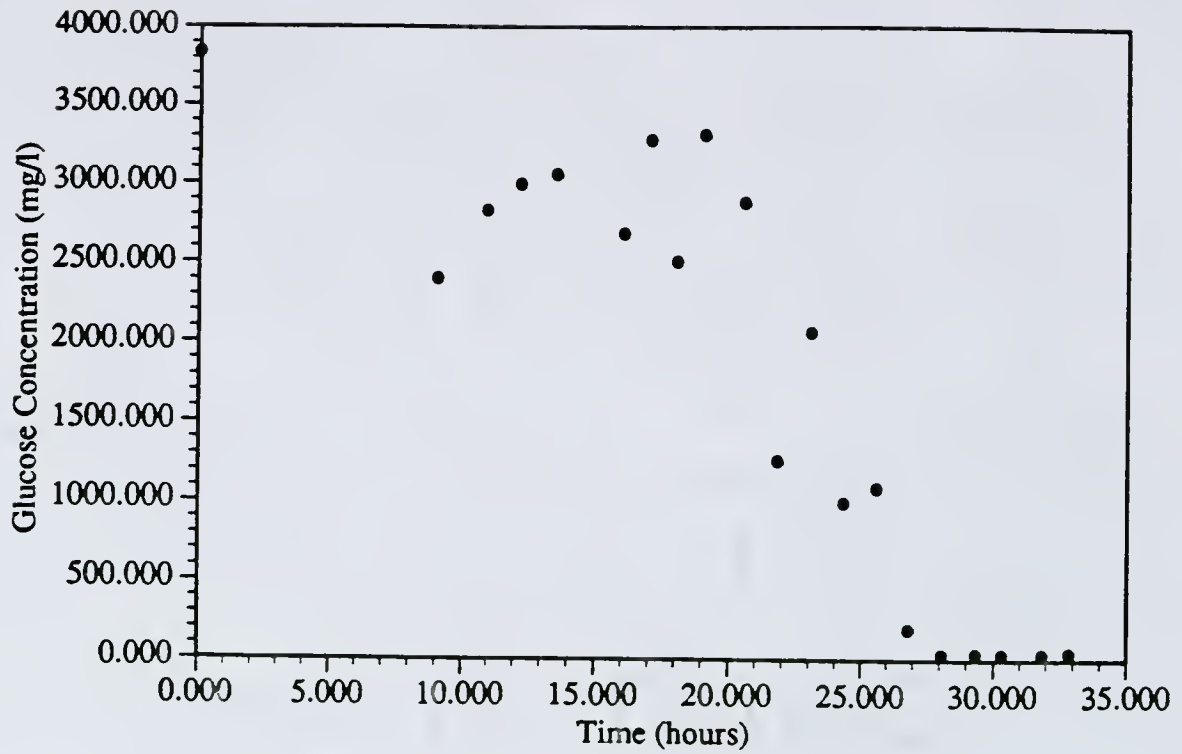


Figure 16. Anaerobic batch run 3. Glucose concentration against time.

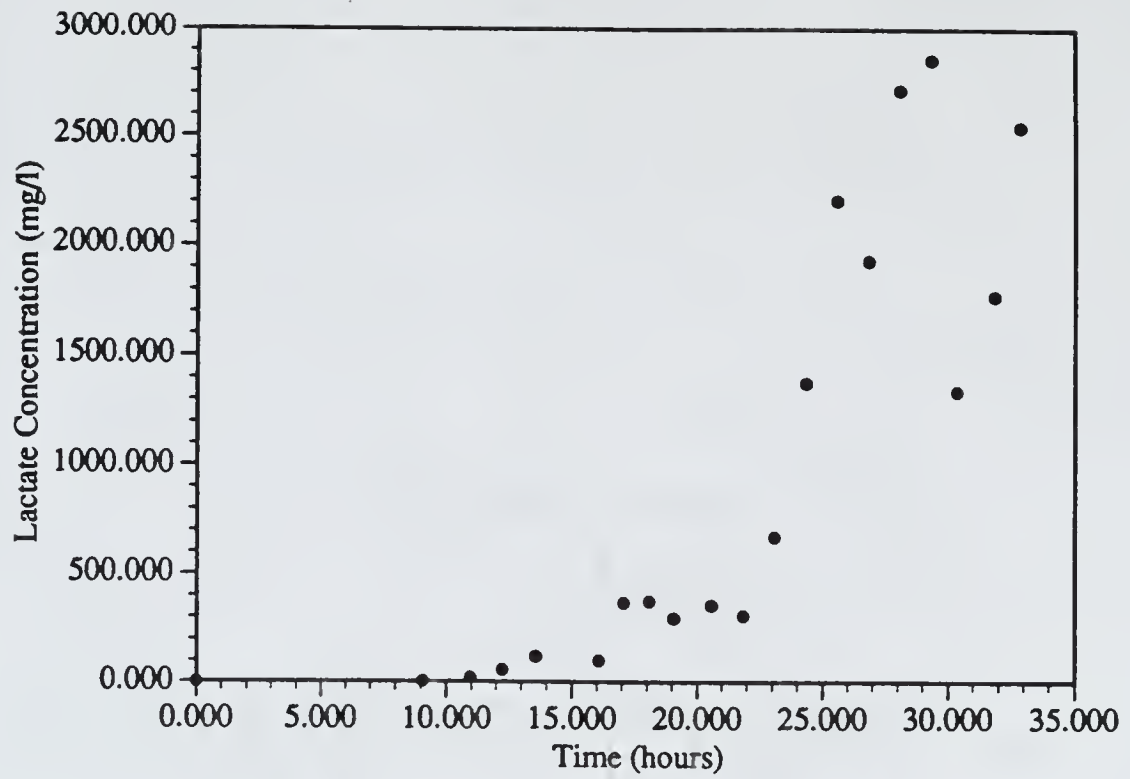


Figure 17. Anaerobic batch run 3. Lactate concentration against time.

did continue to increase beyond 27 hours, but this may be explained by a slow release of the lactate from the cells. The low lactate concentration seen at 27 hours was probably due to experimental error in the measurement, as the previous point indicated a lactate concentration approximately 300 mg/l higher. Appropriate values for growth parameters for this run will be given later in this chapter. Approximately 2 hours after entering the stationary phase, the lactate measurements shown in figure 17 showed an interesting response. The lactate showed a sharp dip with a subsequent increase. Ordinarily this may have been simply dismissed as experimental error. A later experimental run was performed under the same conditions as anaerobic batch run 3, to be designated anaerobic batch run 4, and its results are shown in figures 18-21. The lactate results for this run are shown in figure 21. The previously mentioned dip was also seen here. This dip was not of major importance to this work as it occurs during stationary phase. This work primarily involved exponential phase growth in continuous operation. However, possible explanations for it are appropriate. The simplest hypothesis is experimental error. This hypothesis is not probable though as it has been seen more than once. Another is that the cells may have been growing diauxically on some other substance in the medium such as acetate, leucine, or threonine. This would have been an unusual diauxy, though, as biomass concentration, shown in figures 14 and 18, did not seem to increase during the period of glucose exhaustion. The cells may have been using one of the listed substances in the medium for maintenance while ingesting d-lactate along with this substance and later releasing the lactate for some unknown reason. Still another hypothesis is that some of the cells may have been genetically reverting to a pfl^+ form (to be discussed further in a later chapter). The properties of the revertant are not completely understood and this could have been some effect of the revertant's growth alongside with the non-revertants. Again, whatever the true explanation for this behavior may be, it was not of primary importance to this work as most of the work performed in this project was on exponential phase growth.

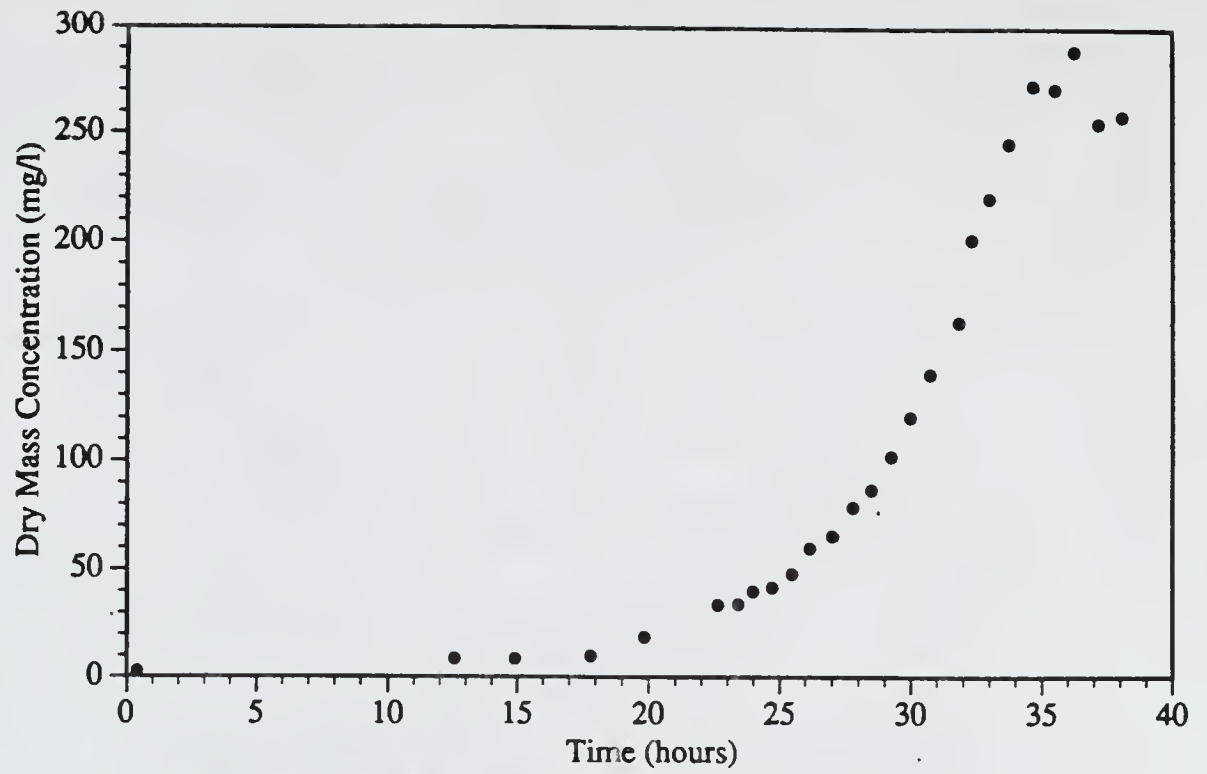


Figure 18. Anaerobic batch run 4. Biomass concentration against time.

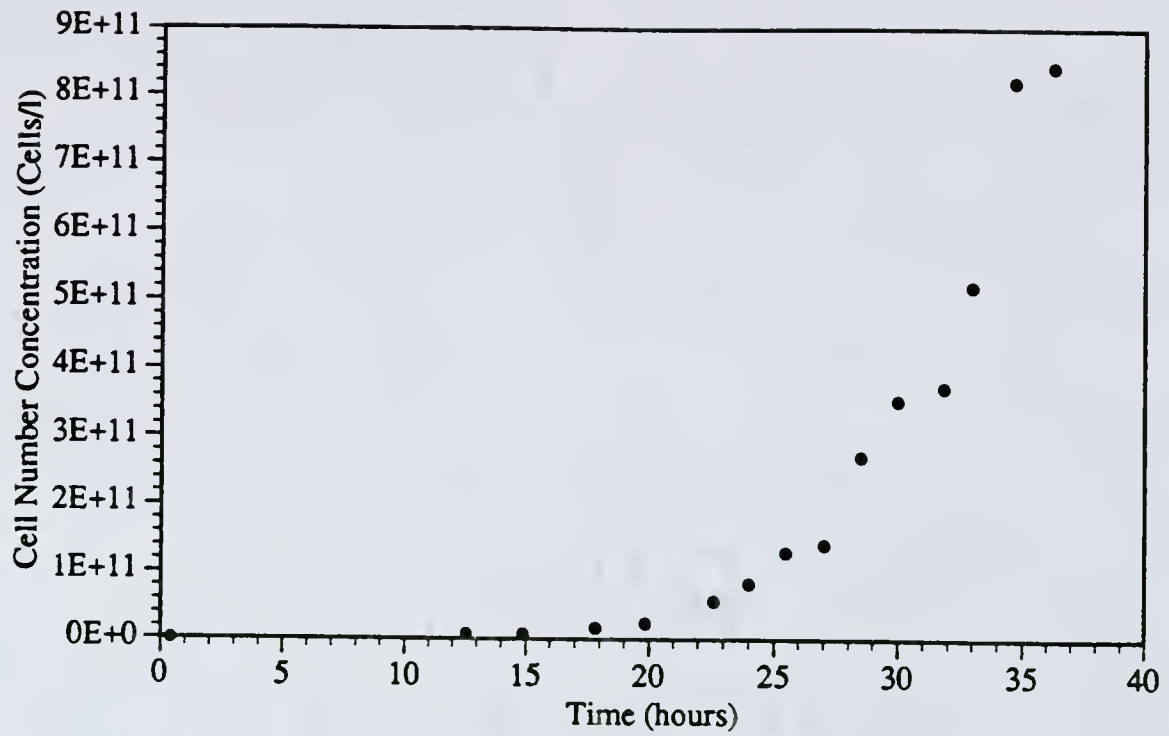


Figure 19. Anaerobic batch run 4. Cell number concentration against time.

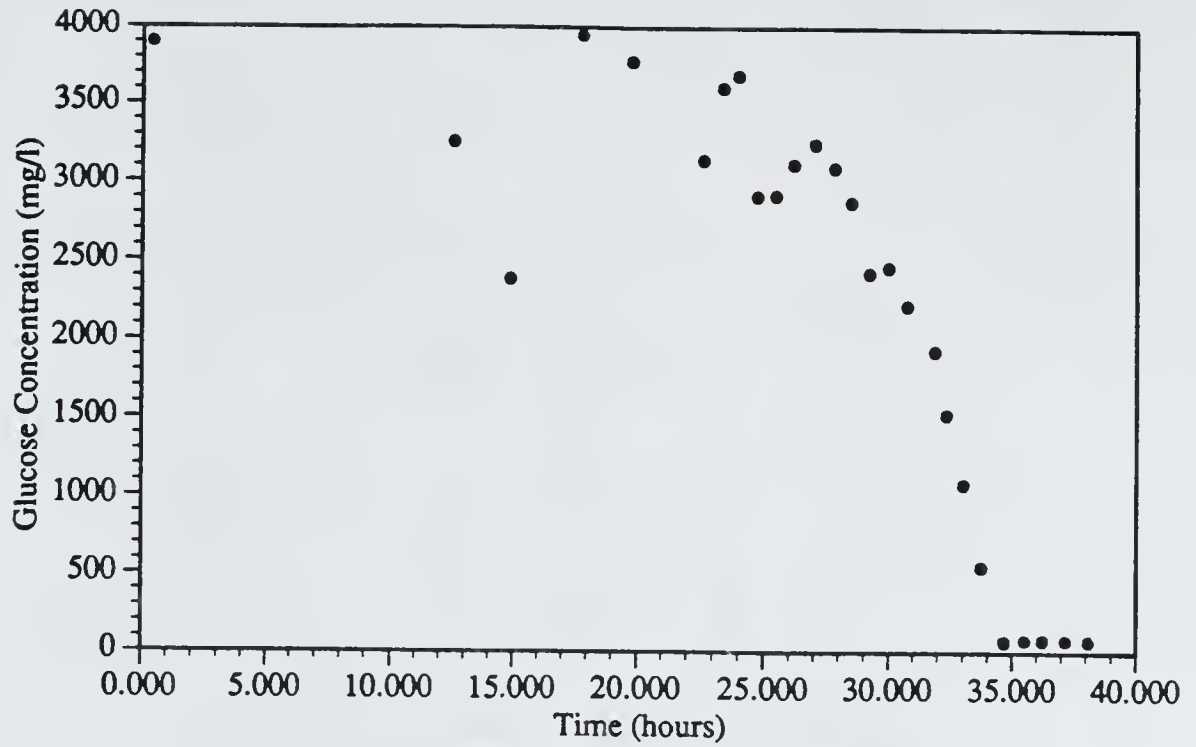


Figure 20. Anaerobic batch run 4. Glucose concentration against time.

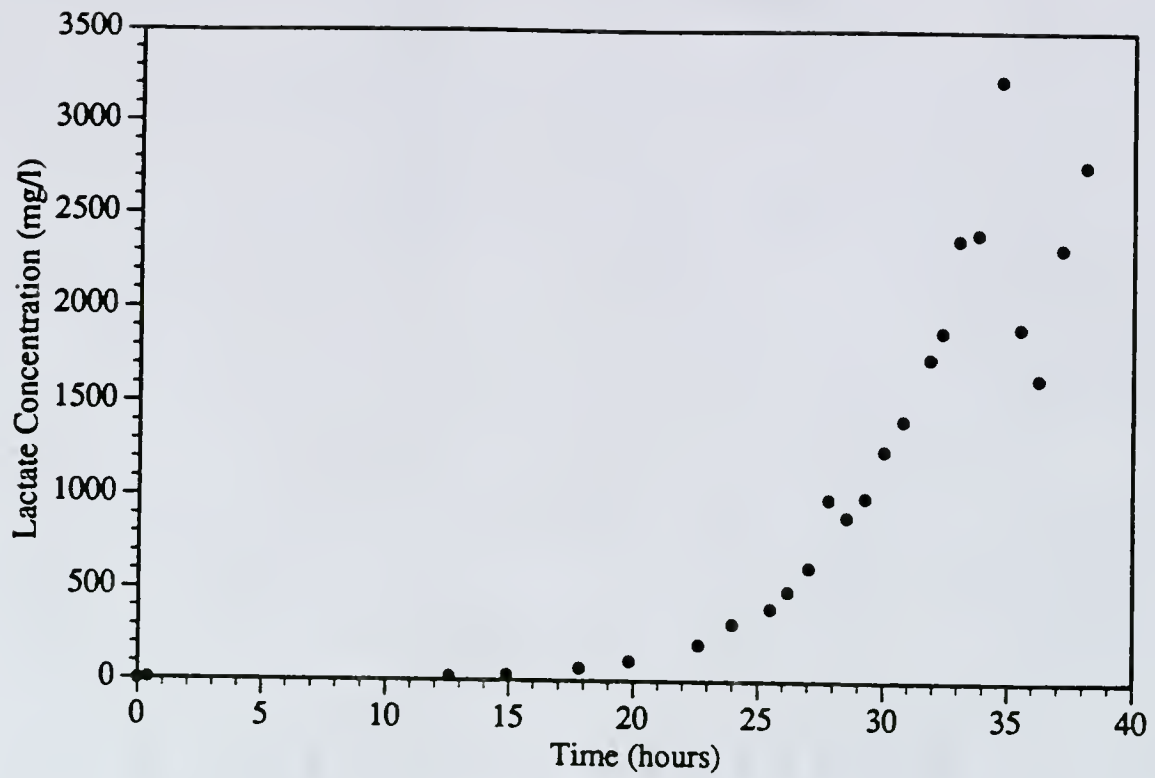


Figure 21. Anaerobic batch run 4. Lactate concentration against time.

4.3 Continuous Growth

All continuous anaerobic experiments were run with the standard feed medium shown in table 1. In all of the following discussions of continuous results, time 0 represents the point at which the reactor was inoculated. The point of switch from batch to continuous operation will be mentioned for each run. It should be reemphasized that all of the continuous runs were started as anaerobic batch runs. The switching point was chosen on the basis of reactor turbidity so as to avoid washout and glucose exhaustion. The results for one of the anaerobic continuous experiments, anaerobic continuous run 1, are shown in figures 22-25. This experiment was performed at a dilution rate of 0.164 hr^{-1} . (Dilution rate is defined as the ratio of flowrate to reactor volume. In reactor engineering terminology, this represents the reciprocal of the residence time.) The switch to continuous operation in this run was done at 83 hours. In figure 22, it is seen that a steady state, defined as where the state variables of the system are unchanging, was seen at approximately 108 hours. Data collected past 130 hours show surprising results and these will be presented and discussed in Chapter 8. Some of the results of another continuous anaerobic experiment (with dilution rate of 0.17 hr^{-1}), anaerobic continuous run 2, are shown in figures 26 and 27. The increased number of data taken at the switch point show the smooth change in system condition from batch to continuous operation. In this experiment, a steady state was seen at approximately 44 hours.

Values for the averaged apparent steady-state values for various dilution rates of cell number, biomass, lactate and glucose concentrations are given in table 4. These values were taken from the shown continuous experiments along with other continuous anaerobic experiments. The results show low values for residual glucose concentration and high conversions to lactate. The biomass concentration is also consistently low. Surprisingly, the biomass concentration seemed to rise with dilution rate, which is not in agreement with normal Monod behavior. These increases were not very large though. In contrast to biomass, glucose did follow the expected Monod behavior of increasing with dilution rate.

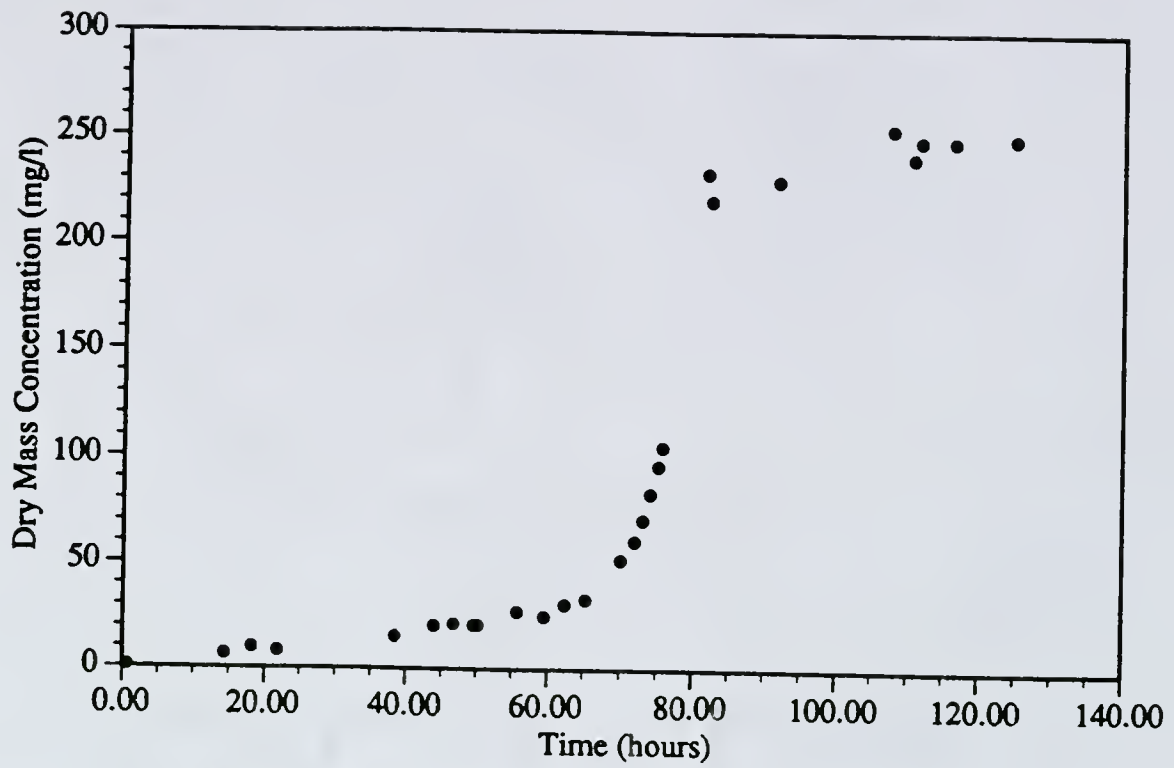


Figure 22. Anaerobic continuous run 1. Biomass concentration against time.

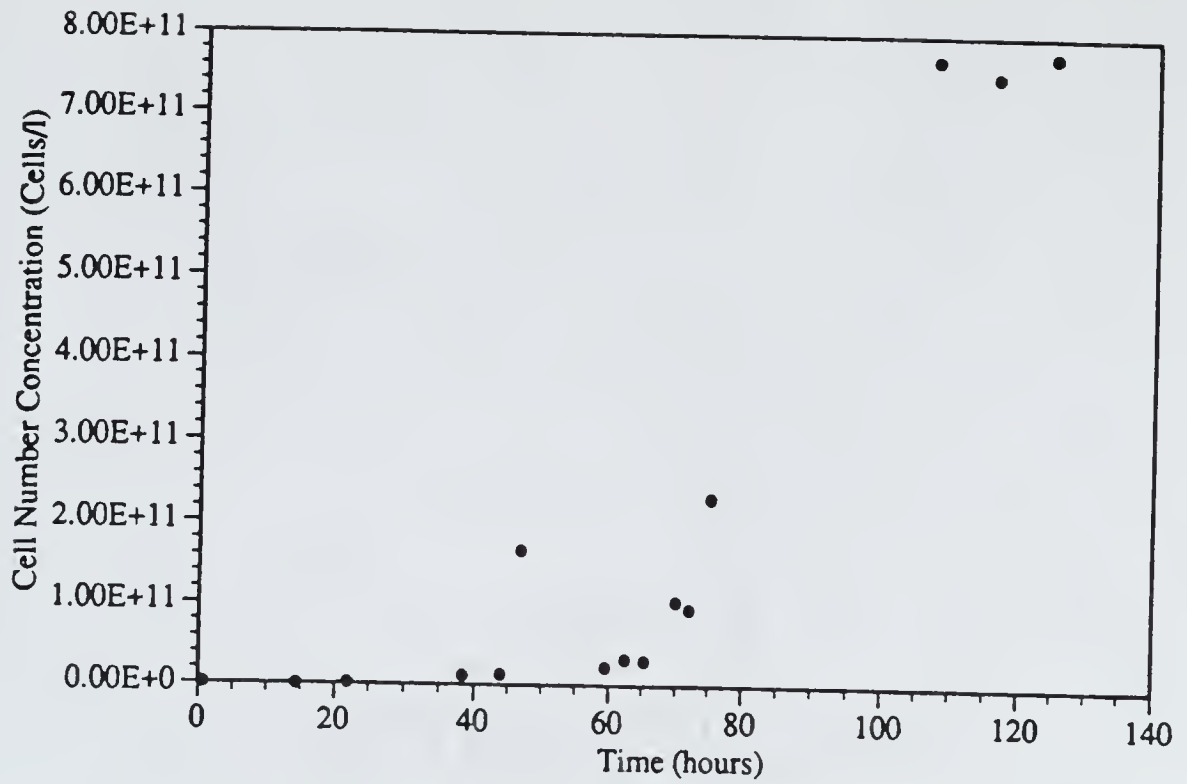


Figure 23. Anaerobic continuous run 1. Cell number concentration against time.

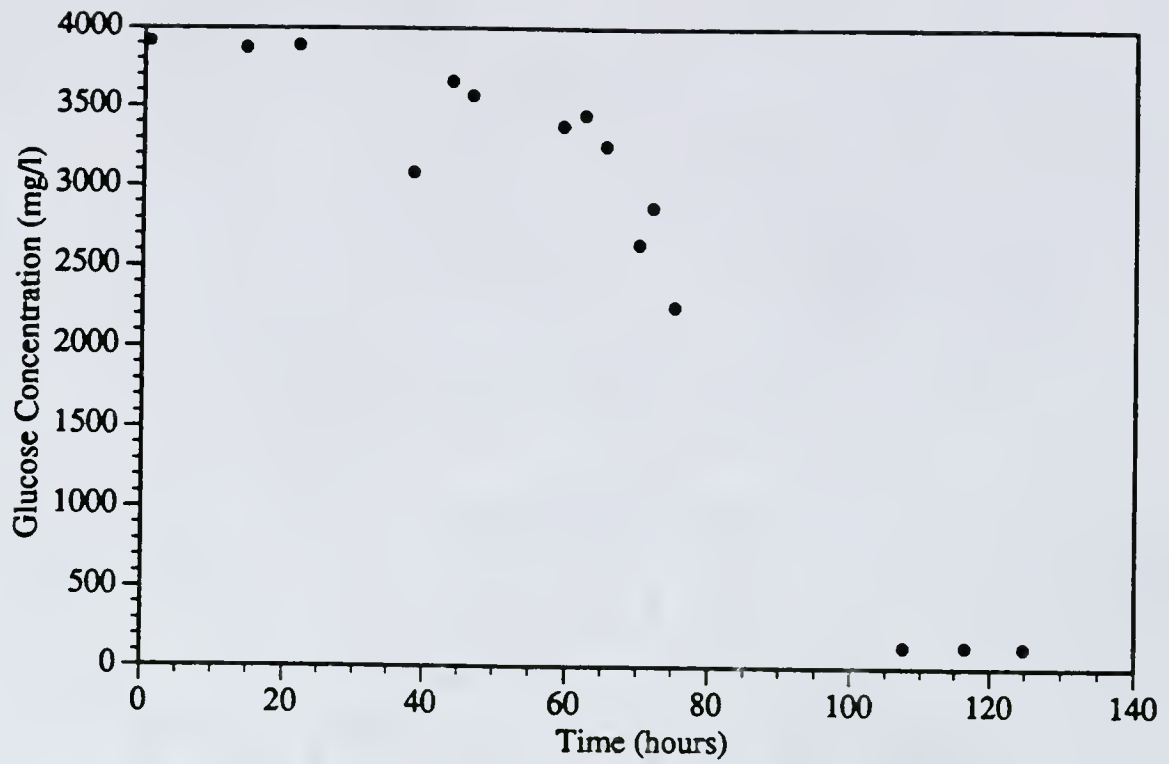


Figure 24. Anaerobic continuous run 1. Glucose concentration against time.

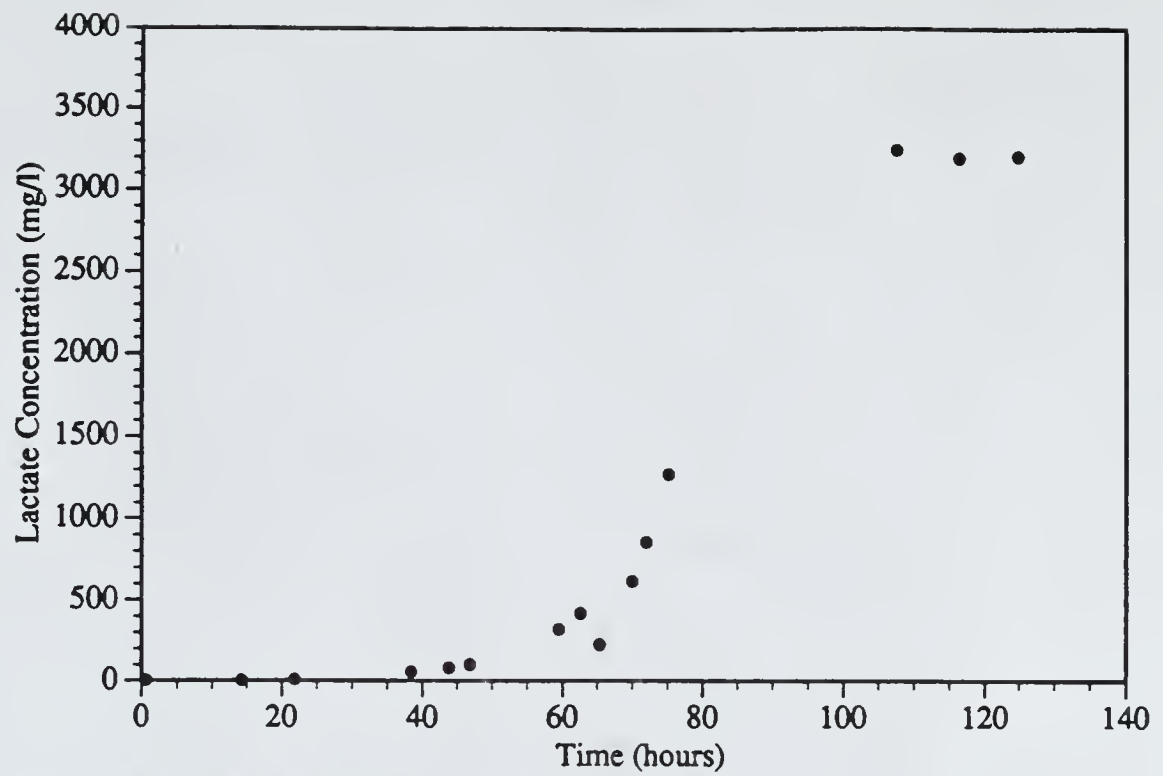


Figure 25. Anaerobic continuous run 1. Lactate concentration against time.

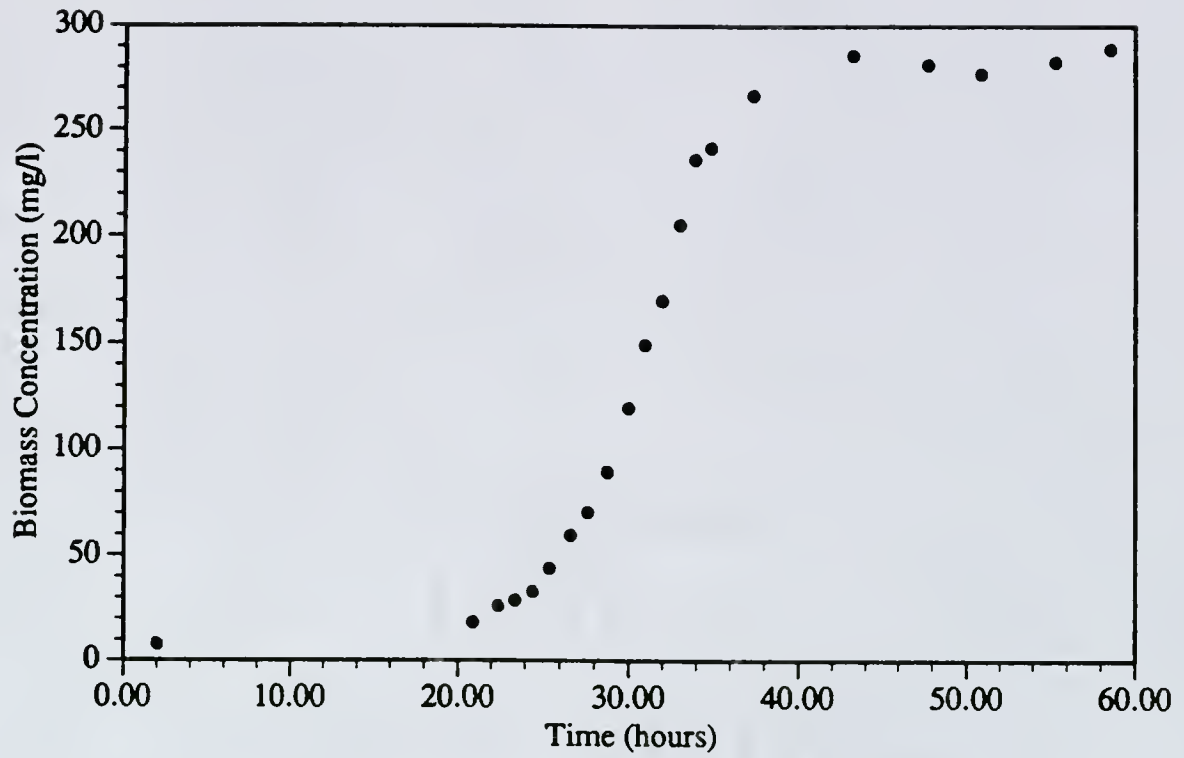


Figure 26. Anaerobic continuous run 2. Biomass concentration against time.

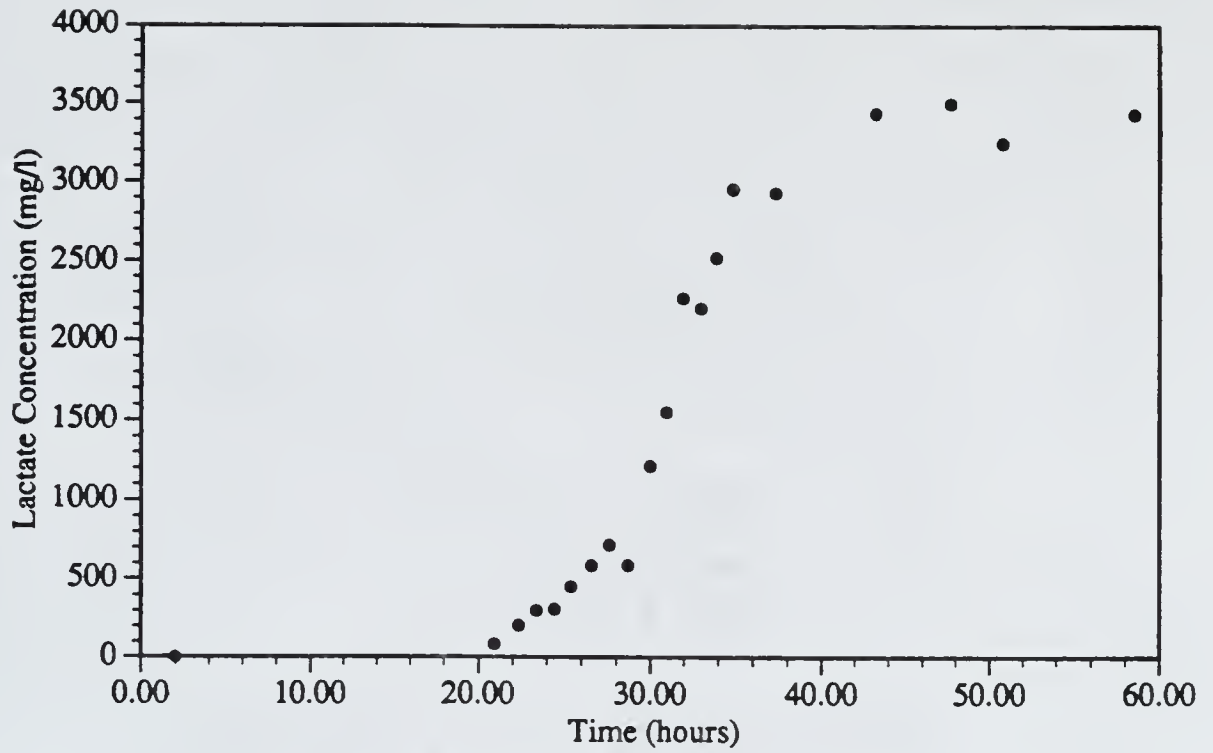


Figure 27. Anaerobic continuous run 2. Lactate concentration against time.

Table 4. Apparent Anaerobic Continuous Steady States

Dilution Rate	Biomass	Cell Number	Glucose	Lactate
	Concentration	Concentration	Concentration	Concentration
(hr ⁻¹)	(mg/l)	(cells/l)	(mg/l)	(mg/l)
.17	283			3402
.164	248	7.65x10 ¹¹	136	3214
.13	240	6.7x10 ¹¹	86	3397

4.4 Modeling

4.4.1 Presentation of Model

The following model was proposed to describe this system under batch anaerobic conditions during exponential growth

$$\dot{x} = \frac{\mu_{\max, \text{anaerobic}} S}{K_{s, \text{anaerobic}} + S} x \quad (27)$$

$$\dot{s} = -\frac{1}{Y_{x/s, \text{anaerobic}}} \frac{\mu_{\max, \text{anaerobic}} S}{K_{s, \text{anaerobic}} + S} x \quad (28)$$

$$\dot{p} = \alpha \frac{\mu_{\max, \text{anaerobic}} S}{K_{s, \text{anaerobic}} + S} x \quad (29)$$

where \dot{q} = time derivative of q

x=biomass (dry mass) concentration in the reactor

s=substrate (glucose) concentration in the reactor

p=product (d-lactate) concentration in the reactor

$\mu_{\max, \text{anaerobic}}$ =maximum growth rate under anaerobic conditions

$K_{s, \text{anaerobic}}$ =saturation parameter under anaerobic conditions

$Y_{x/s, \text{anaerobic}}$ =yield of biomass on substrate under anaerobic conditions

α =growth-associated lactate production parameter

The first model equation, equation 27, shows simple Monod dependence of biomass growth rate on glucose concentration. Equation 28, representing the time derivative of glucose concentration, was chosen with the assumption that all glucose consumed during exponential growth was consumed for the purpose of producing biomass. The third equation, equation 29, gives the time derivative of d-lactate concentration in such a system.

It was assumed that the d-lactate production under exponential growth conditions was strictly anaerobically growth-associated.

A continuous form of this model is as follows

$$\dot{x} = \frac{\mu_{\max, \text{anaerobic}} S}{K_{s, \text{anaerobic}} + S} x - Dx \quad (30)$$

$$\dot{s} = -\frac{1}{Y_{x/s, \text{anaerobic}}} \frac{\mu_{\max, \text{anaerobic}} S}{K_{s, \text{anaerobic}} + S} x + D(s_F - s) \quad (31)$$

$$\dot{p} = \alpha \frac{\mu_{\max, \text{anaerobic}} S}{K_{s, \text{anaerobic}} + S} x - Dp \quad (32)$$

where $D = \text{dilution rate} = \frac{\text{Flowrate}}{\text{Volume}}$

$s_F = \text{feed substrate (glucose) concentration}$

The above continuous form of the model was developed for a continuous stirred tank reactor under conditions of perfect mixing. No biomass or product was introduced in the feed, so no feed lactate or biomass was accounted for in this model. Inlet substrate was accounted for in the substrate equation. The equations were simply extensions of equations 27-29 with additional terms for dilution of the biomass, substrate, and product out of the reactor.

4.4.2 Model Parameter Fitting

The batch run measurements were the primary ones used for parameter computation. The primary justification for this was that the anaerobic continuous runs described previously were not performed until the ending of this work. Also, they showed problems with reversion, which will be described in a later chapter, and measured steady states were difficult to find. The parameters used in later modeling will be given here, along with justification for their determination. Improved values for model parameters are

also given, but these were not the ones used in designing the later cycling operations still to be described.

The first parameters to be discussed are the maximum growth rate, $\mu_{\max, \text{anaerobic}}$, and the saturation constant, $K_{s, \text{anaerobic}}$. These parameters would usually be determined by use of a Lineweaver-Burke plot [56, p.106] of continuous data. In these types of plots, a large number of continuous steady states are necessary. Under steady-state conditions, the time derivatives of the continuous form of the model are all equal to zero. By manipulation of the steady-state version of 30, the following relation can be obtained

$$\frac{1}{D} = \frac{K_{s, \text{anaerobic}}}{\mu_{\max, \text{anaerobic}}} \frac{1}{s_{ss}} + \frac{1}{\mu_{\max, \text{anaerobic}}} \quad (33)$$

where s_{ss} =steady-state residual glucose concentration in the reactor

A plot could then be made of reciprocal dilution rate against reciprocal residual glucose concentration. A least-squares fit would then be made to the data. The intercept would be equivalent to the reciprocal of the maximum anaerobic growth rate, and the slope would be equal to the saturation parameter divided by the maximum anaerobic growth rate.

Unfortunately, due to the reversion problems mentioned above, it was very difficult to obtain continuous steady-state data. Equation 33 can be used on one data point to find one of the two unknown parameters if the other can be satisfactorily estimated. It can be seen that at a dilution rate equal to half of the maximum growth rate, the residual substrate in the reactor is equal to $K_{s, \text{anaerobic}}$. In anaerobic batch run 3 the dry-mass growth rate was 0.190 hr^{-1} and in anaerobic batch run 4 it was 0.23 hr^{-1} . These were obtained by simple exponential fitting of the biomass data during exponential phase. For example, the data used to calculate anaerobic batch run 3's growth rate was the dry mass data taken between 16 and 27 hours. The correlation coefficient for the fit (R^2) was greater than 0.99. It was assumed that these growth rates were at the maximum, as the glucose concentration was very high during most of the duration of the runs. Were this not the case, the R^2 would not

have been so close to 1. For the sake of consistency, anaerobic batch run 3 was the run that served as the source of the data used for fitting model parameters. The reason why this run was chosen over anaerobic batch run 4, was that the run 4's growth rate of 0.23 hr^{-1} was significantly higher than that seen in other experiments performed. Most experiments, including anaerobic batch run 1 and 2, indicated growth rates of the culture having values between 0.19 and 0.20 hr^{-1} . Therefore, the final value of $\mu_{\text{max, anaerobic}}$ used was 0.190 hr^{-1} . The two $K_{\text{s, anaerobic}}$ parameters then calculated using equation 33 for the anaerobic continuous steady states given in table 4 are then 22.4 and 40.4 mg/l for dilution rates 0.164 and 0.13 hr^{-1} , respectively. An average $K_{\text{s, anaerobic}}$ of 31.4 mg/l would then be the apparent value to be used. For several of the simulations described later the anaerobic continuous experiments had not yet been performed. For these, a $K_{\text{s, anaerobic}}$ value of 98 mg/l , based on preliminary continuous data using the feed medium listed in table 2, was used for several of the later simulations in this dissertation. Use of the revised parameter value of 31.4 mg/l is suggested for future work with this model.

The next parameter to be determined was the yield of biomass on glucose under anaerobic conditions, $Y_{\text{x/s, anaerobic}}$. Using equations 30 and 32 and the assumption of steady state the following relation for continuous operation can be stated

$$x_{\text{ss}} = Y_{\text{x/s, anaerobic}}(s_{\text{F}} - s_{\text{ss}}) \quad (34)$$

where x_{ss} = steady-state biomass concentration in the reactor

Using this relation, yield values of $.064$ and $.061 \frac{\text{mg biomass}}{\text{mg glucose}}$ were indicated for dilution rates 0.164 and 0.13 hr^{-1} , respectively. Anaerobic batch run 3 was the base run used and the biomass yield was computed for this using a material balance argument which is very similar to equation 34.

$$x = Y_{\text{x/s}}(s_0 - s) \quad (35)$$

where s_0 =initial glucose concentration in the batch

In figure 28, a plot of biomass against consumed substrate is shown. The line fit to the data and forced through zero is also exhibited. The slope of this line gives the value of $Y_{x/s, \text{ anaerobic}}$ determined by this experiment. The fit indicates a yield value of $0.063 \frac{\text{mg biomass}}{\text{mg glucose}}$. However, as can be seen from the large amount of scatter around the line, this was not a very good fit. The correlation coefficient for this curve, R^2 , was only 0.90. Since the correlation coefficient was so low, the yield used in calculation was computed by simply averaging the biomass concentrations found in the stationary phase and dividing the average by the initial glucose concentration of 4000 mg/l. The yield computed in this manner was $0.068 \frac{\text{mg biomass}}{\text{mg glucose}}$. This was the value used in the modeling work. The fit value of $0.063 \frac{\text{mg biomass}}{\text{mg glucose}}$ turned out to be in good agreement with the later continuous results, and, thus, this result should be used in the future.

The final parameter to be discussed for the anaerobic model is the anaerobic growth associated lactate production parameter, α . Using equations 30, 32, and the steady-state assumption, the following continuous steady-state relationship holds

$$\alpha = \frac{P_{ss}}{x_{ss}} \quad (36)$$

where p_{ss} =steady-state product (d-lactate) concentration

The continuous runs indicate values for α of 12.02, 12.95, and $14.15 \frac{\text{mg d-lactate}}{\text{mg biomass}}$ for dilution rates of 0.17, 0.164, and 0.13 hr^{-1} , respectively. The variability in these values is quite large and leaves some of the d-lactate measurements in question. The determination of α for a batch run is done by using equation 27 and equation 29 to obtain

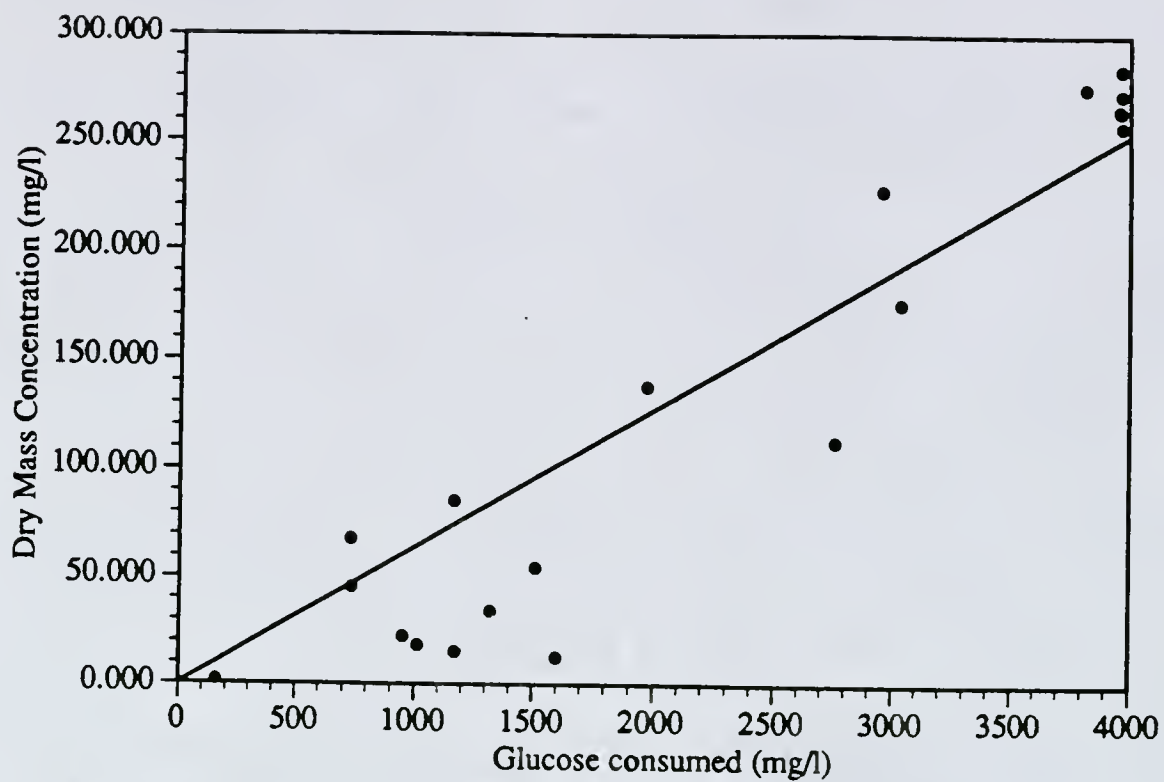


Figure 28. Anaerobic batch run 3. Biomass concentration against glucose consumed.

$$\dot{p} = \alpha \dot{x} \quad (37)$$

Subsequent integration yields

$$p = \alpha x + p_0 + \alpha x_0 \quad (38)$$

where p_0 = initial d-lactate concentration

x_0 = initial biomass concentration

The slope of a plot of biomass against d-lactate concentration during exponential phase for a batch run is equivalent to the α parameter. This plot for anaerobic batch run 3 is shown in figure 29, along with the results of a linear least squares fit to the data. The problem with this method is that, due to the scatter of the d-lactate values seen in figure 29, the final value is very dependent on where exponential phase is declared to begin. For example, if all of the data that were used for the computation of anaerobic batch run 3's growth rate was used, an α parameter of 8.64 mg/mg (with a correlation coefficient, R^2 , of only 0.88) would be the determined value. This correlation coefficient was unacceptably low. If the last data point, due to its questionable reliability, was ignored the α parameter value increased to 9.64. If the only points considered on this figure were those between 100 and 250 mg/l biomass, an α parameter of 16.7 mg/mg would be found. Due to all of this scatter, a batch value for α had to be determined by another batch run. Anaerobic batch run 4, in spite of its high growth rate, was then examined and used to obtain an estimate of α . The results of the corresponding lactate against biomass curve are presented in figure 30, along with linear least squares fitting results. The data showed a much higher degree of linearity than that seen for anaerobic batch run 3. The α parameter fit for these data was 10.8 with a correlation coefficient, R^2 , of 0.98. This was the value used in later simulations. Upon comparison of this value with those given by the continuous runs, this

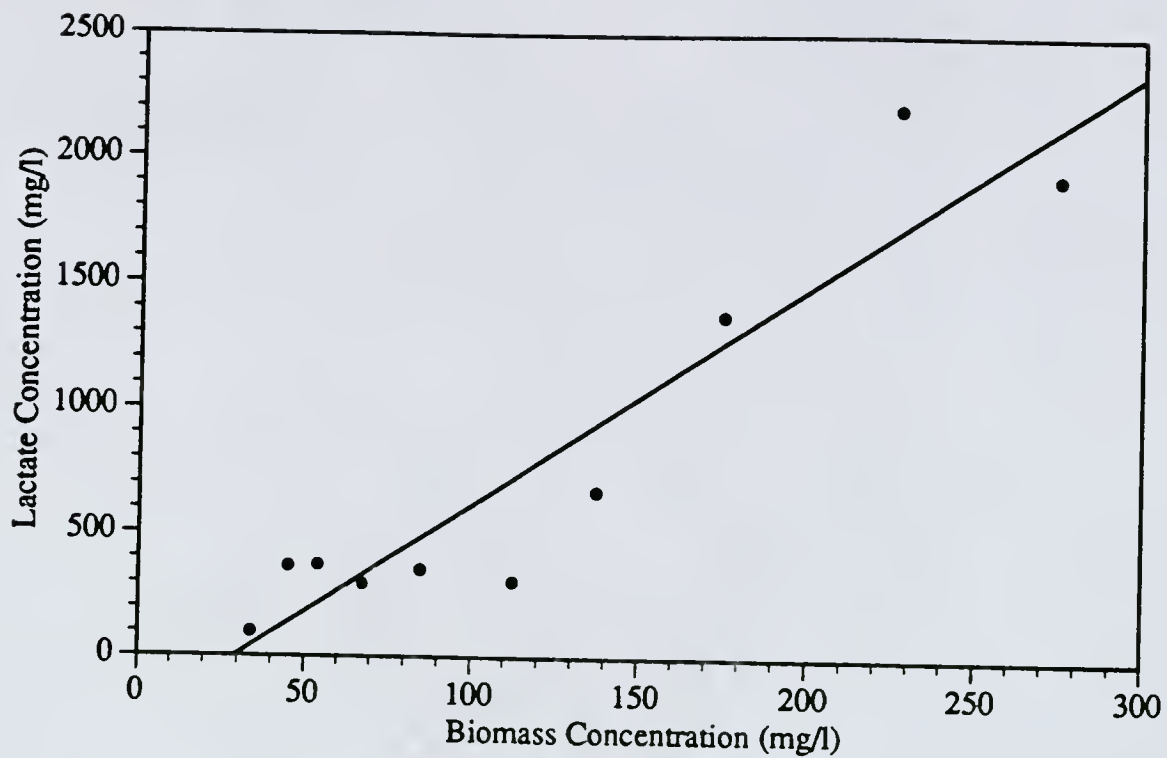


Figure 29. Anaerobic batch run 3. Lactate concentration against biomass concentration.

value for α would underpredict lactate concentration by approximately 20%. Increased values of α should be considered in future use of the model.

The parameter values are summarized in table 5. The suggested revised α parameter was based on averaging the results for the determined α parameters of the three continuous experiments. The large differences in updated parameter values for yield, saturation and α parameters suggested that use of the model in designing any operation must be checked for sensitivity to these parameters.

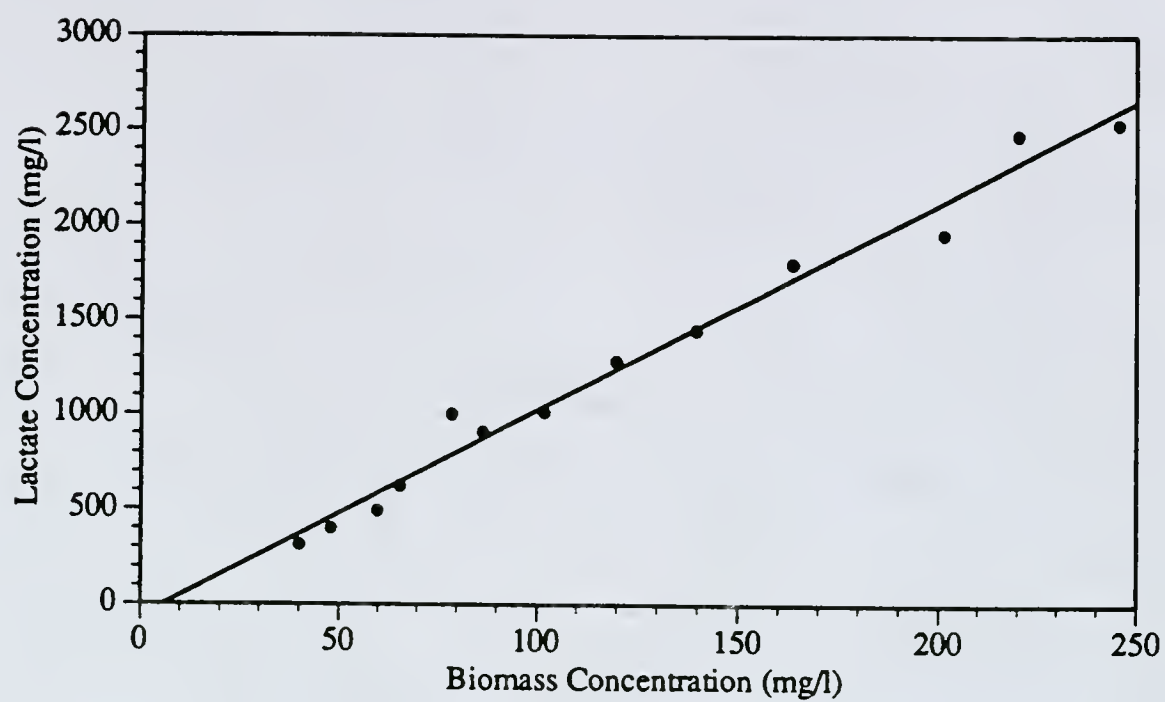


Figure 30. Anaerobic batch run 4. Lactate concentration against biomass concentration.

Table 5. Anaerobic Model Parameter Values

Parameter	Value used in later work	Possible improvement
$\mu_{\text{max, anaerobic}}$.19 hr ⁻¹	.19 hr ⁻¹
$K_{\text{s, anaerobic}}$	98 mg/l	31.4 mg/l
$Y_{\text{x/s, anaerobic}}$.068 mg/mg	.063 mg/mg
α	10.77 mg/mg	13 mg/mg

CHAPTER 5 AEROBIC GROWTH OF *E. COLI* LCB898

5.1 Background

Under aerobic conditions most facultative aerobes, such as *E. coli*, will adjust their metabolism to take advantage of available oxygen and increase its production of biomass.

The first part of aerobic metabolism of glucose is production of pyruvate. This part was described in the previous chapter on anaerobic growth. The only major difference to be mentioned here is that 25% of the glucose will enter the pentose-phosphate pathway under aerobic conditions [50,51]. Where the major difference between fermentation and aerobic respiration on glucose lies, is in the fate of pyruvate. The aerobic metabolism of glucose for a wild-type *E. coli* is shown in figure 31 [49, p. 155, 45]. The aerobic metabolism of *E. coli* LCB898 shouldn't deviate significantly from this as no significant aerobic metabolism genes are mutated in its genome. Pyruvate dehydrogenase, which is only produced aerobically [39], is the enzyme responsible for aerobic conversion of pyruvate to acetyl-CoA. After it is formed, acetyl-CoA is sent through the TCA cycle. In the TCA cycle only one ATP molecule (per molecule of pyruvate) is produced by substrate-level phosphorylation, specifically the conversion of succinyl-CoA to succinate [48, p. 54]. All of the other ATP molecules are generated by oxidative phosphorylation, where the energy is produced by the transfer of electrons from NADH, NADPH, and FADH₂ to oxygen [49]. As can be seen in figure 31, from each turn of the cycle two molecules of NAD⁺, one of NADP⁺, and one of FAD⁺ are reduced, with one additional NAD⁺ reduction occurring in the conversion of pyruvate to acetyl-CoA. In *E. coli*, two molecules of ATP can be generated for each molecule of NADH or NADPH, and one molecule of

ATP can be produced for each molecule of FADH_2 oxidized [48, p. 43]. To sum up, ten molecules of ATP can be produced, when the TCA cycle is employed, for every molecule of pyruvate processed. When one adds, per glucose molecule, the two ATP molecules generated by fermentation, the 2 ATP's that can be generated from the 2 molecules of NADH produced (and not needed in d-lactate formation) and the TCA generated ATP's from the two pyruvate molecules formed, 26 molecules of ATP can be produced for every glucose molecule, as opposed to the synthesis of just two molecules of ATP for each glucose molecule strictly fermented.

Of course, these ATP yields are theoretical. Fermentative efficiency can be as high as 50%, as opposed to the TCA cycle efficiency of 39% [47, p. 134]. Nonetheless, even though pure fermentation has higher efficiency, the aerobic metabolism will give much higher amounts of ATP per glucose molecule consumed than will pure fermentation. Since growth requires ATP for energy, aerobic growth should show higher biomass yields on glucose.

There are two main products of aerobic growth of *E. coli* on glucose, specifically biomass and CO_2 [57, p.802]. Three CO_2 molecules are produced by the TCA degradation of each pyruvate molecule, and thus 6 CO_2 molecules are produced for every glucose used strictly for catabolism.

5.2 Experimental and Modeling Results Introduction

Most of the aerobic experiments were performed in conjunction with a master's thesis project performed by Christina Stalhandske [58]. The experiments were jointly performed by this author and Stalhandske and the modeling work, while contained in that work, was mostly performed by this author. Thus, most of the results, both experimental and modeling, are taken from this thesis.

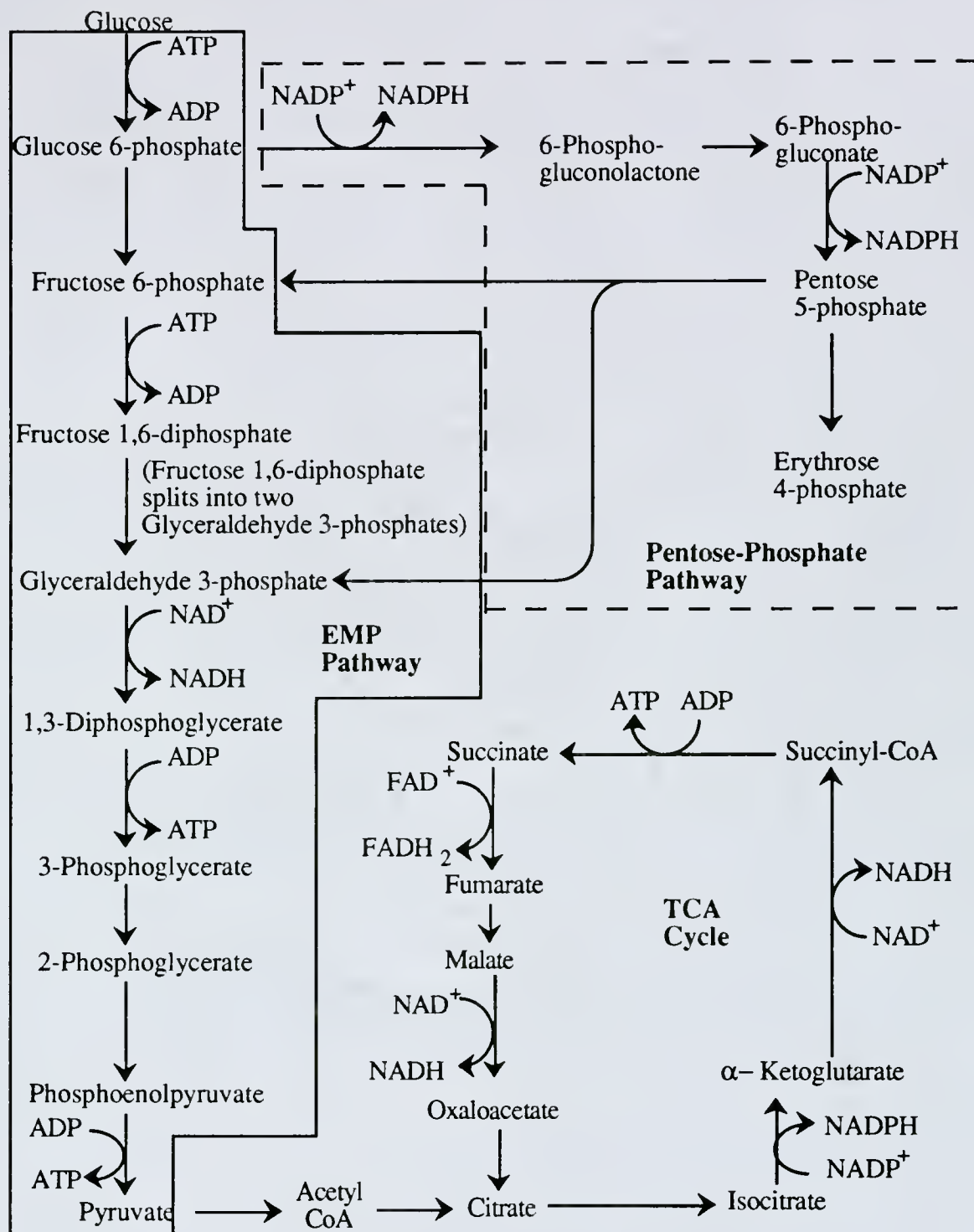


Figure 31. Main Aerobic Biochemical Pathways in *E. coli* LCB898

5.3 Batch Growth

In all of the following discussed batch results, time 0 represents the point at which the reactor was inoculated. The results for one of the aerobic batch runs, to be designated aerobic batch run 1, are shown in figures 32-35. This was one of the preliminary runs to help determine a final feed composition. As can be seen from figure 32, glucose was not exhausted when biomass concentration stopped rapidly increasing at 14 hours. Biomass did increase slightly after 14 hours, but not in an exponential manner. Glucose did continue to drop, but it is hypothesized that this glucose was largely used for maintenance. Amino acid analysis showed that threonine was exhausted before glucose. The lactate and ethanol concentrations of each sample were measured to see if they were produced in a significant amount. These quantities turned out to be negligible. Thus, in the following strictly aerobic batch and continuous runs ethanol and lactate measurements were not measured regularly.

The results of a batch run with sufficient amino acids, aerobic batch run 2, are shown in figures 36-38. This time the cells grew exponentially until glucose was exhausted, which indicated that glucose was the limiting substrate. It appeared that 15 hours after starting the run, cell number and biomass concentration stopped increasing in an exponential manner. Further increases in dry mass can be attributed to diauxy on remaining amino acids or acetate present.

5.4 Continuous Growth

All continuous aerobic experiments were operated with the standard feed medium. In all of the following discussed continuous results, time 0 represents the point at which the reactor was inoculated. The point of switch from batch to continuous operation will be mentioned. It should be reemphasized that all of the continuous runs were started as aerobic batch runs. The switching point was determined on the basis of turbidity and chosen so as to avoid washout and glucose exhaustion.

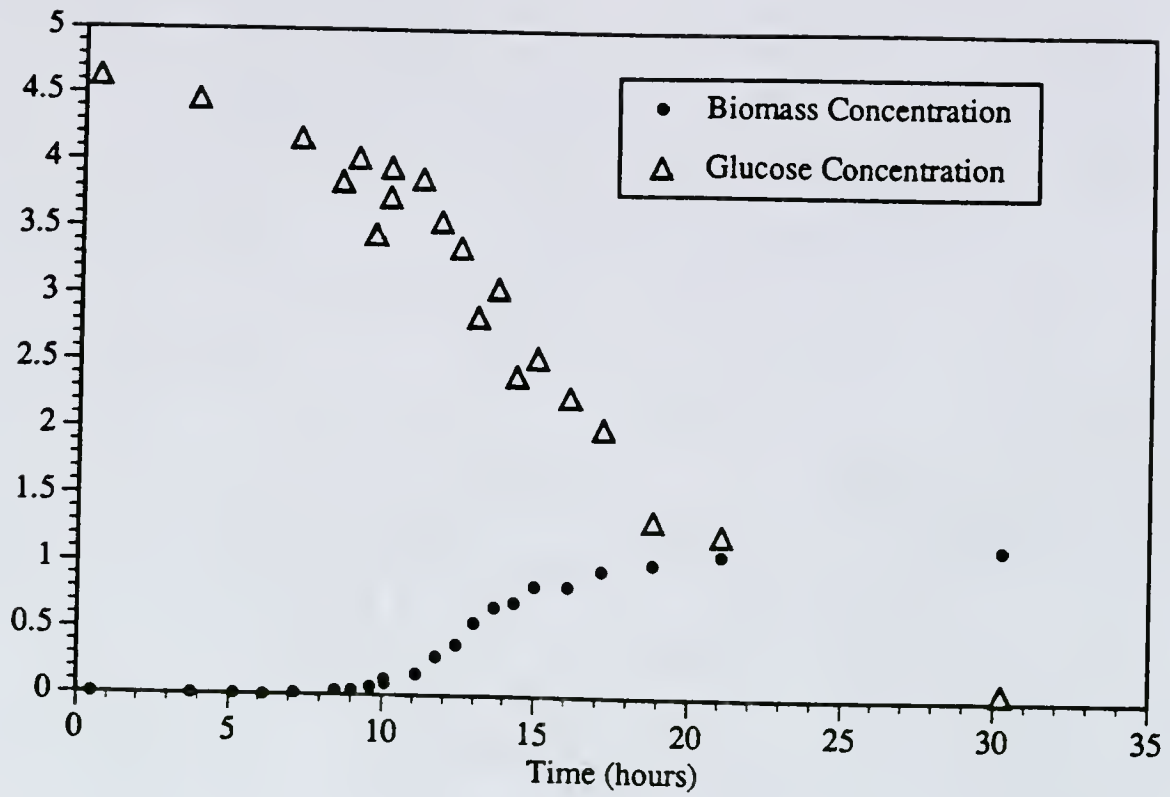


Figure 32. Aerobic batch run 1. Glucose and biomass concentration against time.

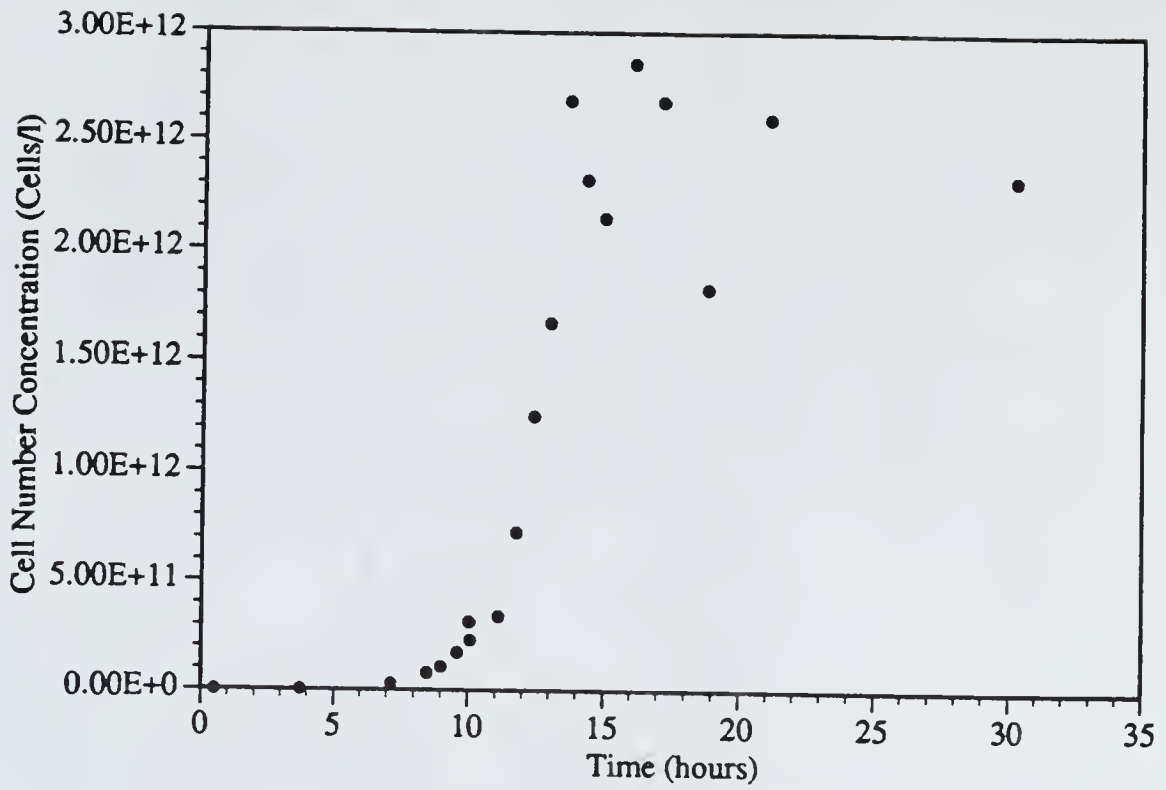


Figure 33. Aerobic batch run 1. Cell number concentration against time.

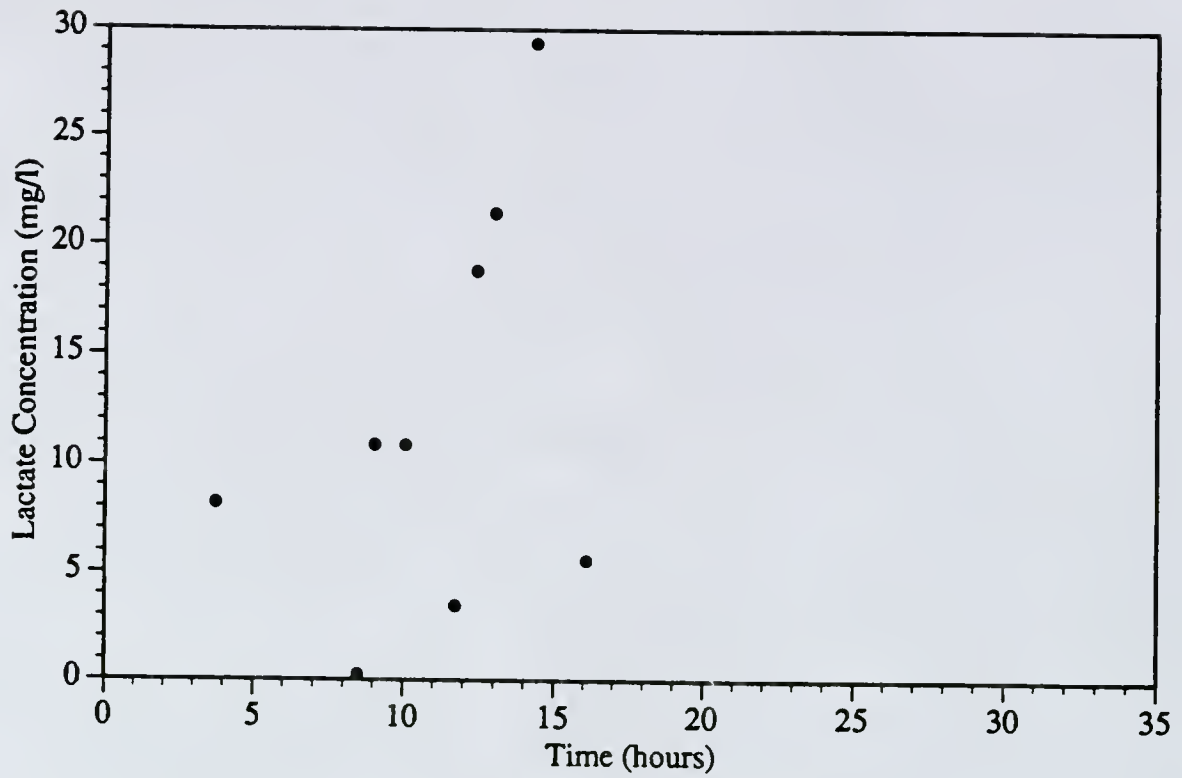


Figure 34. Aerobic batch run 1. Lactate concentration against time.

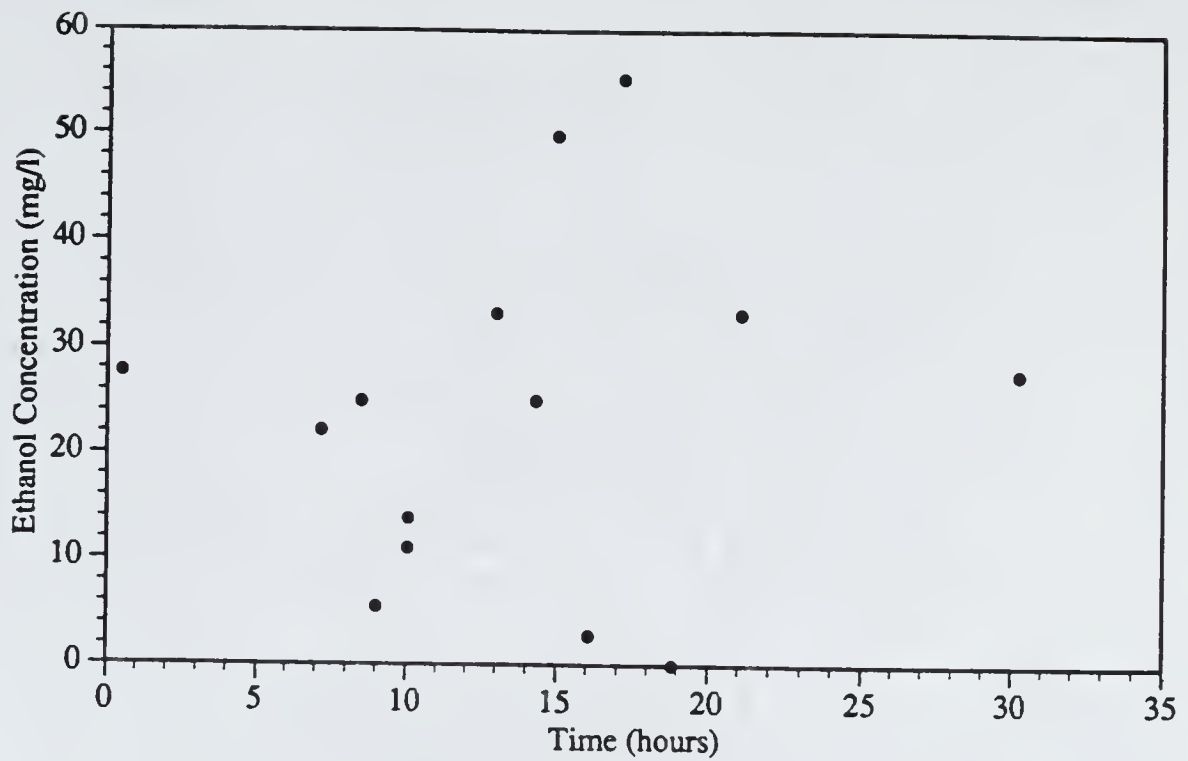


Figure 35. Aerobic batch run 1. Ethanol concentration against time.

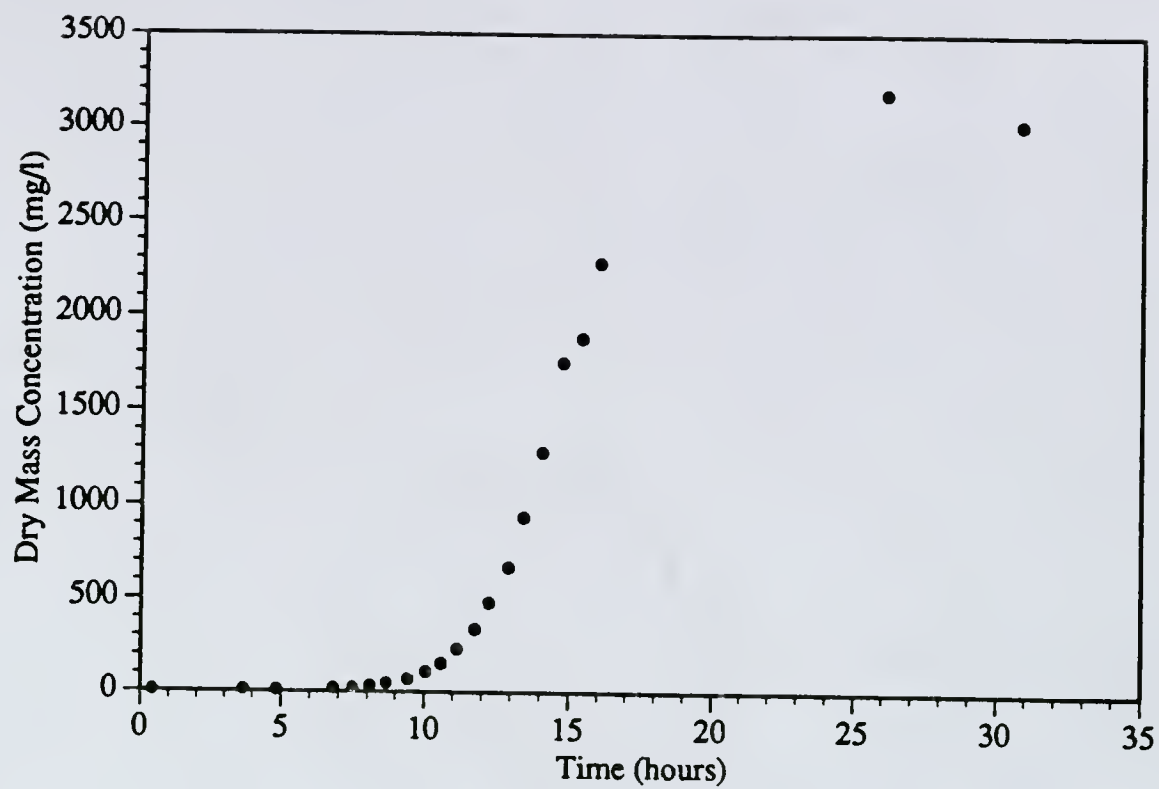


Figure 36. Aerobic batch run 2. Biomass concentration against time.

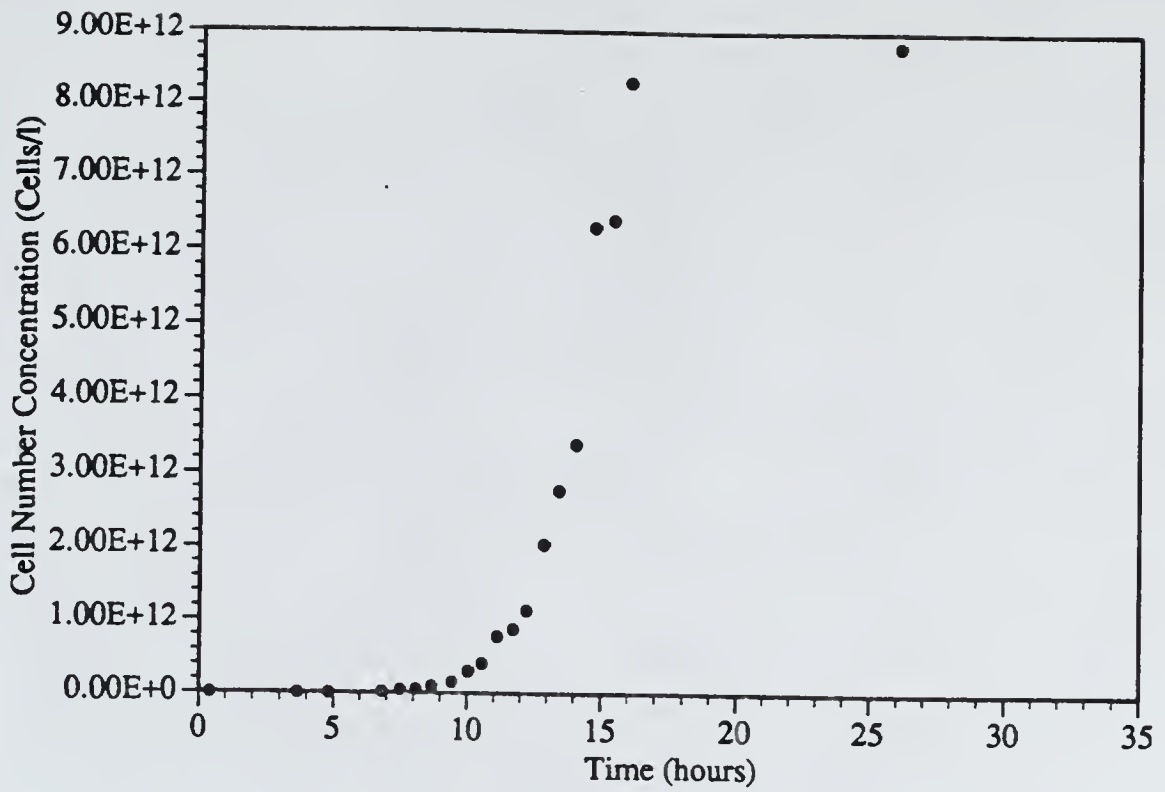


Figure 37. Aerobic batch run 2. Cell number concentration against time.

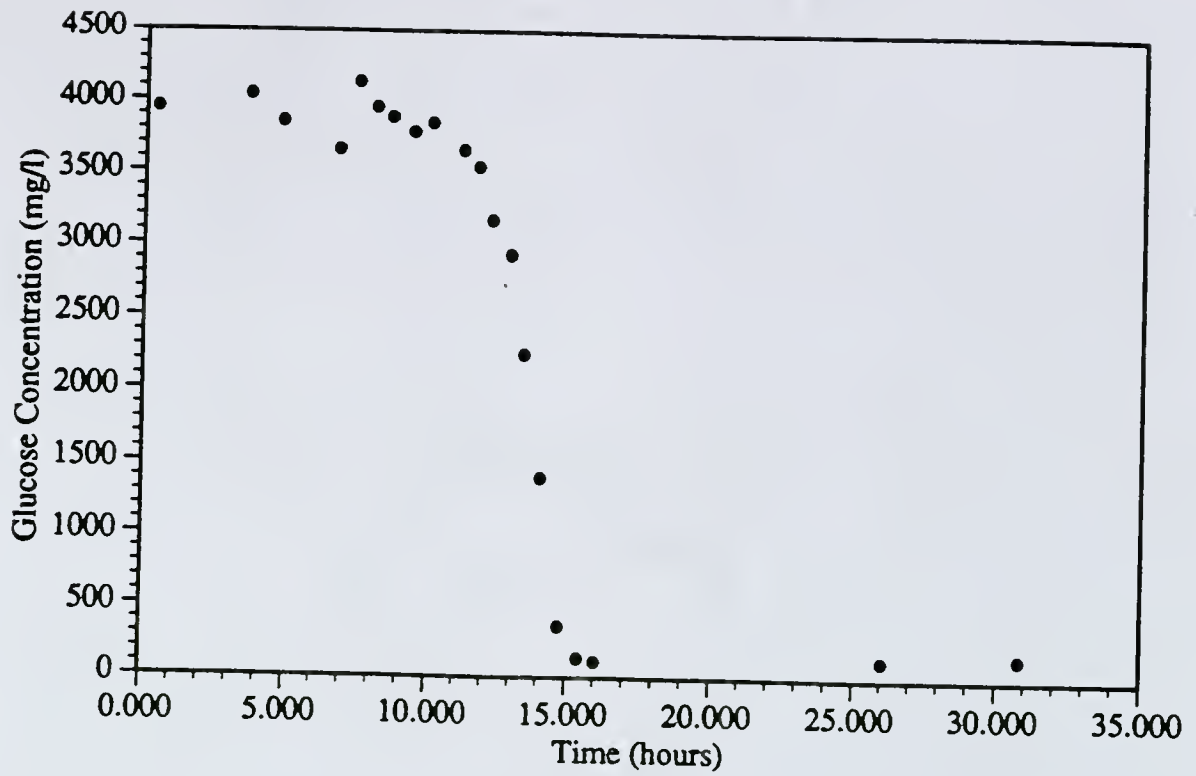


Figure 38. Aerobic batch run 2. Glucose concentration against time.

The results for one of the aerobic continuous experiments, aerobic continuous run 1, are shown in figures 39-41. This experiment was performed at a dilution rate of 0.335 hr^{-1} . The switch to continuous operation was done at 13.5 hours. In figure 39, it is seen that a steady state, defined as where the state variables of the system are unchanging, is reached at approximately 59 hours.

Values for the averaged apparent steady-state values for various dilution rates of cell number, biomass, glucose, and cell number concentrations are given in table 6. These values were taken from the shown experiments along with other continuous anaerobic experiments. All of the lactate measurements for these runs only showed trace amounts. The results show low values for residual glucose concentration. The biomass concentration is also consistently high. The biomass concentration dropped, the residual glucose concentration increased and the average cell size increased with increasing dilution rate. This behavior of the biomass and glucose concentration is in agreement with standard Monod behavior [59,11, p.101].

5.5 Modeling

5.5.1 Presentation of Model

The following model was proposed to describe this system under batch aerobic conditions during exponential growth

$$\dot{x} = \frac{\mu_{\max, \text{aerobic}} S}{K_{s, \text{aerobic}} + S} x \quad (39)$$

$$\dot{s} = -\frac{1}{Y_{x/s, \text{aerobic}}} \frac{\mu_{\max, \text{aerobic}} S}{K_{s, \text{aerobic}} + S} x \quad (40)$$

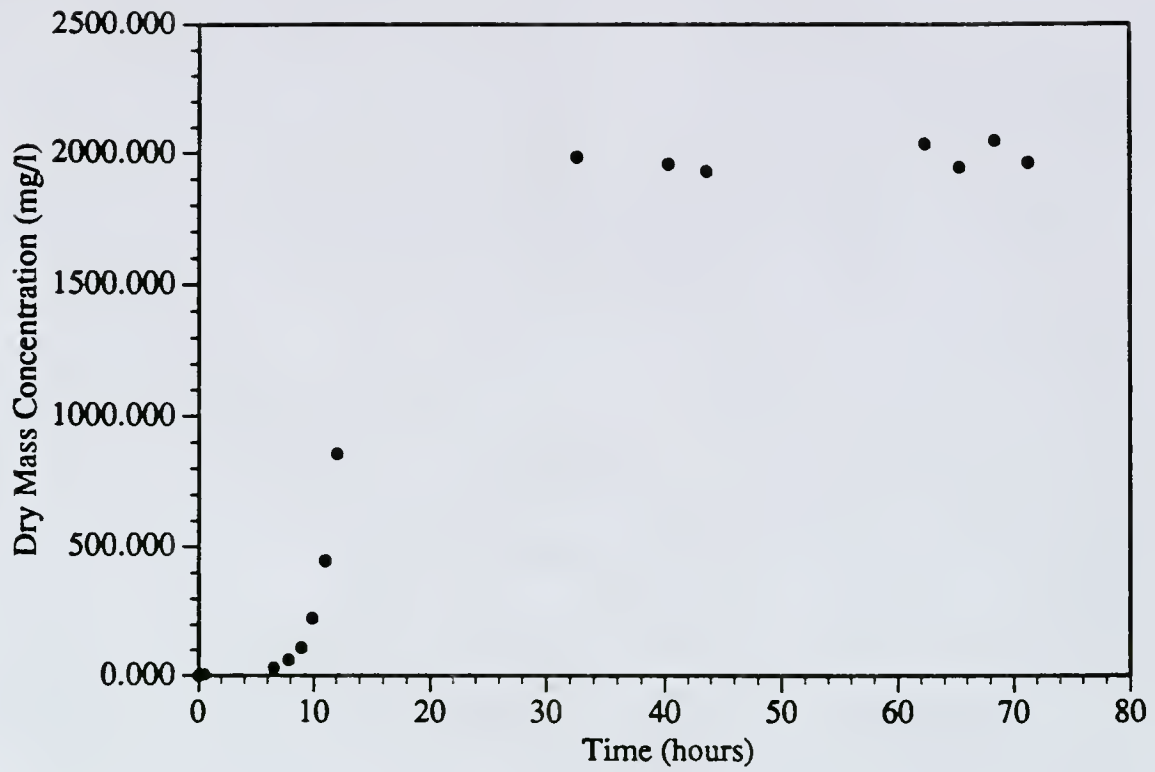


Figure 39. Aerobic continuous run 1. Biomass concentration against time. $D=.335 \text{ hr}^{-1}$

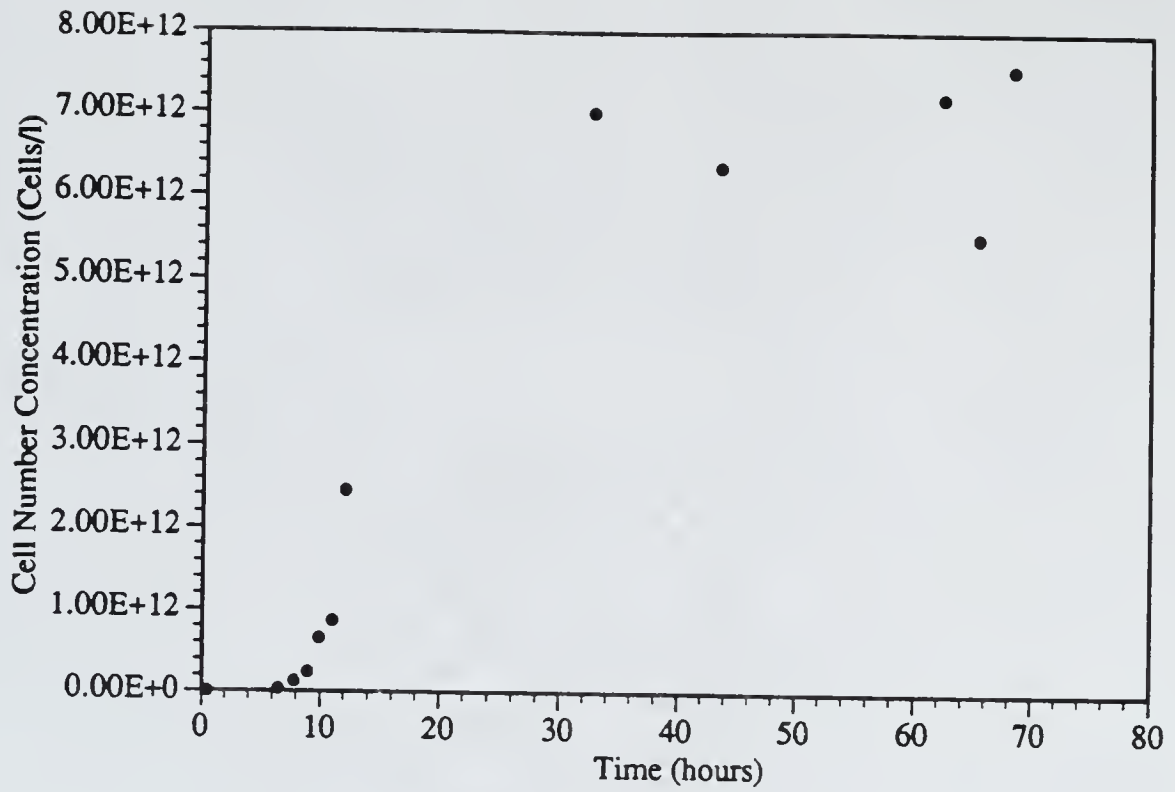


Figure 40. Aerobic continuous run 1. Cell number concentration against time. $D=0.335 \text{ hr}^{-1}$

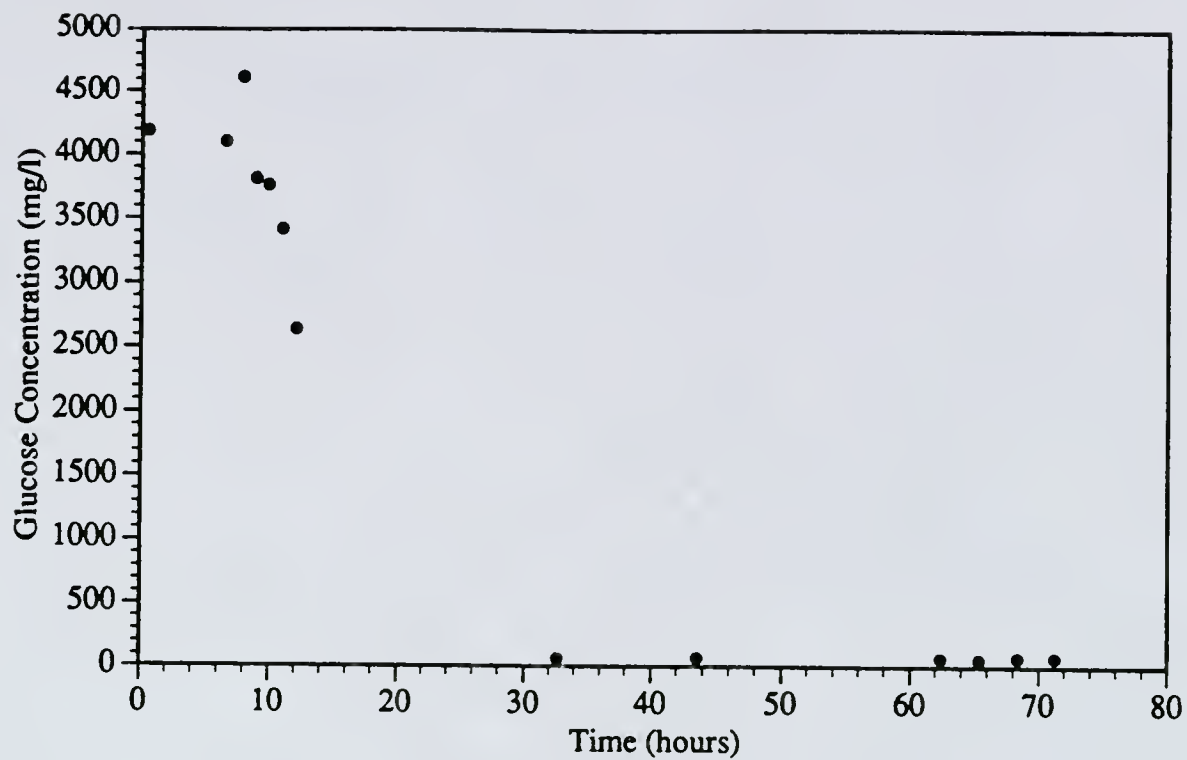


Figure 41. Aerobic continuous run 1. Glucose concentration against time. $D=0.335 \text{ hr}^{-1}$

Table 6. Apparent Aerobic Continuous Steady States

Dilution Rate (hr ⁻¹)	Biomass Concentration (mg/l)	Cell Number Concentration (cells/l)	Glucose Concentration (mg/l)	Per Cell Mass (mg)
.263	2200	1.2x10 ¹³	70	1.83x10 ⁻¹⁰
.45	1920	4.9x10 ¹²	203	3.92x10 ⁻¹⁰
.335	2000	6.7x10 ¹²	93	2.99x10 ⁻¹⁰

$$\dot{n} = \frac{\mu_{\max, \text{aerobic}} S}{K_{s, \text{aerobic}} + S} n \quad (41)$$

where \dot{q} = time derivative of q

x = biomass (dry mass) concentration in the reactor

s = substrate (glucose) concentration in the reactor

n = cell number concentration in the reactor

$\mu_{\max, \text{aerobic}}$ = maximum growth rate under aerobic conditions

$K_{s, \text{aerobic}}$ = saturation parameter under aerobic conditions

$Y_{x/s, \text{aerobic}}$ = yield of biomass on substrate under aerobic conditions

The first model equation, equation 39, shows simple Monod dependence of biomass growth rate on glucose concentration. Equation 40, representing the time derivative of glucose concentration, was chosen with the assumption that all glucose consumed during exponential growth was consumed for the purpose of producing biomass. Equation 41 is similar to 39, and was based on the assumption of constant cell mass.

A continuous form of this model is as follows

$$\dot{x} = \frac{\mu_{\max, \text{anaerobic}} S}{K_{s, \text{anaerobic}} + S} x - Dx \quad (42)$$

$$\dot{s} = -\frac{1}{Y_{x/s, \text{anaerobic}}} \frac{\mu_{\max, \text{anaerobic}} S}{K_{s, \text{anaerobic}} + S} x + D(s_F - s) \quad (43)$$

$$\dot{n} = \frac{\mu_{\max, \text{anaerobic}} S}{K_{s, \text{anaerobic}} + S} n - Dn \quad (44)$$

where D = dilution rate = $\frac{\text{Flowrate}}{\text{Volume}}$

s_F = feed substrate (glucose) concentration

The above continuous form of the model was developed for a continuous stirred tank reactor under conditions of perfect mixing. No biomass was introduced in the feed, so no feed biomass is accounted for in this model. Inlet substrate was accounted for in the substrate equation. The equations were simply extensions of Equations 39-41 with additional terms for dilution of the biomass and substrate out of the reactor.

5.5.2 Model Parameter Fitting

Methods similar to those used for determining the anaerobic model parameters could have been used for the aerobic model parameters as well. However, these methods, except for the yield determination, were not used here. The project described in the thesis of Stalhandske [58] involved nonlinear least squares methods that were described in the prior chapter on theoretical methods. The parameters from her thesis were the ones used in later simulations. In this thesis an alternate model, originally described elsewhere [11,61,62], was also presented and modeling results were also given for this model. This model will only be briefly presented. This alternate model, designated as the RLS model, is represented by the following equations

$$\dot{x} = \frac{vs}{K_{s,aerobic} + s} \left(\frac{n}{x} \right)^{\frac{1}{3}} x \quad (45)$$

$$\dot{s} = -\frac{1}{Y_{x/s,aerobic}} \frac{vs}{K_{s,aerobic} + s} \left(\frac{n}{x} \right)^{\frac{1}{3}} x \quad (46)$$

$$\dot{n} = \frac{\mu_{max,aerobic} z}{K_{s,aerobic} + z} n \quad (47)$$

$$\dot{z} = \alpha(s - z) \quad (48)$$

where v =parameter incorporating both geometric and maximum growth rate factors

$K'_{s, aerobic}, K_{s,aerobic}$ =saturation constants

α =adaptability parameter

z =weighted average of previous substrate concentrations

This model was derived by considering cellular surface area-to-volume ratio and normal Michaelis-Menten kinetics. Basically, in equation 45, $(n/x)^{1/3}$ is proportional to surface area-to-volume ratio for the cell and $s/K'_{s,aerobic} + s$ is proportional to specific glucose uptake per unit surface area of the cell. Thus v represents a lumped proportionality factor for the geometric and maximum growth rate terms. This model predicts instantaneous change in biomass specific growth rate (actually it predicts an overshoot to the new steady state), but a more gradual, monotonic change in number of cells specific growth rate. A chemostat form of this model, similar to that given in Equations 42-44, is presented below. For the sake of simplicity, this form was based on the assumption of instantaneous adjustment of \dot{n} to changing substrate conditions. This would mean that α would have infinite value.

$$\dot{x} = \frac{vs}{K'_{s,aerobic} + s} \left(\frac{n}{x} \right)^{\frac{1}{3}} x - Dx \quad (49)$$

$$\dot{n} = \frac{\mu_{max,aerobic}s}{K_{s,aerobic} + s} n - Dn \quad (50)$$

$$\dot{s} = -\frac{1}{Y_{x/s,aerobic}} \frac{vs}{K'_{s,aerobic} + s} \left(\frac{n}{x} \right)^{\frac{1}{3}} x + D(s_F - s) \quad (51)$$

The yield was computed by plotting biomass against glucose consumed, using the data from aerobic batch run 2 with the method previously described in the anaerobic growth chapter. The results of this are shown in figure 42, along with a linear least squares fit forced through zero. Only the exponential growth biomass points are shown and used in the fit. The slope of this line is the determined yield for this experiment. This yield was found to be $0.493 \frac{\text{mg biomass}}{\text{mg glucose}}$ with a correlation coefficient, R^2 , of 0.99. The yield used in the later simulations had a slightly inaccurate value of 0.486 used. The 0.493 value should be the one considered for future use. All of the other model parameters were determined by the use of aerobic batch run 2's exponential phase data (all but the last 2 points are shown). In addition to the parameters, starting amounts of biomass and cell number concentrations were fit. The results of these curve fits are shown in figures 43-45. The only preset model parameters were yield and initial glucose concentration. In the batch simulations, for the sake of simplicity, the adaptability parameter, α , was assumed to have infinite value. The biomass plot shows the RLS model to give slightly better fits than the Monod model does. The Monod model does give a somewhat better fit of the residual glucose concentration results, but the RLS model gives significantly better predictions for the cell number data, especially towards the end of the run. Finally the sum of squared residuals for the RLS model is about 25% lower than that of the Monod model, indicating a slightly better overall fit by the RLS model. The lower sum of squared residuals is not surprising as two additional parameters were available for fitting. The model parameters in the Stalhandske thesis [58] are given in table 7.

Under steady-state continuous operation, equations 42-44, 49, and 51 give

$$x_{ss} = Y_{x/s, \text{aerobic}} (s_F - s_{ss}) \quad (52)$$

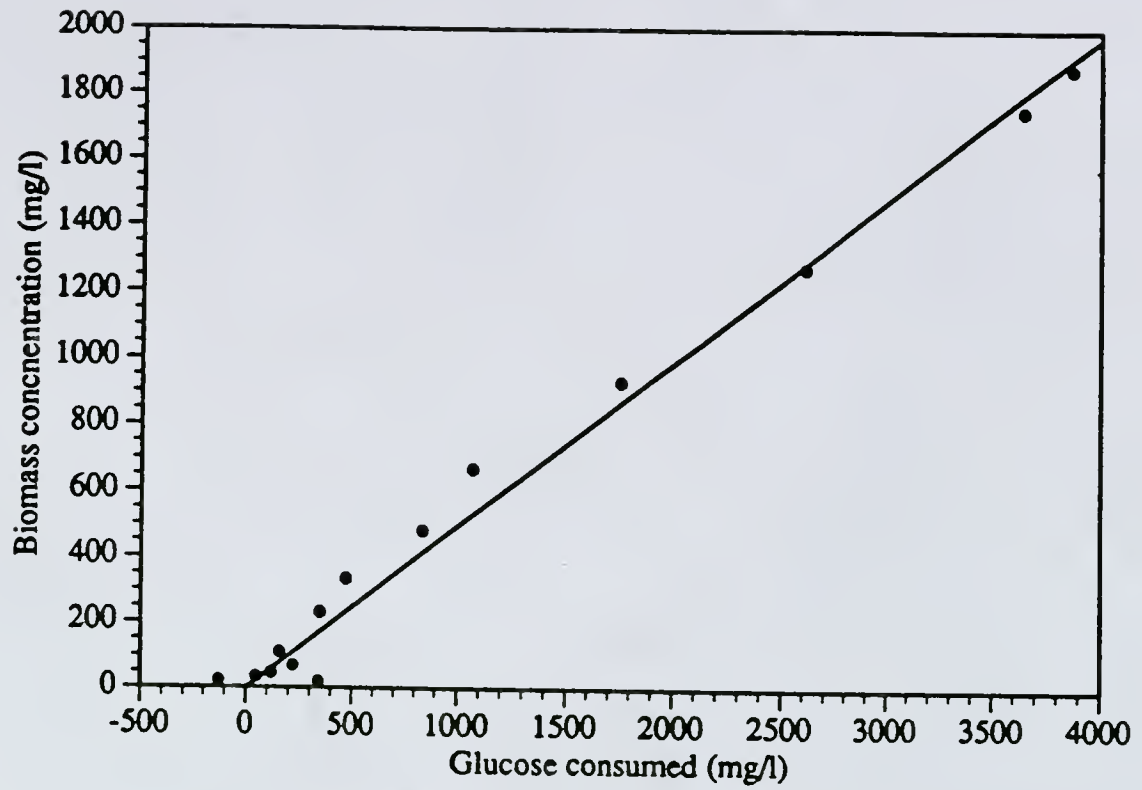


Figure 42. Aerobic batch run 2. Biomass concentration against glucose consumed.

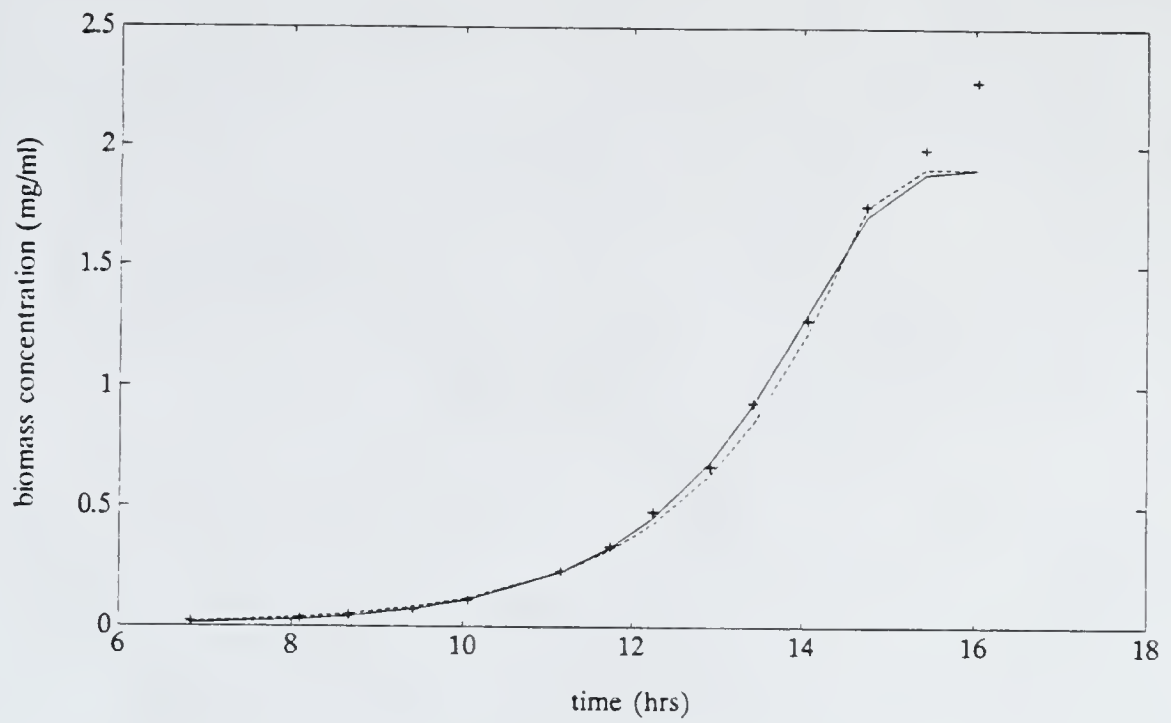


Figure 43. Aerobic batch run 2. Biomass concentration against time. Dashed line represents Monod model fit, and solid line represents RLS model fit.

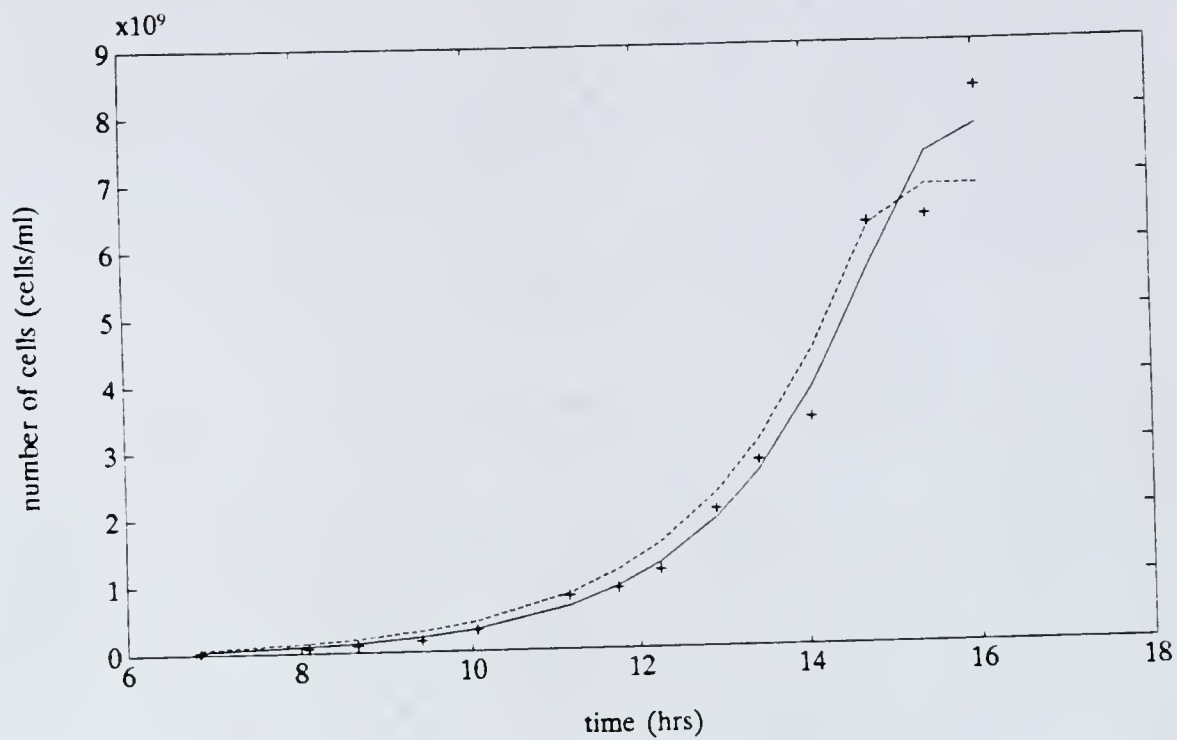


Figure 44. Aerobic batch run 2. Cell number concentration against time. Dashed line represents Monod model fit, and solid line represents RLS model fit.

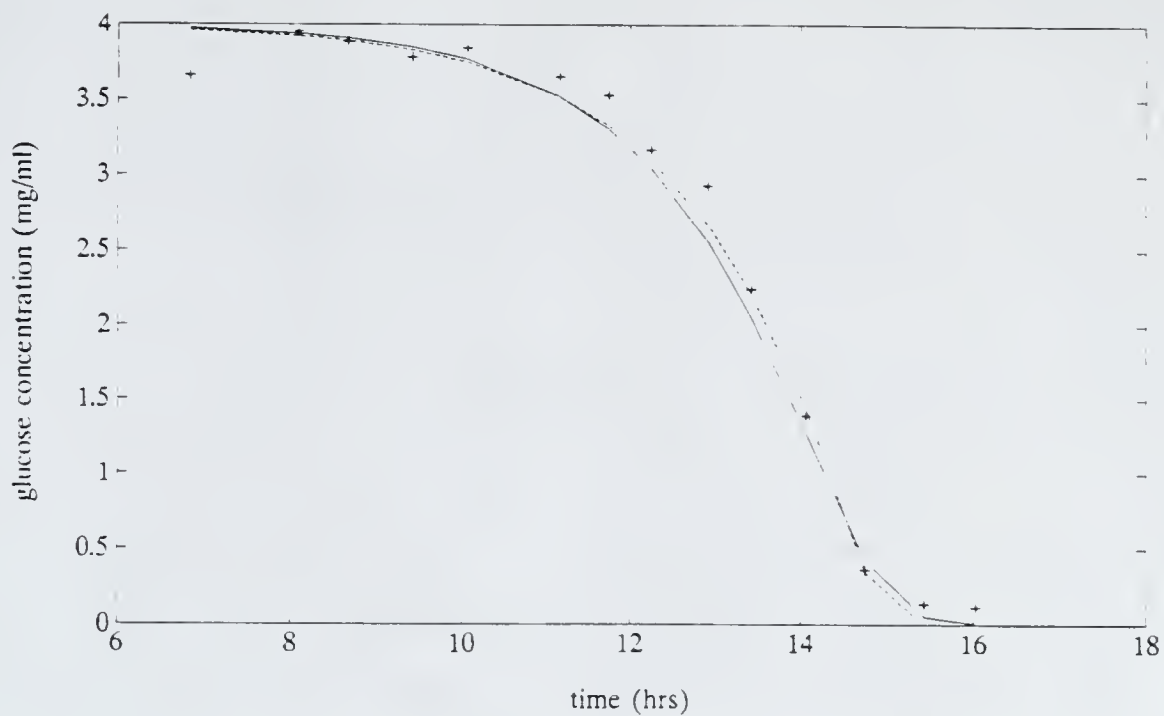


Figure 45. Aerobic batch run 2. Glucose concentration against time. Dashed line represents Monod model fit, and solid line represents RLS model fit.

Table 7. Aerobic Model Parameters

Model Parameter/Starting Condition	Monod Model Fit	RLS Model Fit
$\mu_{\max, \text{aerobic}}(\text{hr}^{-1})$.6129	.6481
$K_{s, \text{aerobic}} (\text{mg/l})$	147.7	108.2
$v \left(\frac{\text{mg}^{1/3}}{\text{cell}^{1/3} \text{hr}} \right)$	N/A	5.79×10^{-4}
$K'_{s, \text{aerobic}} (\text{mg/l})$	N/A	897
Initial cells (cells/l)	1.12×10^9	5.54×10^8
Initial biomass (mg/l)	.312	.0354
Σ residuals	.028	.021

$$s_{ss} = \frac{DK_{s,aerobic}}{\mu_{max,aerobic} - D} \quad (53)$$

$$n_{ss} = \left(D \frac{K'_s + s_{ss}}{v s_{ss}} \right)^3 x_{ss} \quad (\text{for the RLS model}) \quad (54)$$

$$n_{ss} = x_{ss} \frac{n_o}{x_o} \quad (\text{for the Monod model}) \quad (55)$$

where x_{ss} =steady-state biomass concentration in the reactor

s_{ss} =steady-state glucose concentration in the reactor

n_{ss} =steady-state cell number concentration in the reactor

n_o =initial cell number concentration in the batch calculation

x_o =initial biomass concentration in the batch

Equation 55 simply indicates constant cell size. These relations were used in Stalhandske's thesis[58] to compare the model predictions to experimental data. The results are shown in tables 8-10. The RLS model gives superior predictions of glucose concentration at all dilution rates, and a somewhat better biomass prediction at the .335 hr⁻¹ dilution rate. However, its cell numbers predictions are very poor.

Table 8. Aerobic model comparison with continuous data for $D=.263 \text{ hr}^{-1}$

Model Used	Dry mass (mg/l)	Glucose (mg/l)	Number of cells/l
Data	2200	70	1.2×10^{13}
Monod	1900	111	6.7×10^{12}
RLS	1900	74	4.0×10^{14}

Table 9. Aerobic model comparison with continuous data for $D=.45 \text{ hr}^{-1}$

Model Used	Dry mass (mg/l)	Glucose (mg/l)	Number of cells/l
Data	1920	203	1.2×10^{13}
Monod	1700	408	6.2×10^{12}
RLS	1810	246	8.4×10^{13}

Table 10. Aerobic model comparison with continuous data for $D=.335 \text{ hr}^{-1}$

Model Used	Dry mass (mg/l)	Glucose (mg/l)	Number of cells/l
Data	2000	93	6.7×10^{12}
Monod	1900	178	6.7×10^{12}
RLS	1900	116	2.4×10^{14}

CHAPTER 6

THE EFFECTS OF SHIFTS IN AERATION ON *E. COLI* LCB898

6.1 Background

The effects of shifts in aeration on some species have been studied by other workers [e.g. 62,63]. Shifts in aeration condition for *E. coli* specifically have also been examined [e.g. 50,64,65]. There are differences between the physiology of the cells under each aerobic and anaerobic conditions[50,65] including what metabolic enzymes and other proteins are present. Smith and Neidhardt[50,65] indicated that these changes manifest themselves in a smooth transition of growth rates of wild-type *E. coli* K12 when sharp shifts were performed from anaerobic to aerobic conditions, with some delay (25 minutes) in the adjustment to the final growth rate. This delay may or may not be applicable to the mutant *E. coli*. Pyruvate processing is one of the key steps in *E. coli* glucose metabolism. Pyruvate dehydrogenase is the enzyme responsible for conversion of pyruvate to acetyl-CoA under aerobic conditions. Production of this enzyme may be inducible by pyruvate under aerobic conditions[65]. Since the *E. coli* mutant may have a different amount of intracellular pyruvate than normal *E. coli* K12 cells under anaerobic conditions, the adjustment to aerobic conditions may be different than that of the strain described in the work of Smith and Neidhardt.

In the other type of shift, aerobic to anaerobic conditions, Smith and Neidhardt [50] showed a complete lag in bacterial growth for 20 minutes before aerobic growth started. However, this observation may or may not be applicable to the organism under study as pyruvate formate lyase (pfl) is a key anaerobic metabolic enzyme in normal *E. coli*, which is absent in this mutant.

6.2 Development of the Combined Aerobic-Anaerobic Model

A simple model to describe *E. coli* LCB898 under both aerobic and anaerobic conditions was developed for later use in developing cycling strategies. The model chosen was a simple blending of the anaerobic and Monod aerobic models to describe biomass, glucose, and product responses to variable aeration conditions. The Monod aerobic model, in spite of its inferior predictive capability compared to the previously described RLS model, was used for the sake of overall model simplicity. The individual models were described earlier and only the special aspects of the combination model will be discussed. The batch equations are as follows

$$\dot{x} = \left(\frac{\mu_{\max, \text{aerobic}}}{K_{s, \text{aerobic}} + s} \bullet \text{doc} + \frac{\mu_{\max, \text{anaerobic}}}{K_{s, \text{anaerobic}} + s} \bullet (1 - \text{doc}) \right) sx \quad (58)$$

$$\dot{s} = \left(-\frac{1}{Y_{x/s, \text{aerobic}}} \frac{\mu_{\max, \text{aerobic}}}{K_{s, \text{aerobic}} + s} \bullet \text{doc} - \frac{1}{Y_{x/s, \text{anaerobic}}} \frac{\mu_{\max, \text{anaerobic}}}{K_{s, \text{anaerobic}} + s} \bullet (1 - \text{doc}) \right) sx \quad (59)$$

$$\dot{p} = \alpha \frac{\mu_{\max, \text{anaerobic}} sx}{K_{s, \text{anaerobic}} + s} \bullet (1 - \text{doc}) \quad (60)$$

where \dot{q} = time derivative of q

x=biomass (dry mass) concentration in the reactor

s=substrate (glucose) concentration in the reactor

p=product (d-lactate) concentration in the reactor

$\mu_{\max, \text{anaerobic}}$ =maximum growth rate under anaerobic conditions

$K_{s, \text{anaerobic}}$ =saturation parameter under anaerobic conditions

$Y_{x/s, \text{anaerobic}}$ =yield of biomass on substrate under anaerobic conditions

α =growth-associated lactate production parameter

$\mu_{\max, \text{aerobic}}$ =maximum growth rate under aerobic conditions

$K_{s, \text{aerobic}}$ =saturation parameter under aerobic conditions

$Y_{x/s, \text{aerobic}}$ =yield of biomass on substrate under aerobic conditions

K_O =oxygen saturation parameter

doc =aeration switching parameter

A chemostat form of this model, developed for the same conditions as the previously described continuous models, is given by the following equations

$$\dot{x} = \left(\frac{\mu_{\max, \text{aerobic}}}{K_{s, \text{aerobic}} + s} \cdot \text{doc} + \frac{\mu_{\max, \text{anaerobic}}}{K_{s, \text{anaerobic}} + s} \cdot (1 - \text{doc}) \right) sx - Dx \quad (61)$$

$$\dot{s} = \left(-\frac{1}{Y_{x/s, \text{aerobic}}} \frac{\mu_{\max, \text{aerobic}}}{K_{s, \text{aerobic}} + s} \cdot \text{doc} - \frac{1}{Y_{x/s, \text{anaerobic}}} \frac{\mu_{\max, \text{anaerobic}}}{K_{s, \text{anaerobic}} + s} \cdot (1 - \text{doc}) \right) sx + D(s_F - s) \quad (62)$$

$$\dot{p} = \alpha \frac{\mu_{\max, \text{anaerobic}} s x}{K_{s, \text{anaerobic}} + s} \cdot (1 - \text{doc}) - Dp \quad (63)$$

where s_F =feed substrate (glucose) concentration

D =dilution rate=flowrate/volume

Cell number concentrations were not modeled here in order to minimize the number of equations.

The parameter doc has physically allowable values of 1 or 0, with 1 denoting aerobic metabolism and 0 anaerobic. In later work it will be convenient to consider imaginary culture states of intermediate doc values. The model has the assumption of no lactate production or consumption under aerobic conditions. It also shows instantaneous adjustment between aeration conditions. This may not be a very good assumption when

switching from aerobic to anaerobic conditions considering the observations of Smith and Neidhardt where a lag phase was observed. However, no such lag is indicated by the experimental results discussed below, or the cycling results of Chapter 7.

The model parameters used are reviewed in table 11.

6.3 Testing of the Model

An experiment was performed to investigate the effect of a shift between aerobic and anaerobic conditions on the mutant. An aerobic continuous steady state for a dilution rate higher than strict anaerobic operation would allow was established, after which aeration was removed. This type of experiment was performed since analysis of a shift from a steady state is relatively straightforward. The starting conditions of a continuous aerobic culture are then well established and time-invariant. Shifts from transient culture conditions, for example aeration shifts in batch cultures, are far more difficult to analyze, as the starting conditions would not be well established.

This experiment was conducted by continuing aerobic continuous run 1. Again, this was run at a dilution rate of 0.335 hr^{-1} , a dilution rate well below the maximum aerobic growth rate, but one which would lead to biomass washout under anaerobic conditions. The results of this experiment, along with model predictions, are shown in figures 46-48. The first points of each of these figures represent the aerobic steady state. The points represent data, and the curves represent the model predictions. The biomass curve indicated a smooth approach towards the expected washout. The biomass model predictions were in excellent agreement with the experimental data. The glucose response showed initial low values, due to the large amount of biomass that was still in the reactor, but washout of the biomass led to increasing glucose concentration at 75 hours. The glucose predictions were very accurate until washout was approached. The lactate response showed a maximum at 75 hours. The lactate concentration rose very quickly after the switch, but began to drop when biomass washout began to take effect. Again, the model did a satisfactory job. The model and its anaerobic parameters thus seemed useful

for later cycling studies, at least as far as description of aerobic to anaerobic shifts are concerned.

Table 11. Model parameter values

Parameter	Value
$\mu_{\max, \text{anaerobic}}$.19 hr ⁻¹
$K_{s, \text{anaerobic}}$	98 mg/l
$Y_{x/s, \text{anaerobic}}$.068 mg/mg
α	10.77 mg/mg
$\mu_{\max, \text{aerobic}}$.6129 hr ⁻¹
$K_{s, \text{aerobic}}$ (mg/l)	147.7
$Y_{x/s, \text{aerobic}}$.486 mg/mg

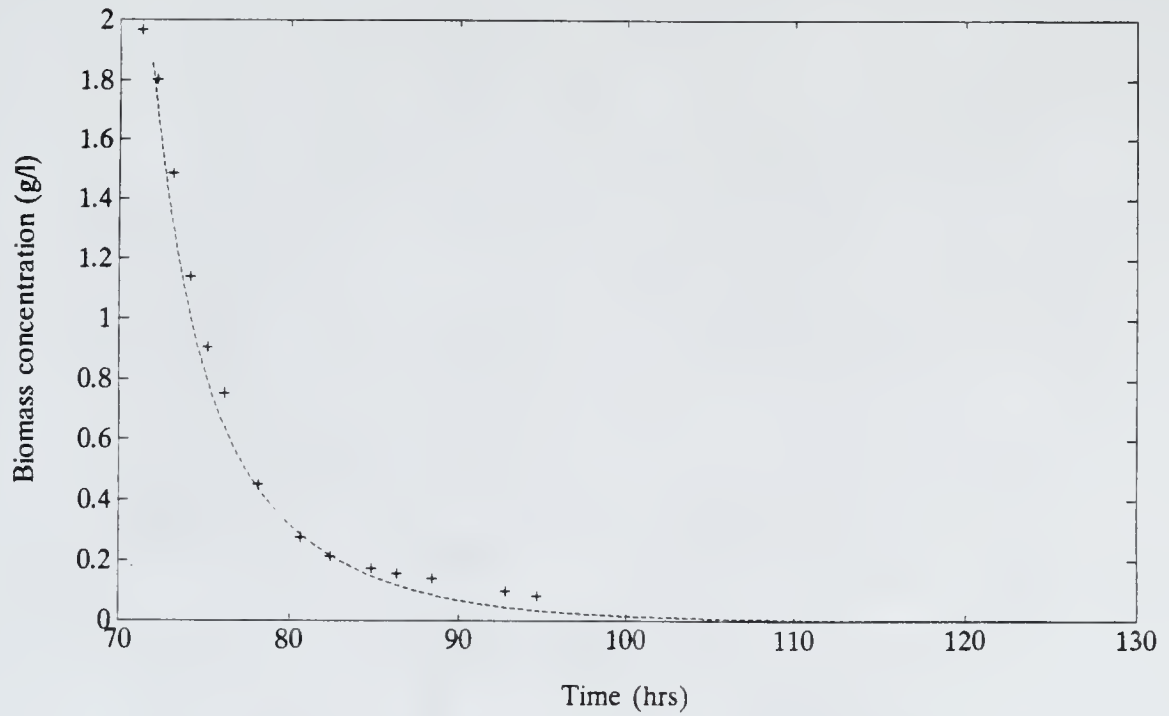


Figure 46. Aerobic to anaerobic shift experiment. Biomass concentration against time. Solid line represents model predictions, pluses represent data

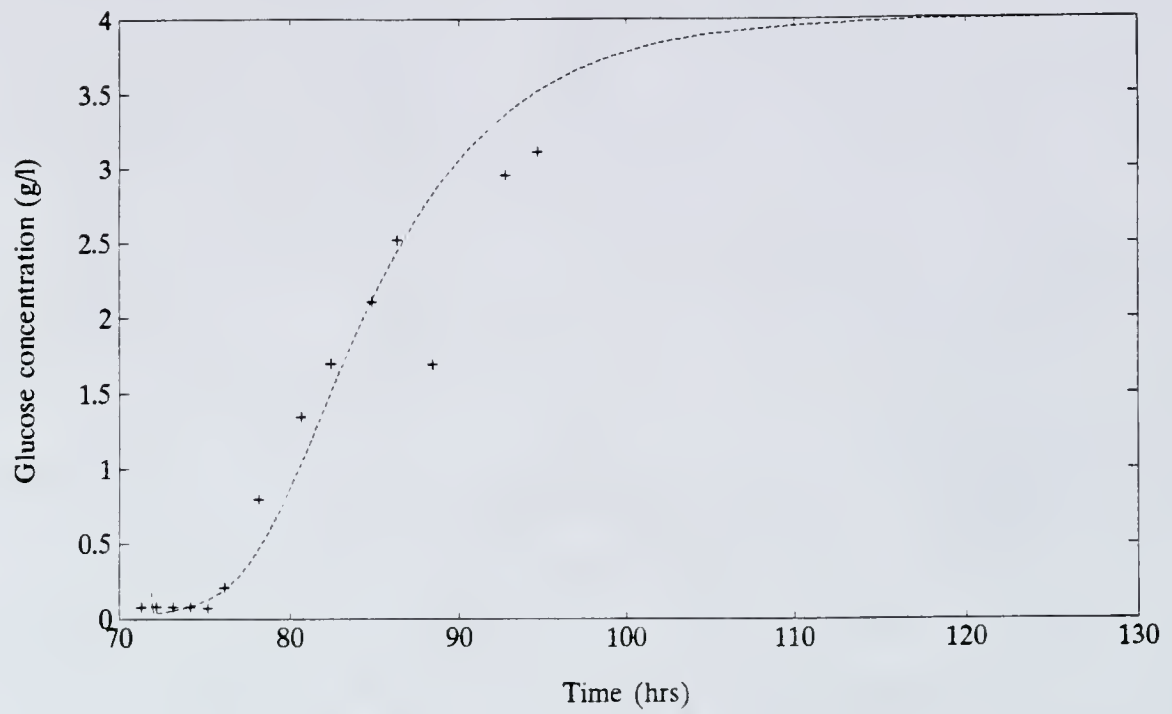


Figure 47. Aerobic to anaerobic shift experiment. Glucose concentration against time. Solid line represents model predictions, pluses represent data

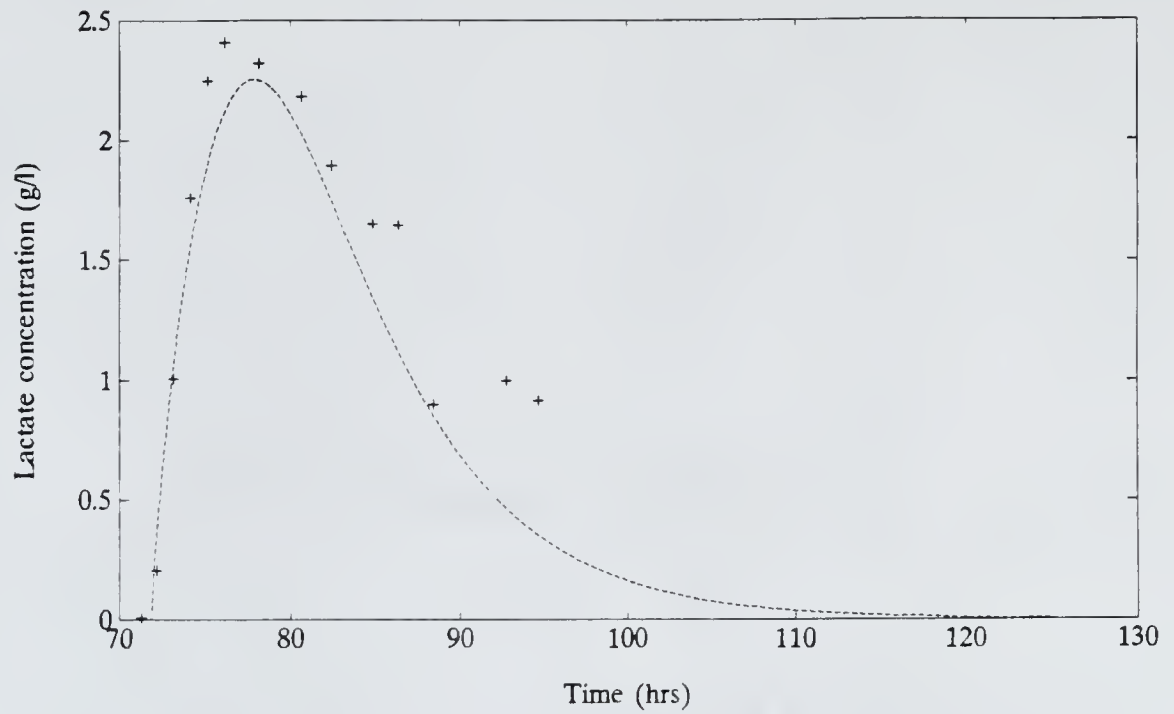


Figure 48. Aerobic to anaerobic shift experiment. Lactate concentration against time. Solid line represents model predictions, pluses represent data

CHAPTER 7

EFFECTS OF AERATION CYCLING ON LACTATE PRODUCTIVITY OF *E. COLI* LCB898

7.1 Background

In previous chapters it was shown that *E. coli* LCB898 has higher growth rates and yields under aerobic conditions than under anaerobic conditions. It was also shown that d-lactate is only produced significantly under anaerobic conditions. This behavior lends itself to examining the possibility of nonconstant aeration of the reactor under continuous operating conditions. Cycling of air into an *E. coli* LCB898 bioreactor is examined in this chapter.

Cycling of operating conditions in a bioreactor has been investigated by other workers. The effects of periodic operation of feed substrate [1,2,5,6] and residual substrate compositions [11] on cellular composition have been studied. Cycling of reactor dilution rate has been used to increase biomass productivity of yeast [66] and plasmid stability of recombinant *E. coli* K12 [67].

In order to investigate aeration cycling, a method had to be used to determine the optimal cycling waveform. In other words, the period of cycling and the fraction spent under aerobic and anaerobic conditions had to be determined. In addition, the best constant dilution rate with which to operate the reactor had to be found. A theoretical method involving Carleman linearization, previously described in the theoretical methods chapter, was used on the previously described combined aerobic-anaerobic model. Aeration cycling can be coupled with more complicated flow strategies, such as simultaneous cycling of dilution rate, variable reactor volume and others. Unfortunately, for these strategies, the

theoretical method used, which approximates the system equations by a Taylor series expansion required too high an expansion order to be practical.

For the sake of later comparison, the optimum model predicted steady-state lactate productivity under anaerobic conditions was determined first. The model predictions for lactate productivity against dilution rate are shown in figure 49. The determined optimal lactate productivity was 408 mg/(l•hour) with the optimum being found at a dilution rate of $.161 \text{ hr}^{-1}$. The corresponding experimentally determined anaerobic steady-state optimum lactate productivities were 527 mg/(l•hour) at a dilution rate of 0.164 hr^{-1} , and 578 mg/(l•hour) at a dilution rate of 0.17 hr^{-1} . As these steady states should be approximately the same, the average of these two productivities were used as the optimal value for later comparison. The average value was 553 mg/(l•hour).

7.2 Theoretical Investigation into Cycling

For the cycling considered, the system is run at a constant dilution rate, with air being turned on and off. This proposed control waveform is shown in figure 50. The measure of performance considered was average lactate productivity over a cycle. The optimization variables were period, fraction spent under each set of conditions, and dilution rate need to be determined. The fraction spent under aerobic conditions, referred to as the aerobic fraction, is symbolized by ϵ in the figure. The period is symbolized by T , and the dissolved oxygen condition, 0 for anaerobic, 1 for aerobic, is symbolized by doc .

According to the model the optimal cycling period is zero. Fast cycling between two values is equivalent to using a constant average value. In other words, if fast cycling between two control settings is performed, the system being controlled will only "see" the average of the two control settings. In the system under study, infinitely fast cycling can then be investigated by setting the doc variable to the aerobic fraction. For example, if an aerobic fraction of 0.3 was simulated with infinitely fast (zero) period, the combined aerobic-anaerobic model would have its doc value set to 0.3. Steady-state solutions of the model were found numerically for various dilution rates and aerobic fractions. The

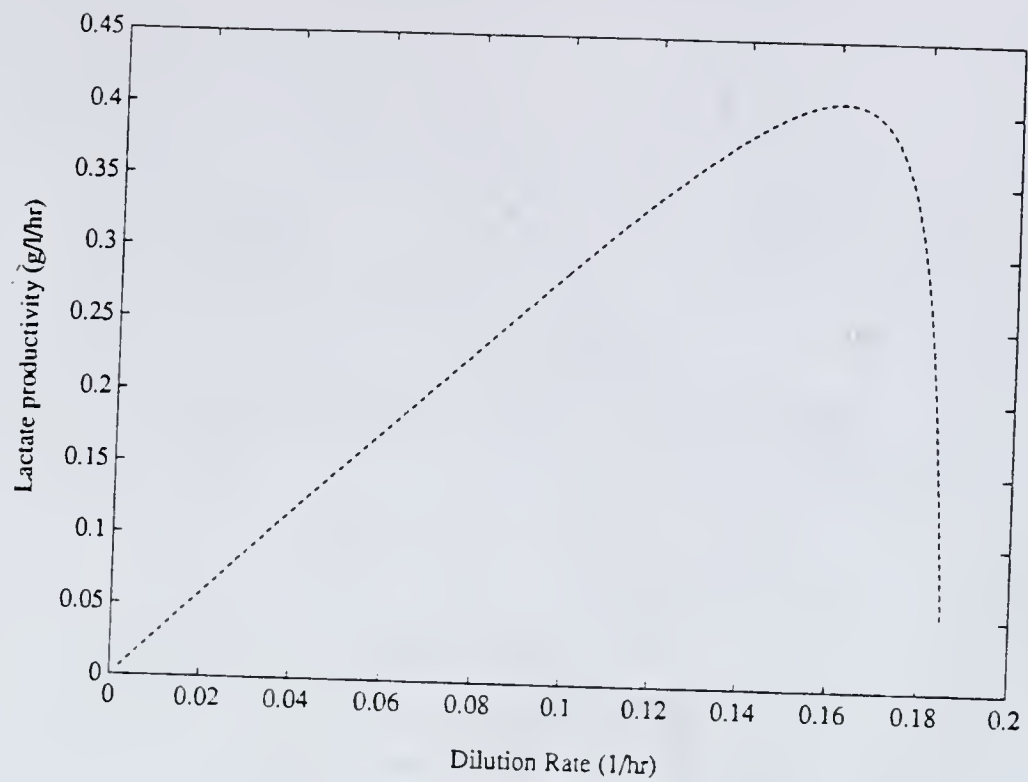


Figure 49. Anaerobic model-predicted lactate productivity against dilution rate.

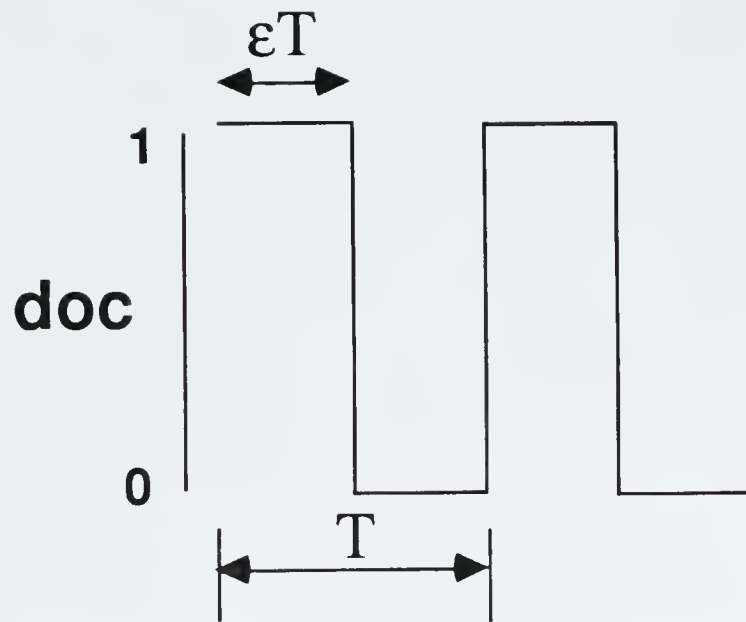


Figure 50. Proposed dissolved oxygen cycling waveform.

corresponding values for the lactate productivity, defined by dilution rate multiplied by lactate concentration, are presented in table 12. Lower aerobic fraction results are only given up to certain dilution rates, because above these rates washout of biomass occurred. The optimum shown in this table is found at an aerobic fraction of 0.45 and a dilution rate of 0.30 hr^{-1} . The value for the lactate productivity at that point was $573.9 \text{ mg}/(\text{l}\cdot\text{hour})$. A more careful search was performed near that point, and the optimal zero period conditions found were aerobic fraction of 0.45 and dilution rate of 0.31 hr^{-1} , with a lactate productivity of $576.2 \text{ mg}/(\text{l}\cdot\text{hour})$.

The effects of increasing period were then examined, as large periods were deemed desirable for three reasons: (1) the actual experimental implementation becomes easier, (2) equipment wear is lessened, and (3) the model is not applicable during the time the cells switch metabolism. The Carleman-linearization-based method previously described as used with deviation variables from the imaginary (since doc is not 0 or 1) steady state: doc 0.45, dilution rate 0.31 hr^{-1} , biomass concentration 597.3 mg/l , glucose concentration 587.9 mg/l , and lactate concentration 1858.8 mg/l . In other words, the zero period optimal solution was the steady state used as basis for the Carleman linearization.

The results for several orders of Carleman linearization are given in table 13. The results of Carleman order 2 and 3, which should be more accurate than order 1 results, indicate that the decrease in lactate productivity is insignificant up to approximately 2 hours, and, as the 3rd order results indicate, productivity only drops 3% from the optimum at 5 hours. The experiments were conducted with period of 5 hours.

The Carleman-linearization-based method was also used to recreate table 12. This was performed to determine the usefulness of this procedure for predicting conditions far away from the point of linearization. The results for a third order Carleman linearization around the zero period steady state for a dilution rate of 0.31 hr^{-1} and an aerobic fraction of 0.45 are shown in table 14. As can be seen in this table, the Carleman linearization did a poor job of predicting lactate productivities at the higher aerobic fractions. Also, washout

Table 12. Zero period lactate productivities (mg/(l•hour) for various conditions predicted by Newton-Raphson solution of model

Aerobic Fraction	Dilution rate (hr ⁻¹)							
	0.1	0.16	0.2	0.25	0.3	0.35	0.4	0.5
0	285.0	407.6						
0.1	276.1	421.8	463.7					
0.2	265.1	410.4	489.8	459.4				
0.3	251.9	391.8	475.3	548.6	323.1			
0.4	236.1	367.7	448.6	534.6	571.2			
0.45	227.1	353.6	431.9	518.1	573.9	463.3		
0.5	217.1	337.9	413.0	497.3	560.9	551.6		
0.6	193.7	300.9	367.8	444.7	509.7	548.8	483.6	
0.7	164.1	254.3	310.5	375.7	433.1	477.8	492.4	
0.8	125.8	194.1	236.5	285.7	329.9	367.0	391.9	192.4
0.9	73.9	113.4	137.7	165.9	191.3	213.3	230.4	222.1
1.0	0	0	0	0	0	0	0	0

was not adequately predicted for high dilution rate, low aerobic fraction, conditions, as can be seen clearly in the first two rows of table 14. When comparison to the table 12 results were made, good predictions of most sub-washout low aerobic fraction productivities were apparent. Good predictions were also seen near the optimum, which was to be expected as this was the point around which linearization was made.

The suggested improvements in parameters shown in table 5 were also investigated. The results of the zero period optima found for different conditions are shown in table 15. Differing anaerobic parameters sometimes slightly changed the optimum operating conditions, but none of these resulted in optimal lactate productivities significantly different from those for the original-parameter optimal conditions.

Simulations, using Runge-Kutta integration of the model equations, for dilution rate of 0.31 hr^{-1} , 5 hour period, and aerobic fraction of 0.45 are shown in figures 51-53. The cycles shown were started off aerobically. The glucose concentration response showed wide swings between about 200 mg/l and 1000 mg/l. The switch to anaerobic conditions is clearly seen in the biomass and lactate plots. Biomass immediately stopped increasing and lactate immediately started increasing at the shift. Corresponding comments apply at the shift from anaerobic to aerobic conditions. The glucose response did not show switches as clearly. During anaerobic conditions glucose initially decreases as the cells consume it at a higher rate than under aerobic conditions, but eventually glucose starts increasing due to cell washout. The switch to aerobic conditions, at every 5 hours, is seen by a sharp increase of slope in the glucose concentration. The glucose response to the shift to anaerobic conditions is similar to that seen in the biomass and lactate curves.

Finally, the optimal periodic lactate productivity of $576.2 \text{ mg}/(\text{l}\cdot\text{hour})$ was approximately 40 % higher than the optimal anaerobic steady-state productivity of $407.7 \text{ mg}/(\text{l}\cdot\text{hour})$.

Table 13. Carleman predictions for average lactate productivity (mg/(l•hour)) over a cycle at a dilution rate of 0.31 hr^{-1} and an aerobic fraction of 0.45 as a function of Carleman order and period.

Period (hours)	Carleman order		
	1	2	3
.00001	576.2	576.2	576.2
.001	576.2	576.2	576.2
.1	576.5	576.2	576.2
1	577.3	575.9	575.9
2	582.3	574.7	574.9
5	584.7	560.5	564.3
6	588.7	550.8	553.9
7.5	595.6	531.4	516.5

Table 14. Zero period lactate productivities (mg/(l•hour) for various conditions predicted by third order Carleman linearization of model

Aerobic Fraction	Dilution rate (hr ⁻¹)							
	0.1	0.16	0.2	0.25	0.3	0.35	0.4	0.5
0	295.0	404.4	407.6	176.1	-1798.7			
0.1	292.8	423	469.1	518.6	573.9			
0.2	284.8	421	490.6	507.2	95.0			
0.3	271.6	402.8	481.4	548.3	464.8			
0.4	253.3	374.5	451.8	535.6	571.4			
0.45	242.8	359.1	434.3	518.6	573.9	471.1		
0.5	232.2	345.8	419	501.0	561.7	554.3		
0.6	216.5	338	415.9	495.1	536.7	549.6	474.9	
0.7	220.5	388.3	528	706.4	624.5	433.0	554.1	
0.8	253.4	622.6	2109.3	-803.2	-191.0	22.5	31.0	438.0
0.9	352.3	-1437.8	-289.5	-63.1	181.2	-137.5	-25.9	205.1
1.0	0	0	0	0	0	0	0	0

Table 15. Optimum Conditions as a Function of Anaerobic Parameter Values, and Lactate Productivity Values for Dilution rate of 0.31 hr^{-1} and aerobic fraction 0.45

α (mg/mg)	K_s , anaerobic (mg/l)	$Y_{x/s}$, anaerobic (mg/mg)	Optimum Conditions	Opt. Lactate Productivity (mg/l/hr)	Lac. Prod. at $D=.31$, $\epsilon=.45$
10.77	31.4	.068	$\epsilon=.45$, $D=.31$	612.3	612.3
10.77	31.4	.063	$\epsilon=.48$, $D=.32$	577.3	577.2
10.77	98	.063	$\epsilon=.48$, $D=.32$	544.4	544.1
13	31.4	.068	$\epsilon=.45$, $D=.31$	739.1	739.1
13	98	.068	$\epsilon=.45$, $D=.31$	695.5	695.5
13	98	.063	$\epsilon=.46$, $D=.31$	656.9	656.8
13	31.4	.063	$\epsilon=.46$, $D=.31$	696.7	696.7

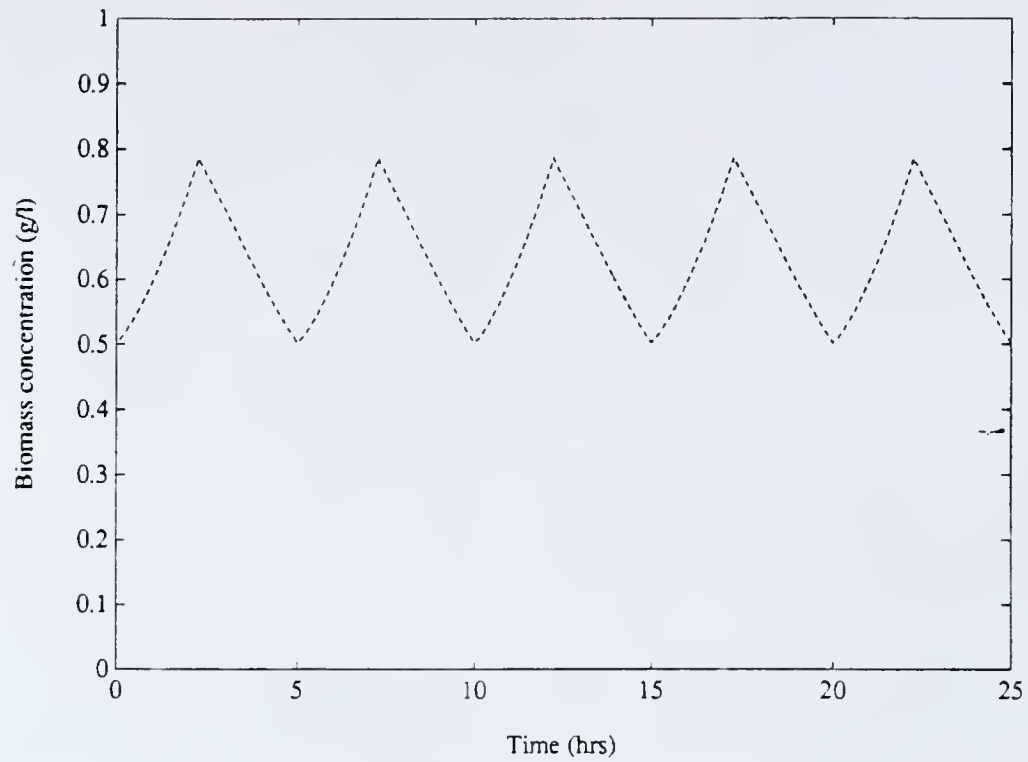


Figure 51. Simulations of effects of periodic operation ($D=.31, \epsilon=.45$) on biomass concentration.

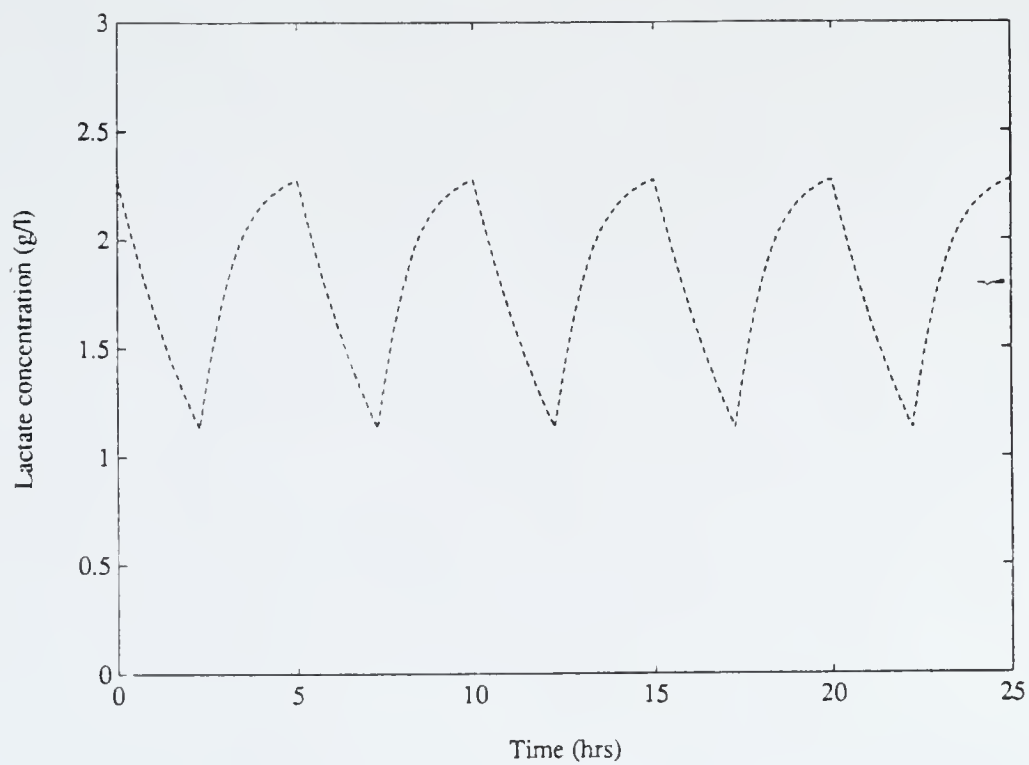


Figure 52. Simulations of effects of periodic operation ($D=.31, \epsilon=.45$) on lactate concentration.

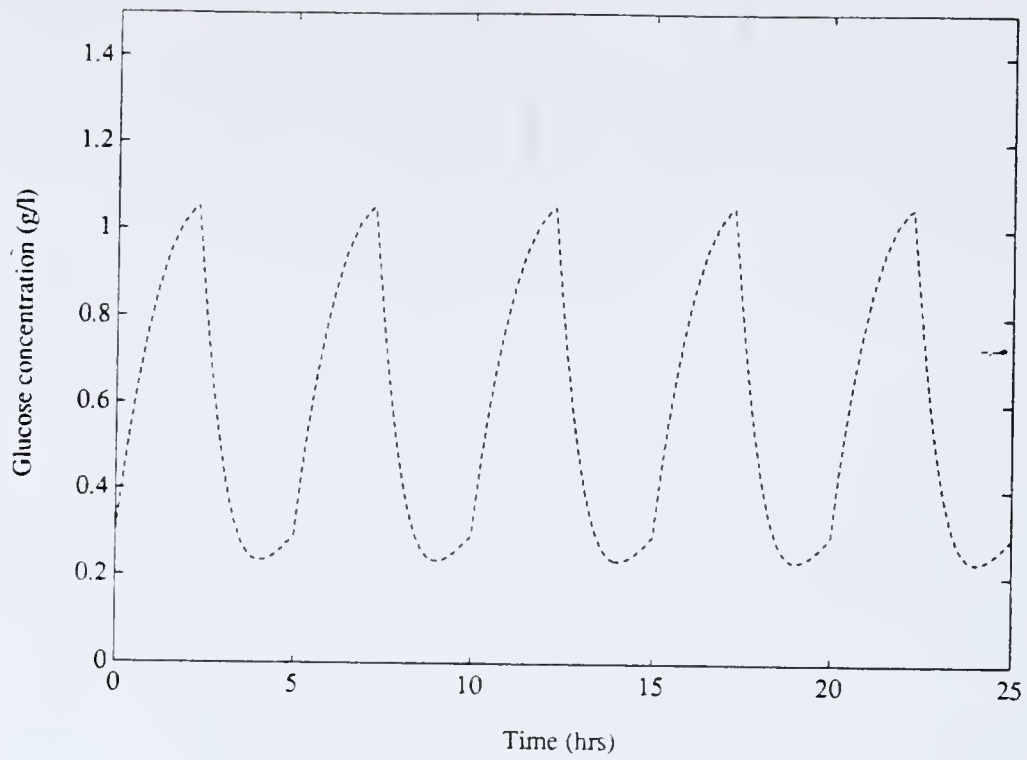


Figure 53. Simulations of effects of periodic operation ($D=.31, \epsilon=.45$) on glucose concentration.

7.3 Experimental confirmation of lactate productivity optimization results

Experiments were performed to confirm an increase of productivity by using cycling. Two periodic operation runs were performed. Both of these experiments were conducted with a dilution rate of 0.31 hr^{-1} , an aerobic fraction of 0.45 and a period of 5 hours. They were initiated as aerobic batches and switched to continuous operation and cyclic aeration when biomass concentration was approximately 800 mg/l, the theoretically predicted value. Each run's results will be described separately.

All of the results for periodic run 1 are shown in figures 54-56. The switch to aeration cycling and continuous operation was performed at 13 hours. These figures are confusing as they present all of the data collected. It is more useful to examine figures 57-59, which only show the results for the switch points between aeration conditions. The biomass results showed a smooth approach to what appears to be a cyclic steady state at about 93 hours. The measured biomass concentrations were significantly higher than the model-predicted values. The glucose measurements showed a decrease, followed by a peak, then again followed by a decrease to what appears to be a cyclic steady state at 103 hours. The glucose measurements were significantly lower than the model-predicted values. The lactate concentration measurements showed a smooth approach to an apparent cyclic steady state at about 93 hours. The lactate concentration measurements were only slightly higher than the model-predicted values. Unfortunately, the experiment ended prematurely due to unforeseen happenings (a line clogged) and without collection of data for an entire control cycle. However, data were taken for the duration of the anaerobic portion of one of the later cycles and the lactate concentration during the aerobic part of the cycle can be accurately estimated since practically no lactate is produced under aerobic conditions.

The following relation describes the effect of lactate concentration during aerobic continuous operation

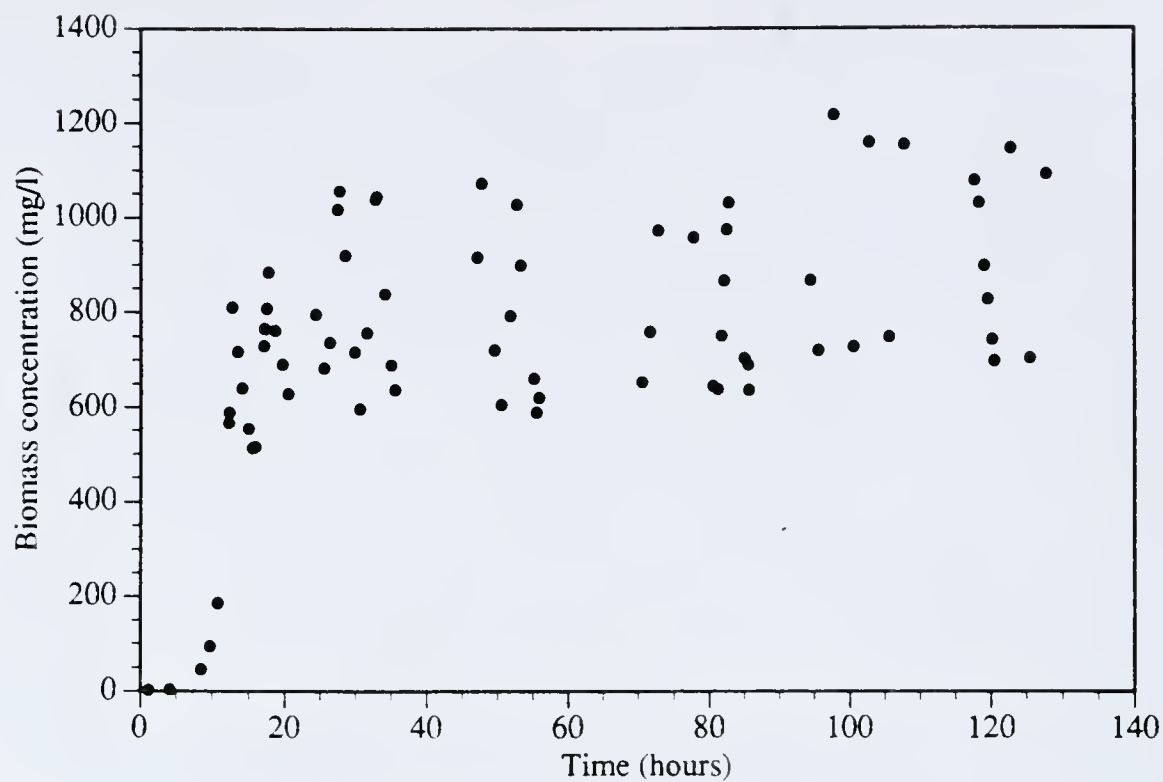


Figure 54. Periodic Run 1. Experimental results of effects of periodic operation ($D=.31, \epsilon=.45$) on biomass concentration.

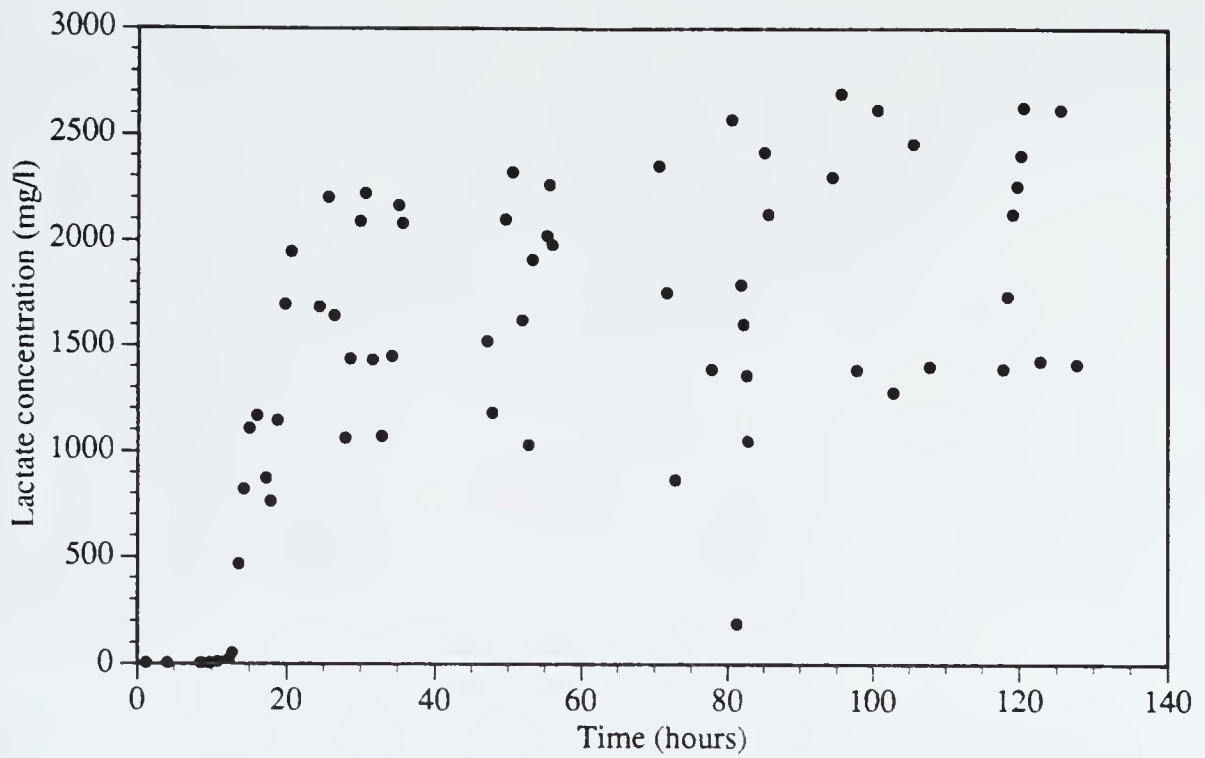


Figure 55. Periodic Run 1. Experimental results of effects of periodic operation ($D=.31, \epsilon=.45$) on lactate concentration.

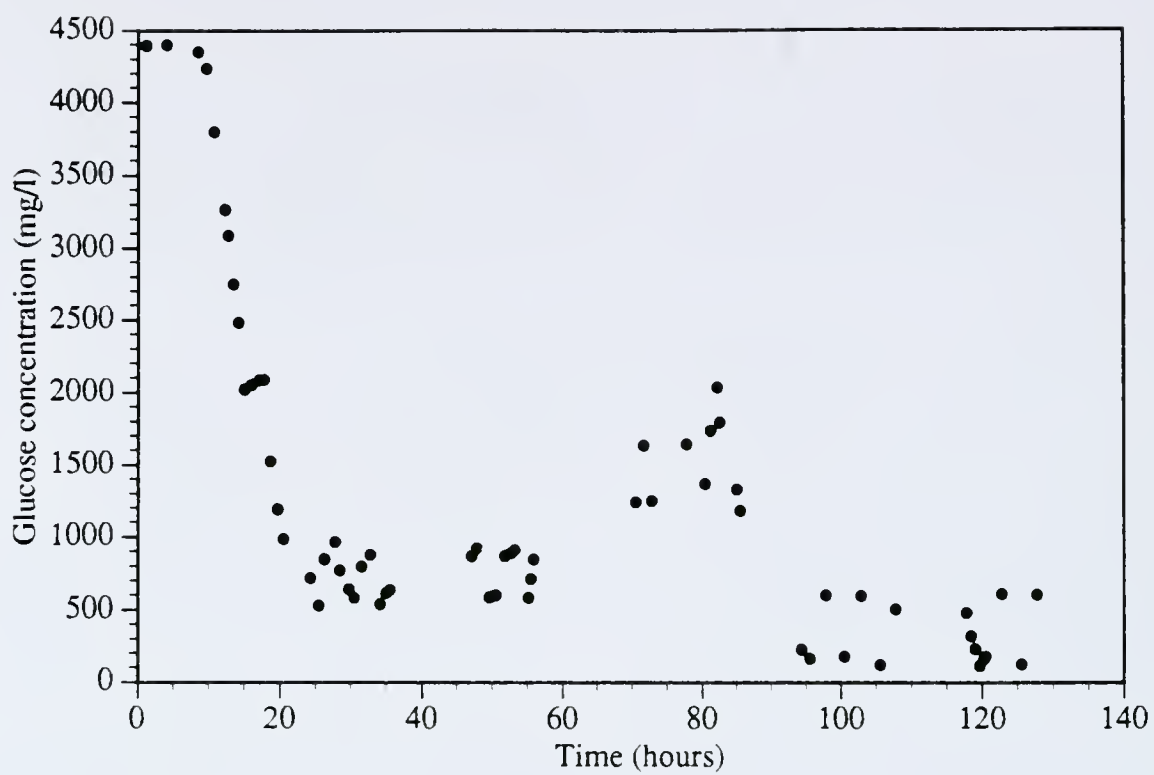


Figure 56. Periodic Run 1. Experimental results of effects of periodic operation ($D=.31, \epsilon=.45$) on glucose concentration.

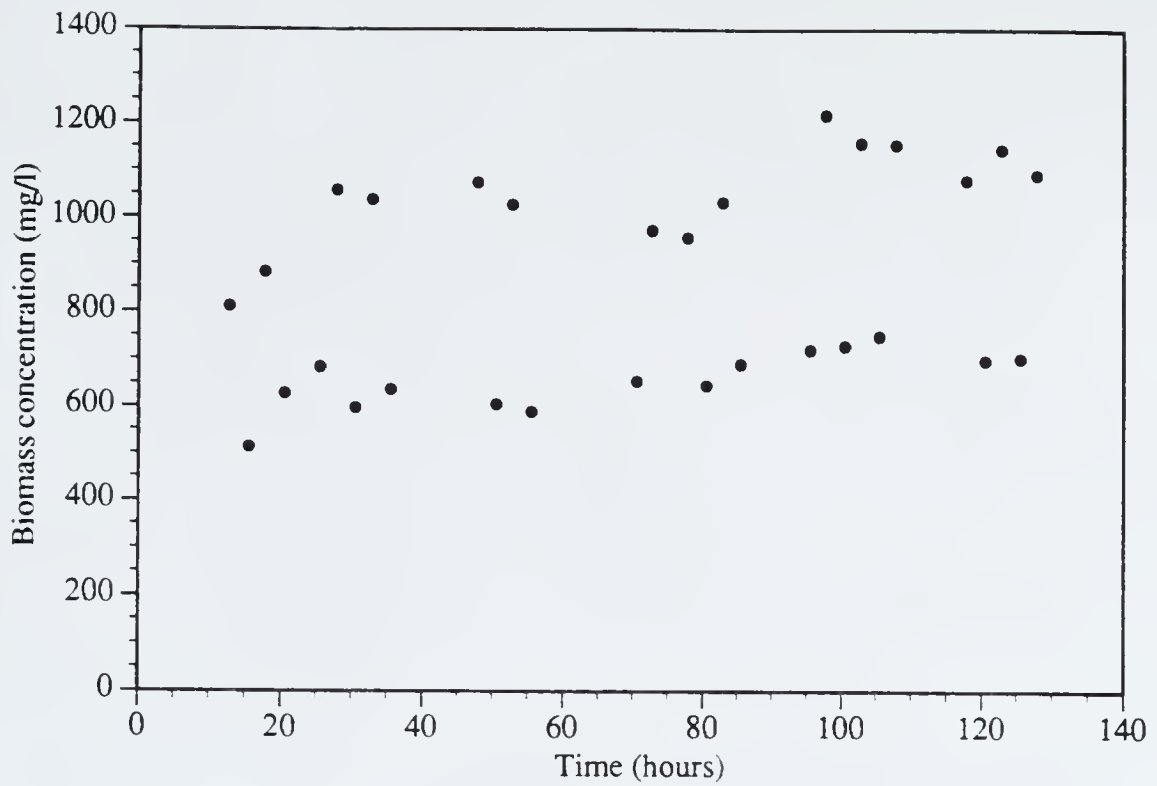


Figure 57. Periodic Run 1. Experimental results of effects of periodic operation ($D=.31, \epsilon=.45$) on biomass concentration. Only the shift points are shown.

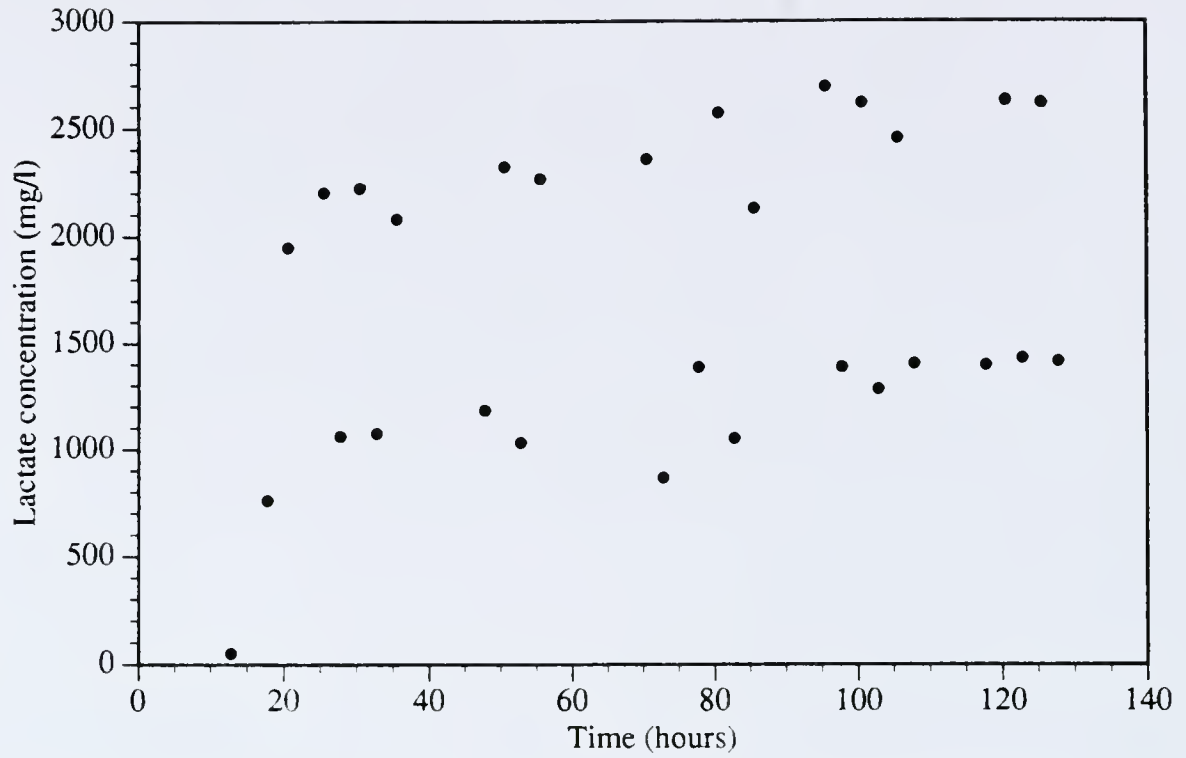


Figure 58. Periodic Run 1. Experimental results of effects of periodic operation ($D=.31, \epsilon=.45$) on lactate concentration. Only the shift points are shown.

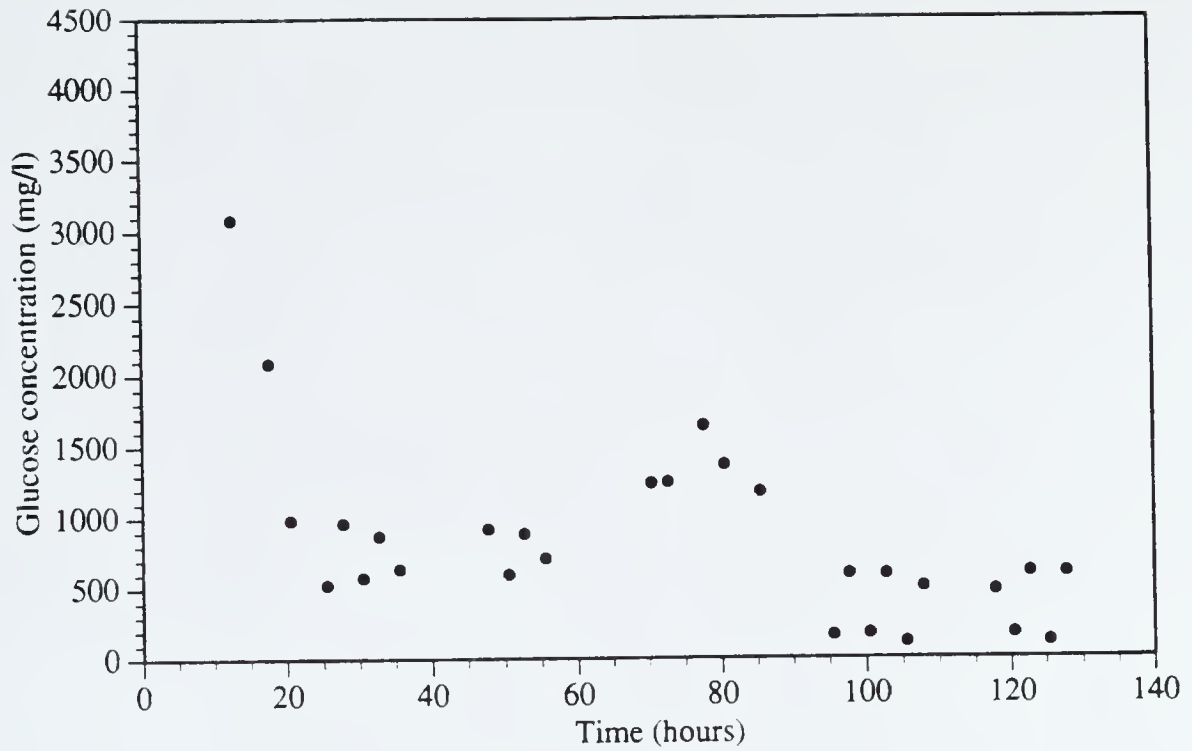


Figure 59. Periodic Run 1. Experimental results of effects of periodic operation ($D=.31, \epsilon=.45$) on biomass concentration. Only the shift points are shown.

$$\dot{p} = -Dp \quad (64)$$

where p =lactate concentration

D =dilution rate

which can be integrated to

$$p = p_0 e^{-Dt} \quad (65)$$

where p_0 =original lactate concentration

t =time

Equation 65 was used with p_0 being set to the lactate concentration at the end of the previous anaerobic phase and D being set to the appropriate dilution rate of 0.31 hr^{-1} . A least squares linear fit to the anaerobic lactate production data was also made, with the results being shown in figure 60. In order to determine the mean value, the anaerobic line and the aerobic exponential curve were then integrated separately. The area under the straight line was divided by 2.75 hours, which was the anaerobic cycle time, and the area under the exponential curve was divided by 2.25 hours. The average lactate concentration determined by this method was 1976 mg/l , which indicated a lactate productivity of $613 \text{ mg/(l}\cdot\text{hour)}$.

The biomass and lactate results for periodic run 2 are shown in figures 61 and 62. The switch to aeration cycling and continuous operation was performed at 13 hours. Again, these figures were confusing as they present all of the data collected. Similar switchpoint-only plots to those for periodic run 1 are shown in figures 63 and 64. The biomass results showed a smooth approach to what appears to be a cyclic steady state at about 60 hours. The lactate concentration showed a smooth approach to an apparent cyclic steady state also at about 60 hours. Three entire cycles were measured in this experiment, with the lactate values shown in figure 65. The second lactate peak was then looked at to obtain an average lactate productivity over a cycle. This was performed by the same procedure as used in the previous run, except that the aerobic cycle was fit to an

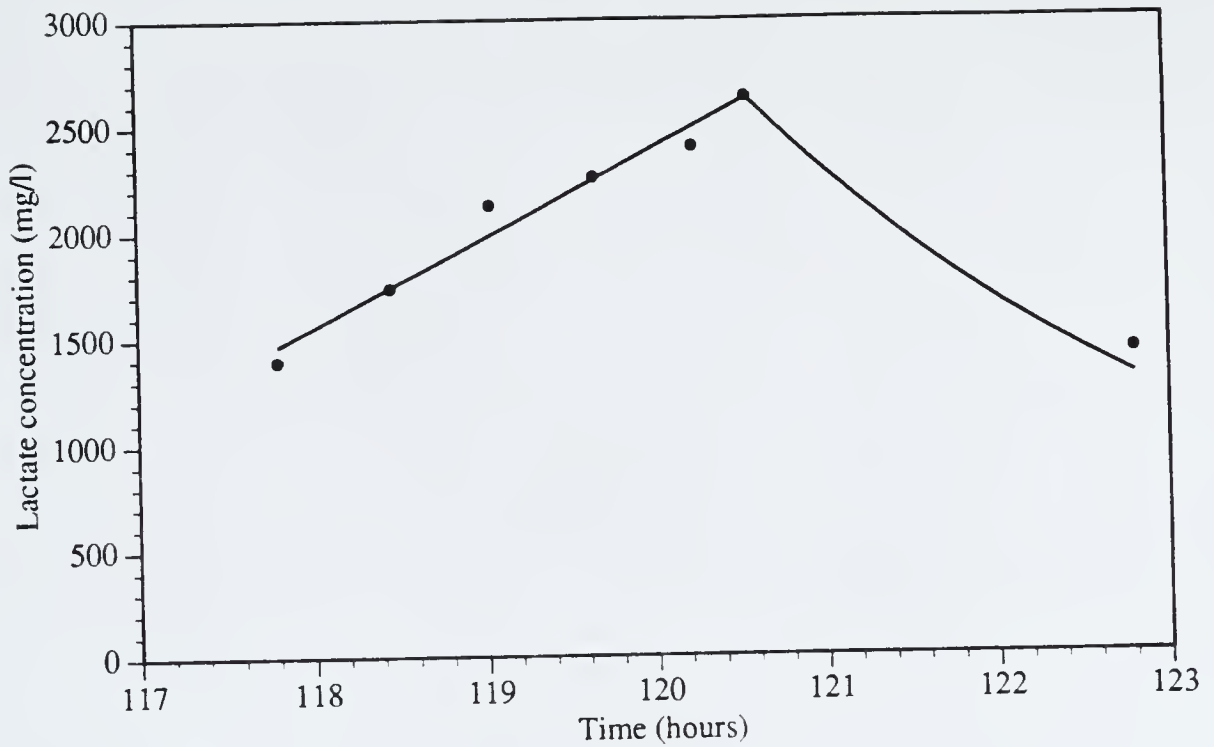


Figure 60. Periodic Run 1. Experimental results of effects of periodic operation ($D=.31, \varepsilon=.45$) on lactate concentration for one cycle. The first line represents a linear fit to the data, and the second curve represents model-predicted lactate dropoff.

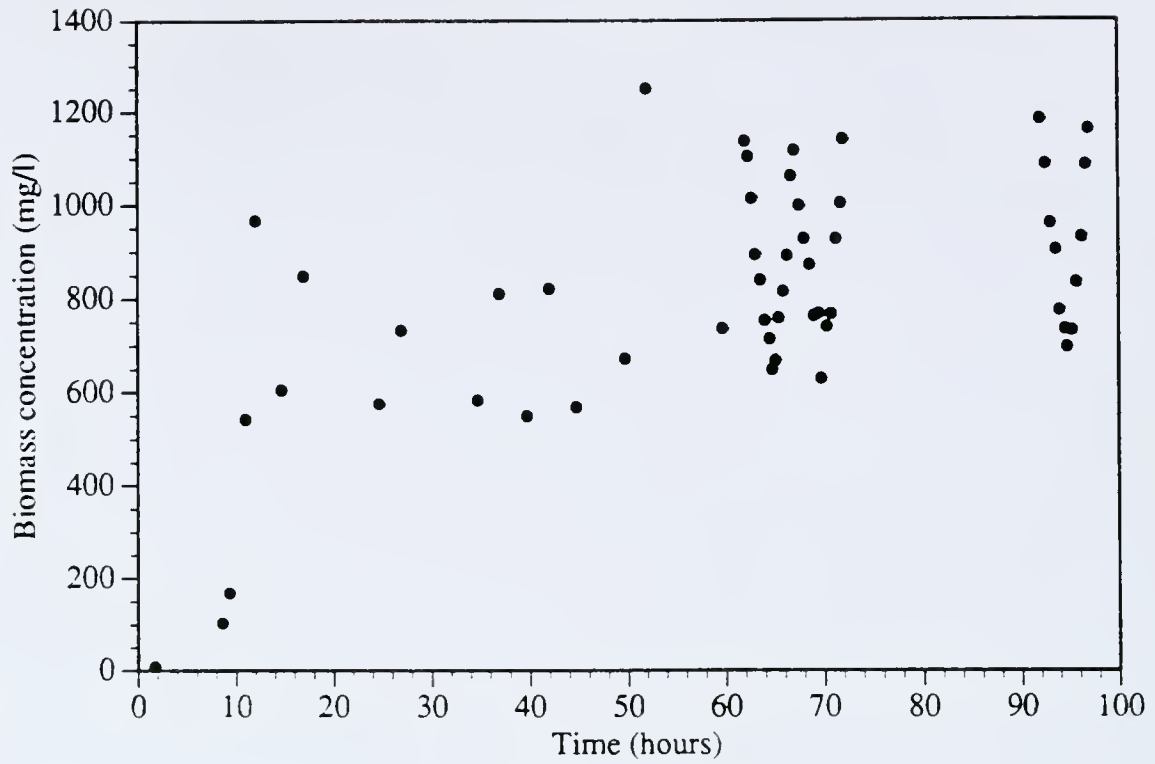


Figure 61. Periodic Run 2. Experimental results of effects of periodic operation ($D=.31, \epsilon=.45$) on biomass concentration.

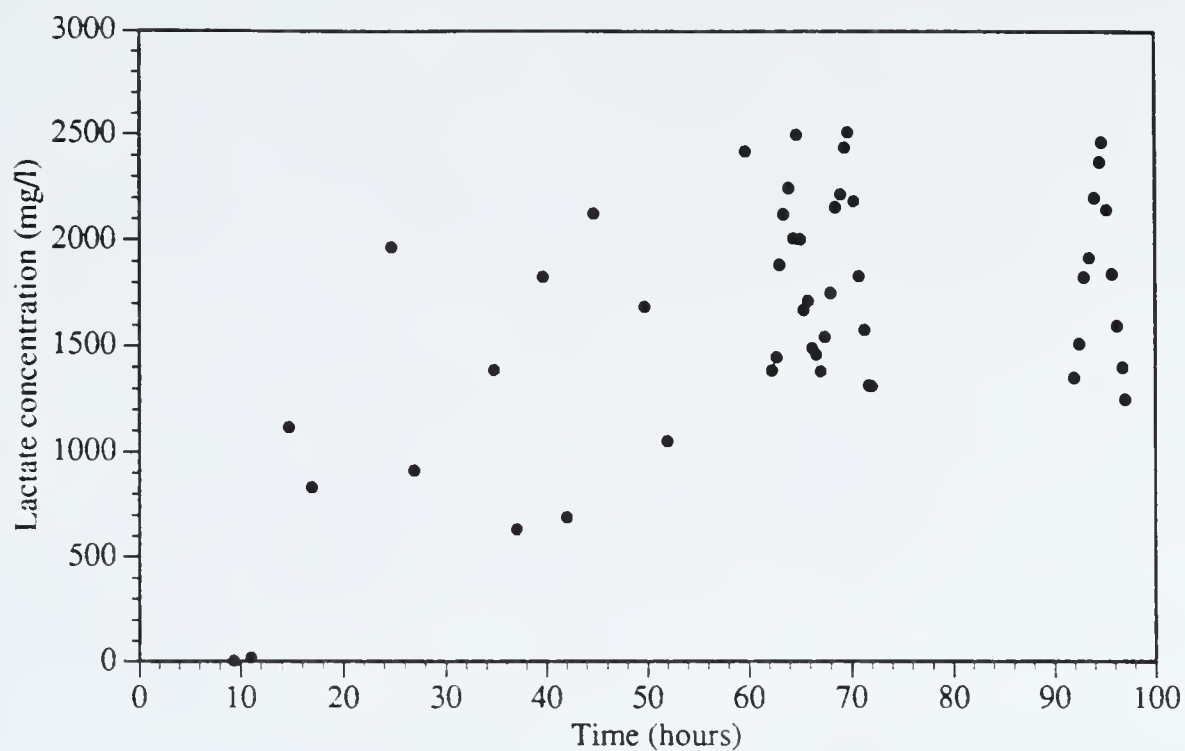


Figure 62. Periodic Run 2. Experimental results of effects of periodic operation ($D=.31, \epsilon=.45$) on lactate concentration.

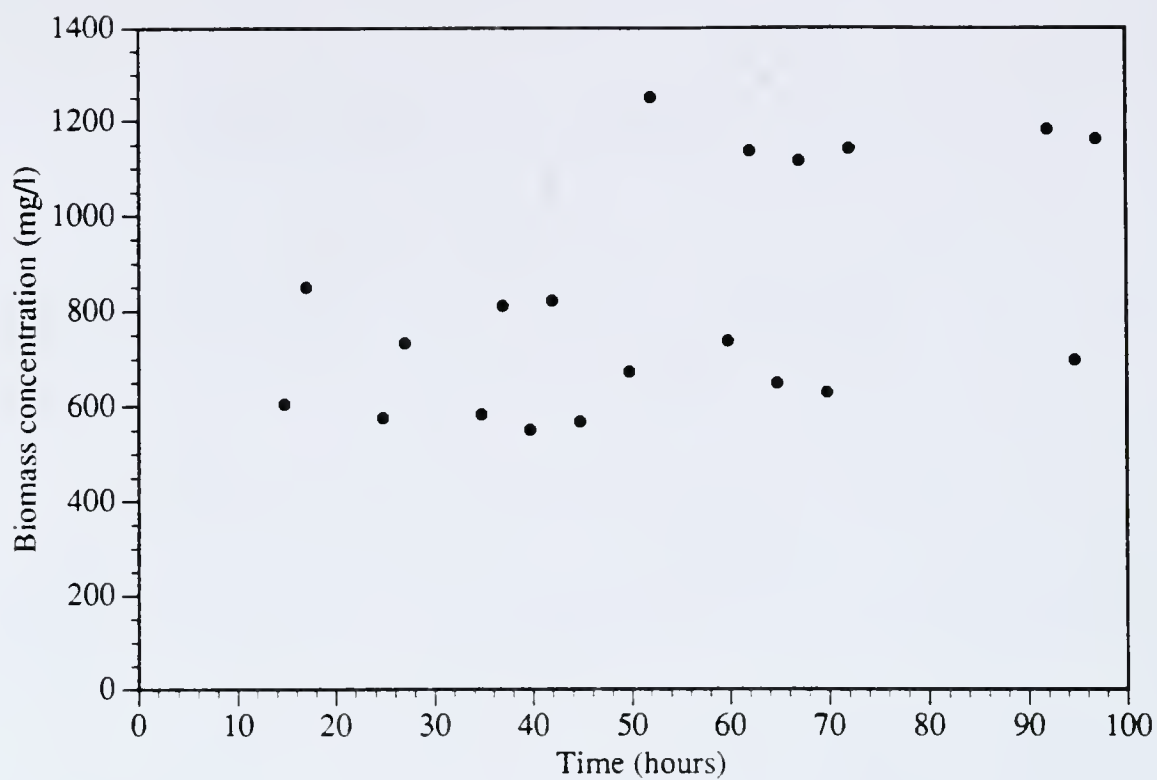


Figure 63. Periodic Run 2. Experimental results of effects of periodic operation ($D=.31, \varepsilon=.45$) on biomass concentration. Only the shift points are shown.

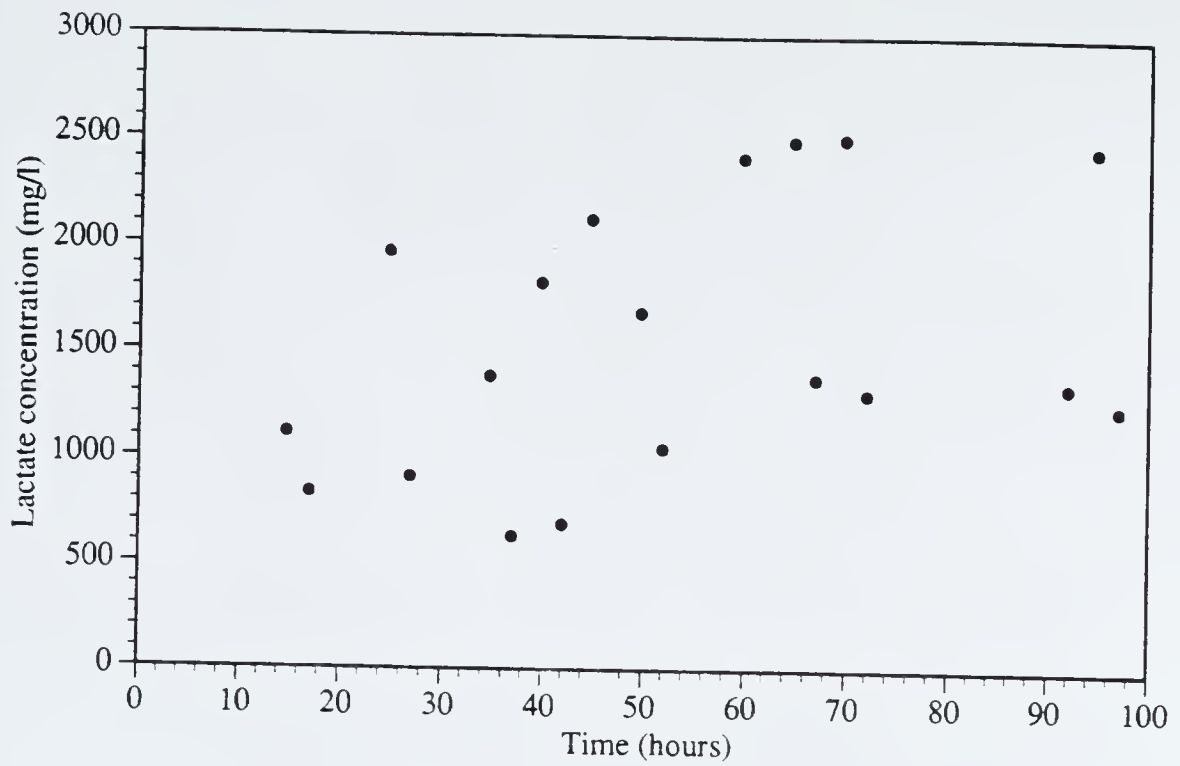


Figure 64. Periodic Run 2. Experimental results of effects of periodic operation ($D=.31, \epsilon=.45$) on lactate concentration. Only the shift points are shown.

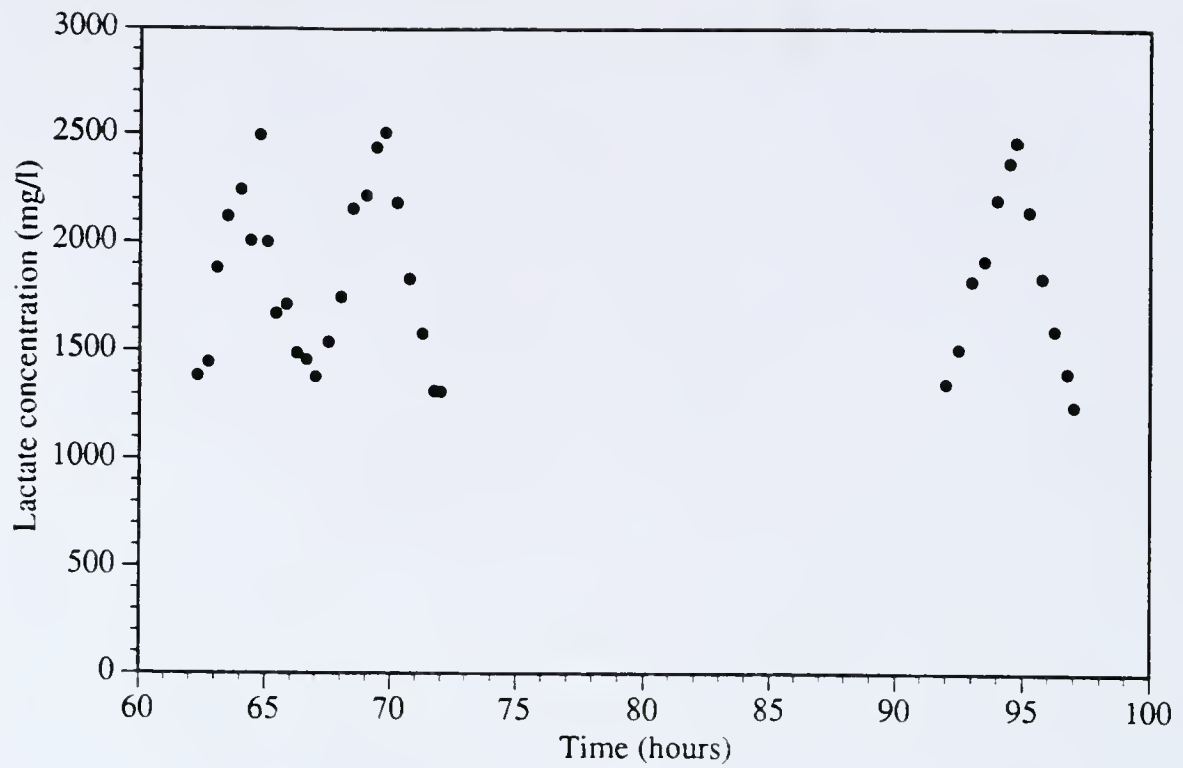


Figure 65. Periodic Run 2. Experimental results of effects of periodic operation ($D=.31, \epsilon=.45$) on lactate concentration. Only three cycles are shown.

exponential curve instead of being estimated. The results of these fits are shown in figure 66. The average lactate concentration determined for this run was 1898 mg/l, giving a lactate productivity of 588 mg/(l•hour).

The average of these lactate productivities is 600 mg/(l•hour). This indicates approximately an 8.5% improvement over the experimentally determined 553 mg/l. While this is not as large an improvement as the model predicted, it must be considered that the model, based on batch anaerobic data does underpredict anaerobic continuous steady-state lactate productivity. It can be argued then that the cycling lactate productivity should have been higher too, but it can also be argued that not enough is known about the transient behavior of *E. coli* LCB898 and microorganisms in general under aeration cycling to accurately describe metabolite production under these conditions. Nonetheless, an improvement by cycling was seen. The more interesting improvement is actually seen in the next chapter on reversion avoidance.

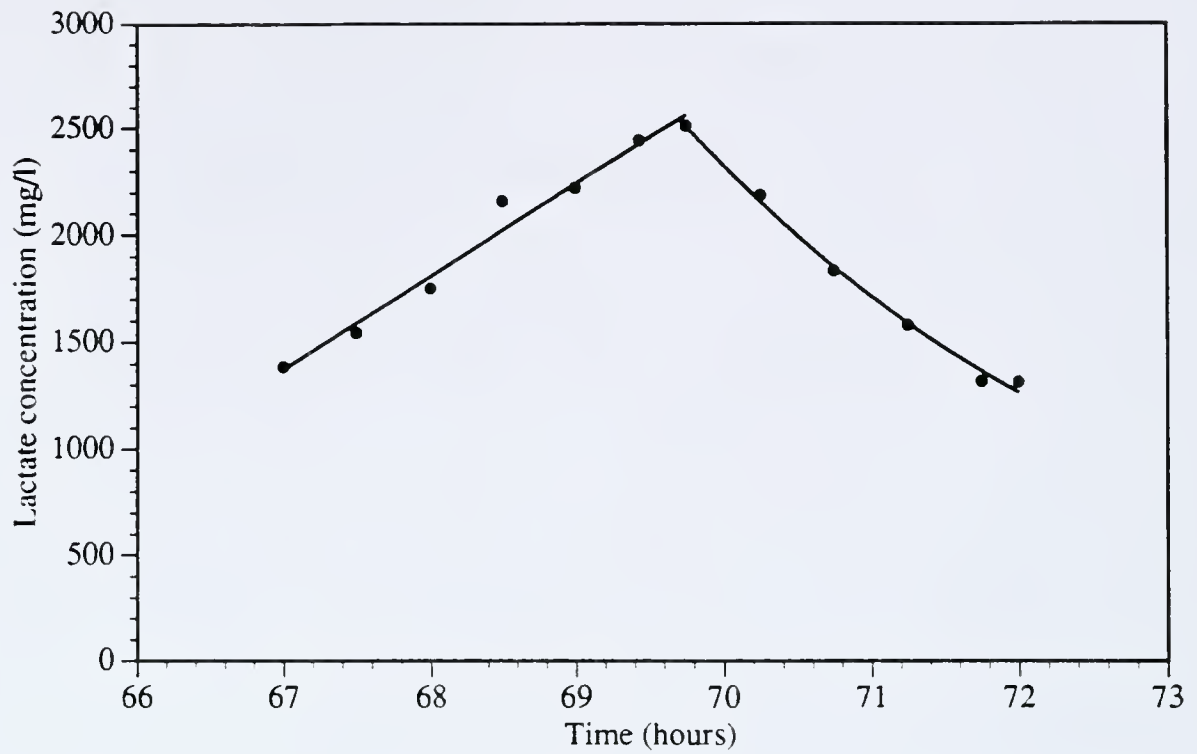


Figure 66. Periodic Run 2. Experimental results of effects of periodic operation ($D=.31, \epsilon=.45$) on lactate concentration for one cycle. The first line represents a linear fit to the data, and the second curve represents an exponential fit to the data.

CHAPTER 8

REVERSION OF *E. COLI* LCB898 AND A POSSIBLE NEW METHOD OF AVOIDANCE OF REVERSION

Mutation frequently occurs in microbial cells grown under continuous steady-state reactor conditions. Examples of mutation in continuous culture have been reported by several workers [e.g. 68-77]. The probable cause of mutation in several of these reports was genetic adaptation of the culture to substrate-limited conditions. As one example, Novick and Szilard [69], in continuous culture experiments with *E. coli* B/1, found that a mutant arose which they designated B/1/f. This mutant showed growth five times as fast as the original strain under tryptophan-limited conditions. They argued that this increased growth rate gave the B/1/f cells a selective advantage over the B/1 cells under the tryptophan-limited conditions seen in their continuous culture experiments, and, in time, the B/1/f cells must displace the original B/1 cells. Another example of mutation under continuous conditions was found in the work of Ruijter [73]. Here it was found that certain continuous operations would induce fast mutation of *Salmonella typhimurium* to a form with improved enzymatic systems for glucose uptake under glucose-limited conditions.

A specific kind of mutation is that of reversion of a previously mutated culture to its original wild-type form. An example of this was found in the work of Kiss and Stephanopoulos[77]. There, reversion of an L-lysine producing *Corynebacterium glutamicum* mutant to its original nonproducing form was investigated. The lysine producing mutant was auxotrophic for threonine, whereas the revertant was not. This gave the revertant an advantage over the mutant, and, in every continuous culture experiment that

was run, the revertant eventually took over with the consequence that the lysine concentration in their cultures fell to near zero.

As will be shown later in this chapter, reversion during anaerobic continuous operation may have been taking place in our system. The mutant, *E. coli* LCB898, may have been reverting to a *pfl*⁺ form. A likely consequence of this reversion would be very low lactate production by the revertant. The cycling of aeration described in the previous chapter has shown promise for delaying this reversion. A possible explanation will be given later.

The biomass, glucose, and lactate measurements for anaerobic continuous run 1 are shown in figures 67-69. These figures were formatted differently than those shown in Chapter 4, in that the time scale has been adjusted to time after the start of continuous operation; they also include later data points. The biomass and lactate figures show the previously described continuous steady state up to about 40 hours after the switch. After this apparent steady state, some sort of change seems to have occurred where the biomass increased and the lactate decreased. Very low lactate concentrations were already seen at 80 hours. The unusual response in glucose and biomass concentrations seen at about 100 hours were due to a system upset where a feed tube was pinched off and reactor volume dropped. A new biomass steady state appears, ignoring the upset, to have been established at 100 hours. The glucose concentration stays low during the entire experiment, again with the exception of the upset.

The biomass and lactate results for anaerobic continuous run 2 are shown in figures 70 and 71. These figures also have been reformatted with more data included in a similar fashion to figures 67-69. The biomass and lactate results show the previously described

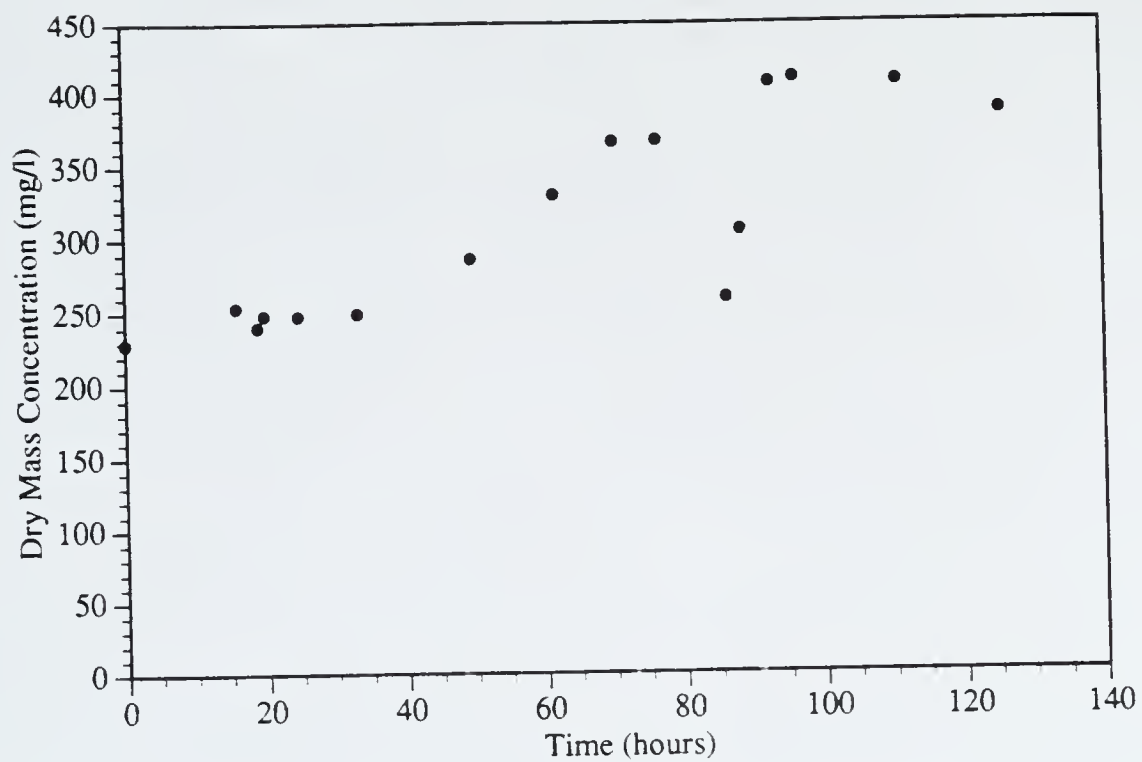


Figure 67. Anaerobic continuous run 1. Biomass concentration against time after switch to continuous.

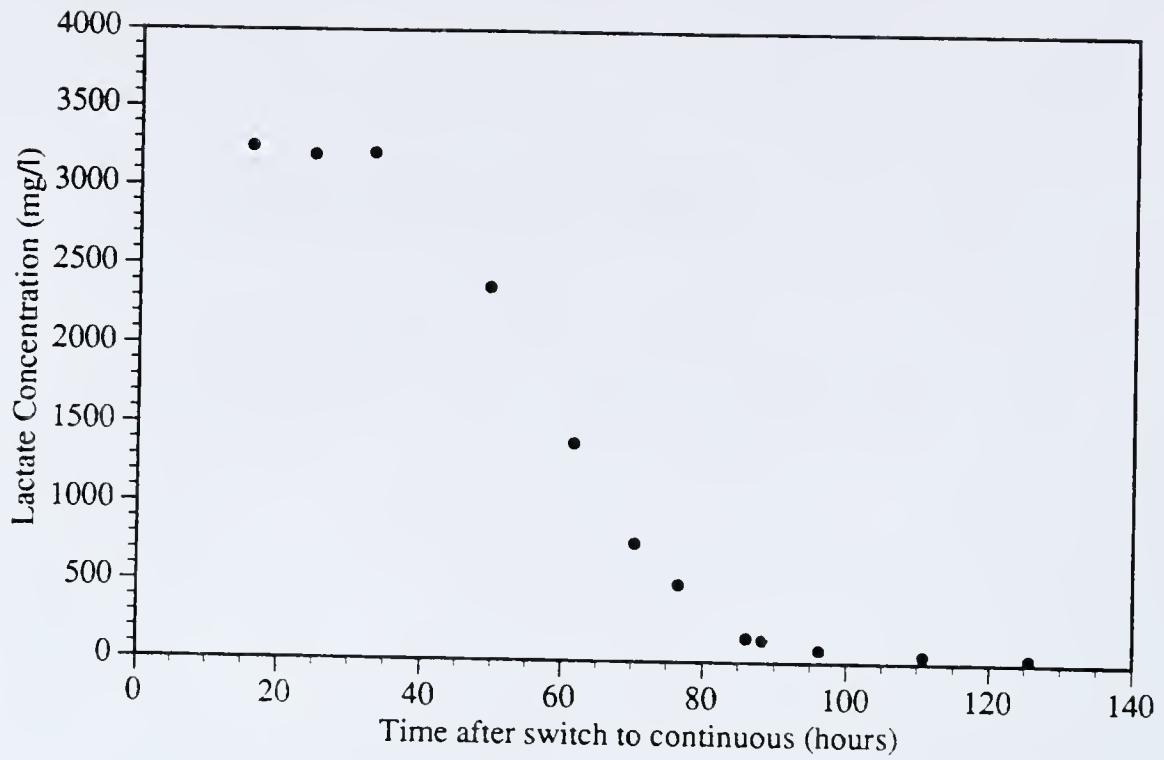


Figure 68. Anaerobic continuous run 1. Lactate concentration against time after switch to continuous.

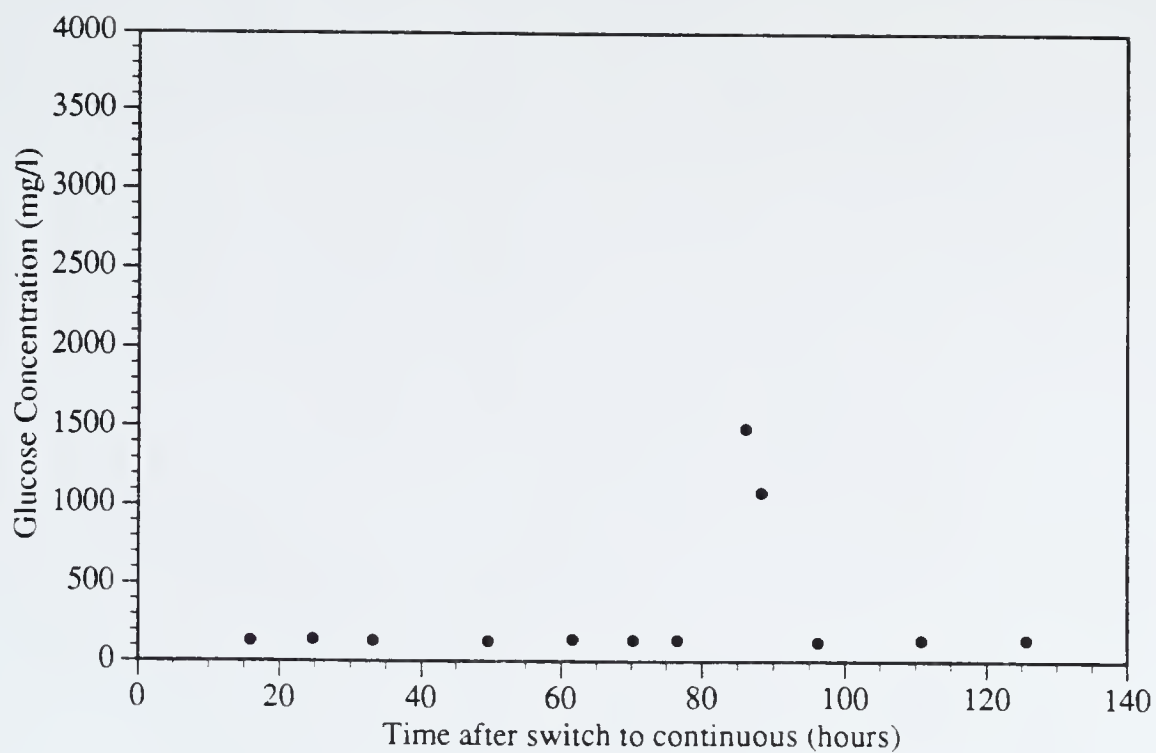


Figure 69. Anaerobic continuous run 1. Glucose concentration against time after switch to continuous.

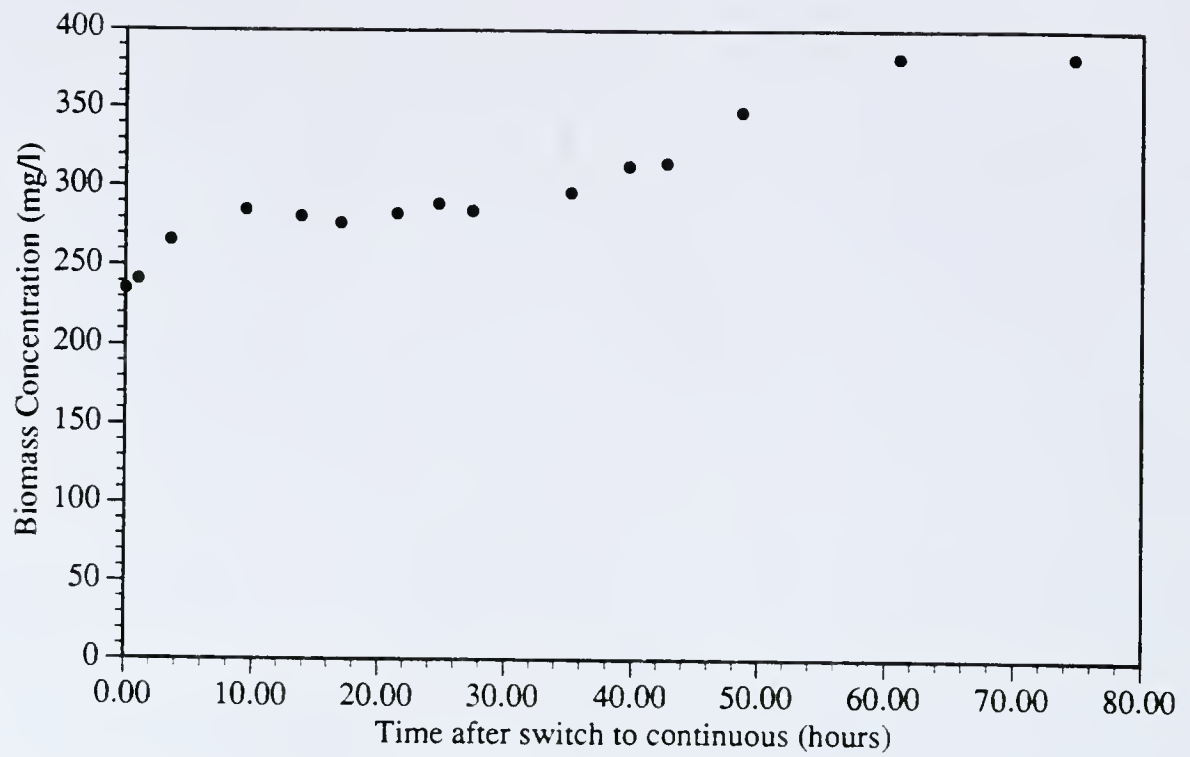


Figure 70. Anaerobic continuous run 2. Biomass concentration against time after switch to continuous.

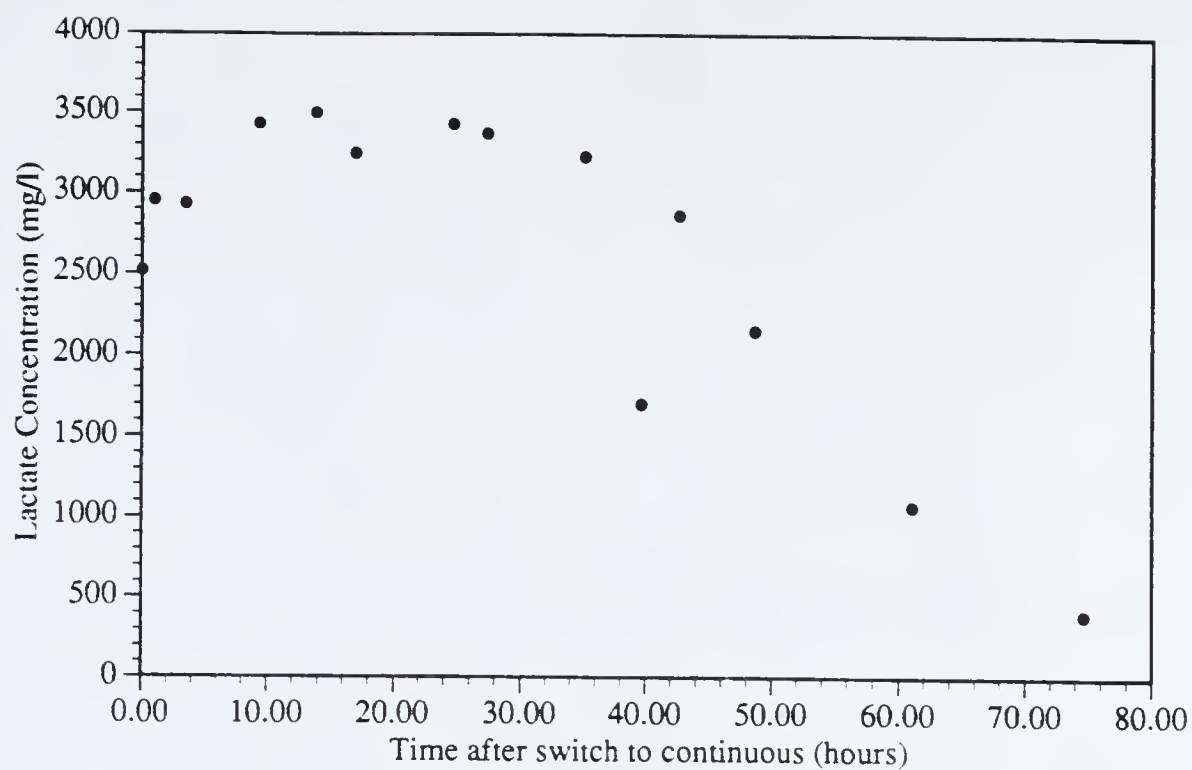


Figure 71. Anaerobic continuous run 2. Lactate concentration against time after switch to continuous.

continuous steady state up to about 30 hours after the switch to continuous operation, then, like in the previously described experiment, some sort of change occurred where the biomass increased and the lactate decreased. In this run, lactate concentration was very low at 60 hours. In order to test for reversion, gas production tests were performed. The principle behind the test was that *E. coli* LCB898 should show little or no gas production due to anaerobic glucose catabolism, as no CO₂ and H₂ production from pyruvate degradation by exclusive action of lactate dehydrogenase is possible. The tests were performed as follows: Two small samples of the reactor contents were taken at 60 hours, spread on to agar plates, and then the plates were incubated overnight. Ten colonies were selected from each of the agar plates and inoculated separately into ten test tubes with 13 ml each of 10 g/l tryptone, 5 g/l NaCl, 1 g/l yeast extract, and 1 g/l glucose solution, along with an inverted Durham tube in each tube. Another small sample was taken at 75 hours and a similar procedure was performed. Additionally sample cultures of the stock culture were also similarly processed. All twenty of the 60 hour samples showed gas production, and eight of the ten 75 hour samples showed gas production. The samples from the stock culture showed no gas production. This appeared to indicate that pyruvate formate-lyase mutation had reverted to an active form. This hypothesis could explain the unusual results from anaerobic continuous runs 1 and 2 and other continuous runs. (The same type of behavior was seen in every anaerobic continuous experiment run.) The pyruvate formate-lyase active revertant appeared to be able to use glucose more efficiently for biomass production, as indicated by the increasing biomass concentrations seen. However, little lactate is seen. The likely explanation for this reversion is that the low glucose concentration seen in a steady-state continuous reactor would provide a selective pressure for those cells that can use the available glucose most efficiently, as the revertants seem to do.

This apparent reversion obviously lowered the lactate productivity after relatively short periods of time. The cycling experiments, besides showing an improvement in lactate

productivity, showed promise in delaying, or perhaps avoiding, this reversion. This was an unexpected additional benefit of the periodic operation. The cycling experimental results for lactate concentration are shown in figures 72 and 73, along with the glucose results for periodic run 1 in figure 74. Only the results at the switch points were shown in these figures, and they were also reformatted for showing the results only after the switch to continuous operation. The experiments were not ended due to reversion. They were ended only due to experimental procedural problems such as feed blockage. Periodic run 1 still showed high lactate productivity at 115 hours, and periodic run 2 still showed high lactate productivity at 85 hours. The glucose results for periodic run 1 showed that average glucose concentration was higher than that for strict anaerobic operation. It appeared that periodic operation helped avoid reversion. A likely explanation as follows. The aerobic portion of the cycle, likely, provided no selective advantage for revertants. In addition, the average glucose concentration was considerably higher than that for strict anaerobic operation, thus lowering the pressure for revertant selection.

The delay or avoidance of reversion by periodic operation shows potential for other applications. The work shown here is preliminary, and further investigations of this phenomenon with *E. coli* LCB898 or other microorganisms should be performed. This idea could be extended to other types of cycling, such as pH, dilution rate, or inlet feed composition. If some organism was showing undesirable mutation in a reactor condition under one set of conditions (for example, acidic or anaerobic) but little or no reversion under another set of conditions (for example, neutral pH or aerobic), then periodic cycling of these conditions might be a useful operating strategy to avoid overall culture reversion.

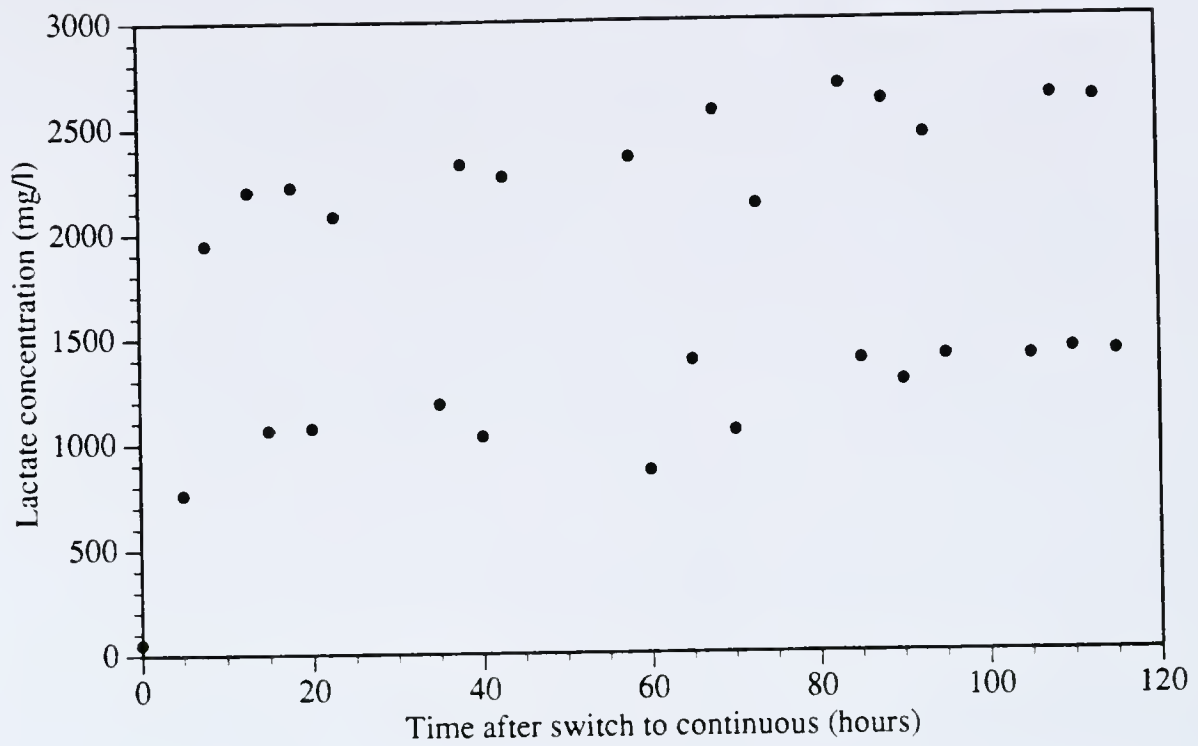


Figure 72. Periodic run 1. Lactate concentration against time after switch to continuous. Only shift points are shown.

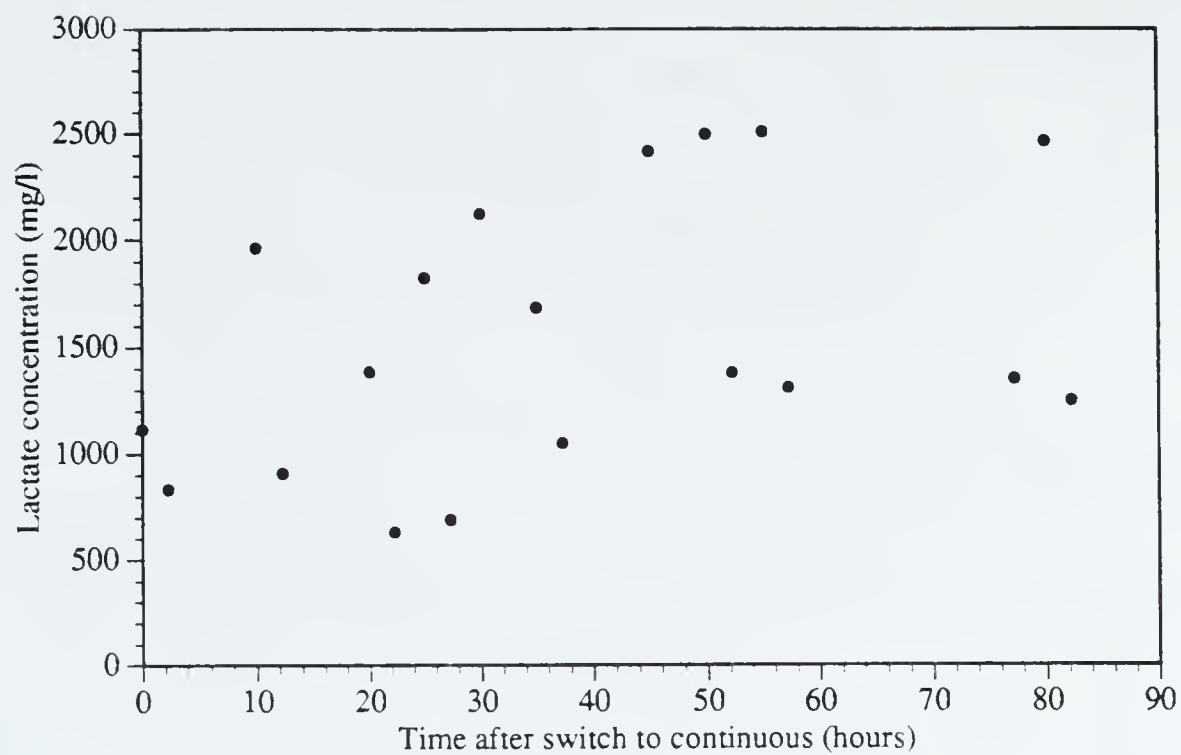


Figure 73. Periodic run 2. Lactate concentration against time after switch to continuous. Only shift points are shown.

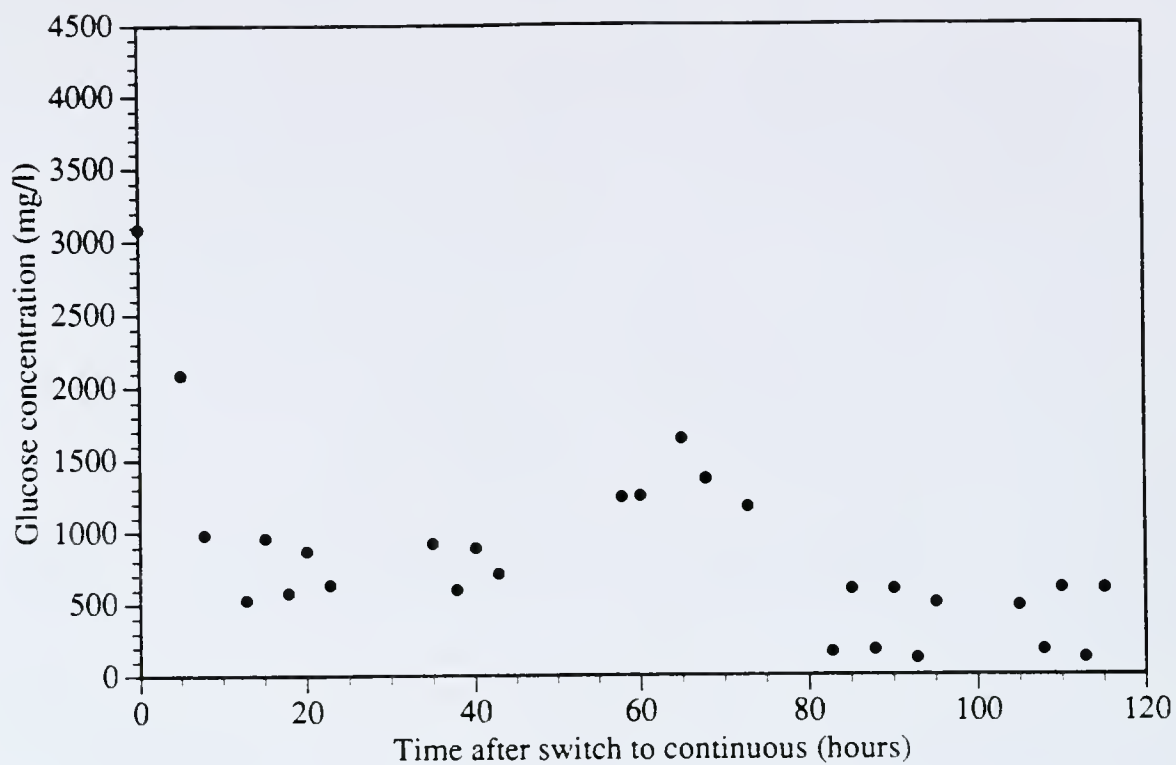


Figure 74. Periodic run 1. Glucose concentration against time after switch to continuous. Only shift points are shown.

CHAPTER 9 CONCLUSIONS

In some biological systems the optimal environmental conditions for producing of a desired metabolic product differ from the conditions that are optimal for cell growth. If producing this metabolite were the objective, one could continuously operate a reactor system at the optimal steady-state production conditions. For a given reactor volume, however, periodically switching conditions could increase overall metabolite production. This is possible since, due to higher growth rates under the optimal growth conditions, one could operate the system at significantly higher flowrates and, thus, obtain higher productivity.

A system involving *E. coli* mutant LCB898 was used as a model system. This mutant lacks the enzyme pyruvate-formate lyase and as a result under anaerobic growth conditions practically all of its pyruvate is converted to d-lactate. Thus it produces large amounts of d-lactic acid under oxygen-poor conditions, whereas it grows at a considerably higher rate under aerobic conditions when almost no lactate is produced. It was experimentally determined that the aerobic maximum specific growth rate is 0.61 hr^{-1} as compared to 0.19 hr^{-1} for anaerobic conditions. The possibility of increasing total lactate productivity by cycling of aeration investigated.

A method for determining the optimal waveform for the proposed cycling was developed by extending previous work by Lyberatos and Svoronos. The method involves Carleman linearization of the system equations around the optimal steady state and subsequent development of an expression for performance measure as a function of period, amplitude and pulse shape. This method was adapted to the present system. However, in

this system, one control variable was aeration which was either on or off with no intermediate values. Thus, an “imaginary” steady state had to be used for linearization. Since the optimization method requires availability of a dynamic model, such a model was developed using the results of both batch and continuous experiments.

The Carleman-based-method was applied to the above described model in order to determine the optimal cycling conditions. The results were very encouraging since a significant improvement in productivity over the optimal steady state (40%) was predicted. Experimental testing of the calculated cycling strategy, however, showed a considerably lower improvement.

Perhaps the most exciting (and accidental) discovery in this work was a possible new method to help delay or avoid mutation or reversion of microorganisms to a nonuseful form in a continuous steady-state bioreactor. This method essentially involves cycling between revertant selective and nonselective conditions. Only preliminary work has been performed, and further investigations are strongly suggested.

APPENDIX MATHEMATICA PROGRAMS FOR COMPUTATION OF CARLEMAN LINEARIZATION MATRICES

On the following pages program listings for two Mathematica programs developed to compute the Carleman linearization of a system of first order differential equations such as that shown in (2). The first program, Kronecker, is an auxiliary program used by the main program, CarlN, to figure Kronecker products. The Mathematica utility program for computing Kronecker products, Outer, did not compute the products correctly, so this auxiliary program was necessary. The second program listed, CarlN, is the main program to compute the Carleman linearization of the system. The program was based on the algorithm described in Chapter 2.

In order to use these programs, they must be installed into an active session of Mathematica. These programs have been tested on both Macintosh and PC systems. The following is the format of an execute statement for this program:

CarlN[cn,list of ode's]

where cn=Carleman order

list of ode's= the list of first order ordinary differential equations for a system to be linearized where the state variables are cast as deviation variables from some steady state and are referred to as $y[i]$

For example, the input statement for the second order linearization of the system given in (3) (assuming the variables are in deviation form) was as follows:

CarlN[2,{-y[1]+3*y[2]+y[2]^2,-y[1]^2+4*u}].

The output is stored in the following arrays:

CC= Contracted Carleman matrix (e.g. the 5×5 matrix in (5))

zvec= Associated Carleman vector (e.g. the 5×1 vector in (5))

wvec the list of approximated variables (e.g. the left-hand-side vector in (4))

Kronecker::usage="Kronecker[m1,m2] figures the Kronecker product of two matrices or vectors m1,m2"

```
Kronecker/: Kronecker[m1_List, m2_List] := Block[{atv,btv,ctv,dtv,av,bv,cv,dv,jv,
kv,nrm1,ekv,ncm1,m1a,nrm2,fkv,ncm2,m2a,iav,jav,rtp,ctp},
jv=Dimensions[m1];nrm1=jv[[1]];ekv=TensorRank[m1]; If[ekv <
1.1,ncm1=1;m1a=Outer[Times,m1,{1}], ncm1=jv[[2]];m1a=m1];
kv=Dimensions[m2];nrm2=kv[[1]];fkv=TensorRank[m2]; If[fkv <
1.1,ncm2=1;m2a=Outer[Times,m2,{1}], ncm2=kv[[2]];m2a=m2];qkv3=1;
Do[Do[qkm3[qkl1,qkl2]=m1a[[qkl1,qkl2]]*m2a,
{qkl2,ncm1}],{qkl1,nrm1}]; m3=Table[{},{nrm1*nrm2}];
Do[Do[qktm1=qkm3[qkv1,qkv2];Do[dope=qkl3-qkv3+1;
m3[[qkl3]]=Flatten[Append[m3[[qkl3]], qktm1[[dope]]]]; ,{qkl3,qkv3,qkv3+nrm2-
1,1}],{qkv2,ncm1}]; qkv3=qkv3+nrm2,{qkv1,nrm1}];]
```

CarlN::usage="CarlN[cn,f] figures the cn order Carleman linearization of an n-dimensional system where f=the list of n equations that describe the system. The variables should be in deviation form.

The equation list should be as follows f={f1,f2,..fn}. The variables should be in the form y[1],y[2], etc.

Output includes wvec=Carleman coordinate vector CC=the contracted Carleman matrix
zvec=the associated Carleman vector wvec=the variable order of the Carleman matrix"

```

CarlN/: CarlN[cn_Integer,f_List] := Block[{a,il,jl, kl,ll,ml,nl,ol,pl,ql,rl,sl,
yv,lvec,gg,gto,vlt,bsv1,bsv2,bsv3,bsv4,ul,tl, gs,tma,tmb,hll,tmc,tmd,ill,wvt,ccdim,wvf,
tpmat,tme,tmh,tmg,tmf,test,lll,mll,pmat2,pmat3,
pmat,uccdim,tvy,tvx,tvv,tmi,tmii,tmij,tvw,TURCC,
UCC,tvs,tvta,tvu,ptva,tvuu,tvt,URCC,ffv,A10m, ffvv },
n=Length[f];yv=Table[0,{n},{1}]; Do[yv[[il,1]]=y[il],{il,n}];vlist[1]=yv;
lvec=Table[0,{cn}];lvec[[1]]=Length[vlist[1]];

```

(* Following big Do statement forms

vlists and initializes uncontracted submatrices of Taylor portion of Carleman matrices *);

```
Do[Kronecker[yv,vlist[(gl-1)]];vlist[gl]=m3;lvec[[gl]]= Length[vlist[gl]],{gl,2,cn,1}];
```

```
Do[A1[il]=Table[0,{n},{lvec[[il]]}];gg=A1[il];
```

```
Do[Do[gg[[pl,ql]]=f[[pl]],{ql,lvec[[il]]}],{pl,n}];A1[il]=gg,{il,cn}];
```

(* Determination of all uncontracted A1x matrices for 1<=x<=cnn *);

```
Do[gto=A1[ml];vlt=vlist[ml]; Do[Do[Do[gto[[nl,ol]]= D[gto[[nl,ol]],{y[rl],
```

```
Exponent[vlt[[ol,1]],y[rl]]}],{rl,n} ],{ol,lvec[[ml]]}],{nl,n}]; A1[ml]=gto (1/(ml!))
```

```
,{ml,cn}]; Do[bsv4=A1[tl];bsv1=Dimensions[bsv4];
```

```
Do[Do[Do[bsv4[[bsv2,bsv3]]=bsv4[[bsv2,bsv3]]/. y[ul]->0,{ul,n}], {bsv3,bsv1[[2]]}],
```

```
{bsv2,bsv1[[1]]}];A1[1,tl]=bsv4,{tl,cn}];
```

(* Determination of A10 submatrix *); A1[0]=f;gs=f; Do[Do[gs[[jl]]=

```
gs[[jl]] /. y[kl]->0,{kl,n} ],{jl,n}]; A1[0]=gs;A1[1,0]=A1[0];
```

(* Determination of Remaining Uncontracted Submatrices *);


```
Do[tma=IdentityMatrix[n]; tmb=IdentityMatrix[n^(hll-1)];Do[ Kronecker[tma,A[hll-1,ill]]
;tmc=m3; Kronecker[A[1,ill],tmb];tmd=m3; A[hll,ill]=tmc+tmd,{ill,0,cn-hll+1,1}},
{hll,2,cn,1}];
```

(* Formation of Contracted variable list *);

```
wvt=Table[0,{cn}];ccdim=0;Do[wvt[[jll]]= vlist[jll];ccdim=ccdim+Binomial[n+jll-1,jll]
,{jll,cn}];wvt=Flatten[wvt];
wvf=Union[wvt];tpmat=Table[0,{ccdim}];pmat=tpmat;
Do[tpmat[[kll]]=Position[wvt,wvf[[kll]]], {kll,ccdim}];
Do[tme=Length[tpmat[[mll]]];tmh={ }; Do[tmg=tpmat[[mll,lll]];
tmf=Length[tmg];If[tmf<1.1, test=99;tmh=Append[tmh,tmg],else=1],
{lll,tme}];pmat[[mll]]=tmh,{mll,ccdim}]; pmat=Map[Flatten,pmat,{1}];
tmi=Table[tva,{tva,ccdim}]; pmat2=pmat[[tmi,{1}]];pmat3=Flatten[pmat2];
pmat2=Flatten[Sort[pmat2]]; ;wvec=wvt[[pmat2]];wvec=Outer[Times,wvec,{1}];
```

```
(* Formation of Uncontracted Carleman matrix *); uccdim=0;Do[uccdim=uccdim +
n^nll,{nll,cn}]; UA[1]=Transpose[A[1,1]];UA[1]={UA[1]};
Do[UA[1]=Append[UA[1],Transpose[A[1,tvz]]] ,{tvz,2,cn,1}];UA[1]=Flatten[UA[1],1];
UA[1]=Transpose[UA[1]]; If[cn>1,
Do[UA[tvy]=Transpose[A[tvy,0]]; UA[tvy]={UA[tvy]}; Do[UA[tvy]=Append[UA[tvy],
Transpose[A[tvy,tvx]]], {tvx,cn-tvy+1}]; UA[tvy]=Flatten[UA[tvy],1];
UA[tvy]=Transpose[UA[tvy]]; tvv=Dimensions[UA[tvy]];
If[ttv[[2]]<uccdim,
tmi=Table[0,{ttv[[1]]},{uccdim-ttv[[2]]}];
tmii=Transpose[tmi];tmij={ Transpose[UA[tvy]]};
```

```
UA[tvy]=Prepend[tmij,tmii]; UA[tvy]=Flatten[UA[tvy],1];
```

```
UA[tvy]=Transpose[UA[tvy]],else=4];
```

```
,{tvj,2,cn,1}],else=2];
```

```
UCC={A[1]}; If[cn>1,
```

```
Do[UCC=Append[UCC,UA[tvw]],{tw,2,cn,1}],else=3]; UCC=Flatten[UCC,1];
```

```
(* Column Contraction of Matrix *); TURCC=Table[0,{ccdim},{uccdim}];
```

```
Do[tvta=pmat3[[tvu]]; tvs=Length[pmat[[tvu]]]; ptva=Flatten[Position[pmat2,tvta]][[1]];
```

```
Do[tvuu=pmat[[tvu,tvt]]; TURCC[[ptva]]=Transpose[UCC][[tvuu]]+
```

```
TURCC[[ptva]],{tvt,tvs}},{tvu,ccdim}];
```

```
URCC=Transpose[TURCC];
```

```
(* Row (and Final!) Contraction of Matrix *);
```

```
CC=Table[0,{ccdim},{ccdim}]; Do[CC[[ffv]]=URCC[[pmat2[[ffv]]]],{ffv,ccdim}];
```

```
(* Final form of z vector *);
```

```
zvec=Table[0,{ccdim},{1}];
```

```
A10m=Outer[Times,A[1,0],{1}]; Do[zvec[[ffvv]]=A10m[[ffvv]],{ffvv,n}]]
```

LIST OF REFERENCES

1. Pickett, A. M., and Bazin, M. J., *Biotech. and Bioeng.*, 21, 1043 (1979).
2. Pickett, A. M., and Bazin, M. J., *Biotech. and Bioeng.*, 22, 1213 (1980).
3. Zines, D. O., and Rogers, P. L., *Biotech. and Bioeng.*, 13, 293 (1971).
4. Welles, J. B., and Blanch, H. W., *Biotech. and Bioeng.*, 18, 129 (1976).
5. Borzani, W., Gregori, R. E., and Vairo, M. L. R., *Biotech. and Bioeng.*, 18, 623, (1976).
6. Sundstrom, D. W., Klei, H. E., and Brookman, G. T., *Biotech. and Bioeng.*, 18, 1, (1976).
7. Abulesz, E-M. and Lyberatos, G., *Biotech. and Bioeng.*, 29, 1059 (1987).
8. Stephens, M.L. and Lyberatos, G., *Biotech. and Bioeng.*, 31, 464 (1988).
9. O'Neil, D. G. and Lyberatos, G., *Biotech. and Bioeng.*, 28, 1323 (1986).
10. MacDonald, N., *Biotech. and Bioeng.*, 18, 805 (1976).
11. Rodin, J. B., "Effect of Transient Operation on the Behavior of Escherichia Coli and Development of an Appropriate Time Delay Model", M.S. Thesis, University of Florida, Gainesville, FL (1989).
12. Pike, R.W., Optimization for Engineering Systems, Van Nostrand Reinhold, New York (1986).
13. Edgar, T.F., and Himmelblau, D.M., Optimization of Chemical Processes, McGraw-Hill, New York (1988).
14. Beightler, C.S., Philips, D.T., and Wilds, D.J., Foundations of Optimization, Prentice Hall, Englewood Cliffs, NJ (1979).
15. Kirk, D.E., Optimal Control Theory: an Introduction, Prentice Hall, Englewood Cliffs, NJ (1970).
16. Bryson. A.E. and Ho, Y.C., Applied Optimal Control, Hemisphere, Washington, DC (1975).
17. Lyberatos, G. and Svoronos, S.A., "Optimal Periodic Square-Wave Forcing: A New Method", *Proc. ACC*, Minneapolis, MN, 257 (1987).
18. Bailey, J.E. and Horn, F.J. M., *J. Opt. Theor. Appl.*, 7, 378 (1971).

19. Horn, F.J. M., and Lin, R.C., I&EC Process Design Dev., 6, 21 (1967).
20. Rinaldi, S., IEEE Trans. Auto. Control, 671 (1970).
21. Bittanti, S., Fronza, G. and Guardabasi, G., IEEE Trans. on Automatic Control, AC-18, 33 (1973).
22. Sincik, D. and Bailey, J.E., Int. J. of Control, 27, 547 (1978).
23. Colonius, F., Optimal Periodic Control, Springer-Verlag, Berlin-Heidelberg (1988).
24. Press, W.H., Flannery, B.P., Teukolsky, S.D., and Vetterling, W.T., "Numerical Recipes Fortran Version", Cambridge, NY (1989).
25. Carleman, T., Acta Math., 549, 63 (1932).
26. Bellman, R. and Richardson, J.M., Quart. Appl. Math., 20, 333 (1963).
27. Drener, A., Proc. at the 1974 Allerton Conf., El. Eng. Dept., U. of Illinois, Urbana-Champaign, IL, 834 (1974).
28. Brochet, R., "Functional Expansions and Higher Order Necessary Conditions in Optimal Control, in Mathematical Systems Theory", G. Marchesmi, S. Mitter, eds. Lecture Notes in Economics and Mathematical Systems, V. 131, Springer-Verlag, New York, 111 (1976).
29. Svoronos, S.A., Stephanopoulos, G. and Aris, R., Int. J. Control, 31, 104 (1980).
30. Steeb, W.H., and Wilhelm, F., J. Math. Anal Appl., 77, 601 (1980).
31. Rugb, W.J., Nonlinear System Theory, The Johns Hopkins University Press, Baltimore (1981).
32. Tsiliogiannis, C.A. and Lyberatos, G., J. Math. Anal. App., 126, 143 (1987).
33. Kowalski, K. and Steeb, W.H., Nonlinear Dynamical Systems and Carleman Linearization", World Scientific, Teaneck, NJ (1991).
34. Hatzimanikatis, V., Lyberatos, G., Pavlou, S., and Svoronos, S. A., "A Method for Pulsed Periodic Optimization of Chemical Reaction Systems," Chem. Eng. Sci., in press.
35. Abulesz, E.M., "Periodic Optimization of Biological Systems", PhD Dissertation, University of Florida, Gainesville, FL (1988).
36. Wolfram, S., Mathematica: A System for Doing Mathematics by Computer, Addison Wesley, Redwood City, CA (1988).
37. Varenne, S., Casse, F., Chippaux, M., and Pascal, M. C., Mol. Gen. Genet., 141, 181 (1975).

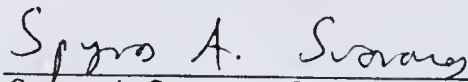
38. Pascal, M. C., Chippaux, M., Abou-Jaoude, A., Blaschkowski, H. P., and Knappe, J., *J. Gen. Micro.*, 124, 35, (1981).
39. Hansen, R. G., and Henning, U., *Biochim. Biophys. Acta*, 122, 355 (1966).
40. Winkelman, J. W., and Clark, D. P., *J. Bac.*, 167, 1 (1986).
41. Miller, J.H., Experiments in Molecular Genetics, Cold Spring Harbor Laboratory, Cold Spring Harbor, NY (1972).
42. Stephens, M.L., "The Effect of Periodic Operation on Mixed and Recombinant Bacterial Populations", PhD Dissertation, University of florida, Gainesville, FL (1989).
43. Sumbrook, J., Fritsch, E.F. and Moiniaris, T., Molecular Cloning: a Laboratory Manual, Vol. 3, Cold Spring Harbor Laboratory, Cold Spring Harbor, NY (1989).
44. Cunningham, P.R., and Clark, D. P., *Mol. Gen. Genet.*, 205, 487 (1986).
45. Winkelman, J.W., and Clark, D.P., *J. Bac.*, 167, 362 (1986).
46. Bridson, E.Y., and Brecker, A., "Design and Formulation of Microbial Culture Media" in Methods in Microbiology , vol. 3A, Norris, J. R. and Ribbons, D.W., eds. Cambridge University Press, Academic Press, London (1970).
47. Brock, T.D., and Madigan, M.T., Biology of Microorganisms, Prentice Hall, Englewood Cliffs, NJ (1988).
48. Dawes, E.A., Microbial Energetics, Blackie & Son, Glasgow (1986).
49. Neidhardt, F.C., Ingraham, J.L., and Schaechter, M., Physiology of the Bacterial Cell: A Molecular Approach, Sinauer Associates, Sunderland, MA (1990).
50. Smith, M.W. and Neidhardt, F.C., *J. Bac.*, 134 (1983).
51. Model, P. and Rittenberg, P., *Biochemistry*, 6, 69 (1967).
52. Knappe, J., "Anaerobic Dissimilation of Pyruvase", in Escherichia Coli and Salmonella Typhimurium, Neidhardt, F.C., Ingraham, J.G., Low, K.B., Magasankik, B., Schaechter, M., and Umgarer, H.E., American Society for Microbiology, Washington, DC (1987).
53. Clark, D.P., *FEMS Microbiology Rev.*, 63, 223 (1989).
54. Belaich, A. and Belaich, J.P., *J. Bac.*, 125, 14 (1976).
55. Clark, D.P., Cunningham, P.R., Reams, S.G., Mat-Jan, F., Mohammedkhani, R., and Williams, C. R., "Mutants of *Escherichia coli* Defective in Acid Fermentation" in *Proc. of the Ninth Symp. on Biotechnology for Fuels and Chemicals*, Humana Press, Clifton, NJ (1982).
56. Bailey, J.E. and Ollis, D. F., Biochemical Engineering Fundamentals, Second ed., McGraw-Hill, New York (1986).

57. Tempest, D.W. and Neijssel, O.M., "Growth Yield and "Energy Distribution", in Escherichia Coli and Salmonella Typhimurium, Neidhardt, F.C., Ingraham, J.L., Low, K.B., Magasanik, B., Schaechter, M., and Umberger, H.E., American Society for Microbiology, Washington, DC (1987).
58. Stalhandske, C., "Experimental Determination of Dynamic Models for the Aerobic Growth of a Mutant Escherichia Coli", M.S. Thesis, Royal Institute of Technology, KTH, Stockholm, Sweden (1991).
59. Monod, J., Ann. Rev. Microbiol., 3, 371 (1949).
60. Rodin, J.B., Lyberatos, G. and Svoronos, S. A., "Modelling the Difference between Biomass and Cell Number Growth Rate", presented at 1990 AIChE Annual Meeting, Chicago (1990).
61. Rodin, J. B., Lyberatos, G. K., and Svoronos, S. A., Biotech. and Bioeng., 37, 127 (1991).
62. San Martin, R., Bushell, D., Leak, D. J., and Hartley, B. S., J. Gen. Micro., 138, 987 (1992).
63. Alexander, M. A., Chapman, T. W., and Jeffries, T. W., Appl. Env. Micro., 55, 2152 (1989).
64. Diaz-Ricci, J. C., Holtzmann, B., Rinas, U. and Bailey, J. E., Biotech. Prog., 6, 326 (1990).
65. Smith, M. W., and Neidhardt, F. C., J. Bac., 154, 344 (1983).
66. Abulesz, E-M. and Lyberatos, G., Biotech. Bioeng., 34, 741 (1989).
67. Stephens, M. L., Christensen, C., and Lyberatos, G., Biotech. Prog., 8, 1 (1992).
68. Fox, M. S., J. Gen. Physiology, 39, 267 (1955).
69. Novick, A. and Szilard, L., Genetics, 36, 708 (1950).
70. Roth, M., and Noack, D., J. Gen. Micro., 128, 107 (1982).
71. Caslavaska, J., and Pazlarova-Kodesova, J., Folia Microbiol., 20, 379 (1975).
72. Miller, R. P., Dykhuizen, D. E., and Harri, D. L., Mol. Biol. Evol., 5, 691 (198).
73. Ruijter, G. J. G., Pogima, P. W., and Van Dam, K. J., Bac., 4, 783 (1990).
74. Wiebe, M. G., Trinci, A. P. J., Cunliffe, B., Robson, G. D., and Oliver, S. G., Mycol. Res., 95, 1284 (1991).
75. Kubitschek, H. E., and Bendigkeit, H. E., Mut. Res., 1, 113 (1964).
76. Kirpekar, A. C., Kirwan, D. J., and Stieber, R. W., Biotech. Prog., 1, 231 (1985).
77. Kiss, R. B. and Stephanopoulos, G., Biotech. Bioeng., 40, 75 (1992).


BIOGRAPHICAL SKETCH

Jonathan Ben Rodin was born on December 6, 1966, in Lincoln, Nebraska. Until he reached the age of twenty, he lived in various cities of the Midwest, including Lincoln, Nebraska, and the Iowa cities of Sioux City and Iowa City. In Iowa City he finished his undergraduate chemical engineering degree at the University of Iowa. He then went to the University of Florida for his graduate work. His future plans are currently undetermined.


I certify that I have read this study and that in my opinion it conforms to acceptable standards of scholarly presentation and is fully adequate, in scope and quality, as a dissertation for the degree of Doctor of Philosophy.


Spyros A. Svoronos, Chairman
Associate Professor of Chemical
Engineering

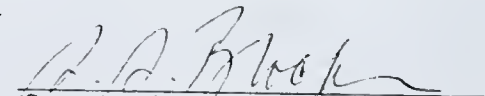
I certify that I have read this study and that in my opinion it conforms to acceptable standards of scholarly presentation and is fully adequate, in scope and quality, as a dissertation for the degree of Doctor of Philosophy.


Gerasimos Lyberatos, Cochairman
Associate Professor of Chemical
Engineering


I certify that I have read this study and that in my opinion it conforms to acceptable standards of scholarly presentation and is fully adequate, in scope and quality, as a dissertation for the degree of Doctor of Philosophy.


Gerald B. Westermann-Clark
Associate Professor of Chemical
Engineering

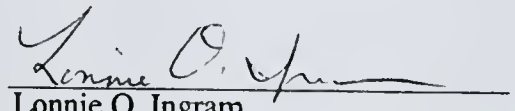
I certify that I have read this study and that in my opinion it conforms to acceptable standards of scholarly presentation and is fully adequate, in scope and quality, as a dissertation for the degree of Doctor of Philosophy.


Seymour S. Block
Professor of Chemical Engineering

I certify that I have read this study and that in my opinion it conforms to acceptable standards of scholarly presentation and is fully adequate, in scope and quality, as a dissertation for the degree of Doctor of Philosophy.

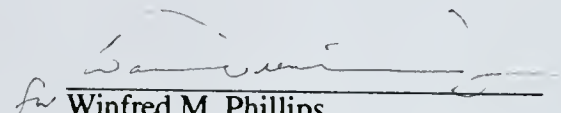

Ben Koopman
Professor of Environmental
Engineering Sciences


I certify that I have read this study and that in my opinion it conforms to acceptable standards of scholarly presentation and is fully adequate, in scope and quality, as a dissertation for the degree of Doctor of Philosophy.


Lonnie O. Ingram
Professor of Microbiology and Cell
Science

This dissertation was submitted to the Graduate Faculty of the College of Engineering and to the Graduate School and was accepted as partial fulfillment of the requirements for the degree of Doctor of Philosophy.

December, 1992


Winfred M. Phillips
Dean, College of Engineering


Madelyn M. Lockhart
Dean, Graduate School

